Propagation Environment Modeling Using Scattered Field Chamber

Abstract

This thesis covers the development of the Reverberation Chamber as a measurement tool for cell phone tests in electronic production. It also covers the development of the Scattered Field Chamber as a measurement tool for simulations of real propagation environments.

The first part is a more ”general knowledge about Reverberation Chambers”-part that covers some important phenomena like unstirred power and position dependence that might occour in a small Reverberation Chamber used for cell phone tests. Knowing how to deal with these phenomenas, give the possibility to use the chamber as a measurement tool for production tests even though it is too complex for a simple test of the antenna function.

The second part shows how to alter some important propagation parameters inside the chamber to fit some real world propagation environments. The 3D plane wave distribution, the polarization and the amplitude statistics of the plane waves are all altered with simple techniques that are implementable all together. A small, shielded anechoic box with apertures is used to control 3D plane wave distribution and polarization. Antennas that introduce unstirred power in the chamber are used to control the statistics.

Sammanfattning

Avhandlingens innehåll kan delas i två delar, den första behandlar utvecklandet av den modväxlande kammaren (Reverberation Chamber) som mätverktyg för mobiltelefontester i elekronikproduktion. Den andra behandlar utvecklandet av den specialiserade modväxlande kammaren (Scattered Field Chamber) som mätverktyg för test av kommunikationsterminaler i simulerade vågutbredningsmiljöer.

Den första delen som behandlar produktionstest kan ses som en del innehållande generell vetskap om vågutbredningsfenomen som kan förekomma i små modväxlande kammare som utvecklats för mobiltelefontester. Genom att veta om och kunna kompensera för dessa fenomen kan kammaren användas för test inom produktion. För enkla funktionstest av enbart antennen på en telefon är metoden dock för komplex och andra metoder finns tillgängliga som är enklare och mer tidseffektiva.

Den andra delen behandlar modellerandet av viktiga vågutbredningsmiljöparametrar i en specialiserad modväxlande kammare kallad Scattered Field Chamber (SFC). Den tredimensionella fördelningen av infallande planvågor, planvågornas polarisation samt amplitudstatistik kan alla modelleras för att simulera en verklig utbredningsmiljö. Vi har använt oss av en skärmad, heldämpad (med avseende på elektromagnetiska vågreflektioner) låda som placeras i kammaren, i denna tas aperturer upp för att kontrollera planvågsinfallet. Dessa aperturer används också för att kontrollera polarisationen av de transmitterade vågorna. Slutligen används antenner som introducerar olika grad av direktvågor för att styra amplitudstatistiken för de infallande vågorna. Alla dessa tekniker är implementerbara på samma gång.

Acknowledgement

This work was realized through financial support and theoretical and practical knowledge from Flextronics in Linköping, Ericsson AB in Kumla, Kista and Mölndal, Sony Ericsson in Lund, Saab Dynamics in Karlskoga and FOI in Linköping. Thank you all for this support.

I would like to thank my supervisor Dag Stranneby for giving me the support I needed. I also want to thank my co-supervisor Mats Bäckström for valuable contacts, a lot of knowledge and feed back. Also thanks to Olof Lundén for his knowledge and help with a lot of measurements and ideas, Kent Madsén for being my everlasting partner in this work, Paul Hallbjörner for the discussions and his many good ideas, Kent Rosengren and Charlie Orlenius for discussions and companionship, Torleif Martin for help with numerical simulations and my wife Lena and Dan Roos for encouraging me to continue to my Ph.D. studies. Stefan Fransson, Boris Westerbacka, Thomas Bolin, Zhinong Ying, Staffan Kindgren, Jan-Erik Berg, Jonas Medbo and Patrik Svensén and all the others that I have met during courses and conferences, thanks for showing interest in my project and for supporting me.

Till Fabian, Tova, Agnes och Saga.

Preface

The work started back in 1997, first with some introductory measurements on a prototype based on an article by Arai and Urakawa [1] and later on as an internal project within Ericsson Mobile Communications in Kumla and Linköping. The intention of the project was to develop a new method for antenna testing on fully assembled cell phones in production. The test should be able to detect cell phones that, for some reason, were unable to communicate via the antenna and the air interface. This test was to be performed on every cell phone in the production line or at least on a sample basis from the line. Since the project was an internal Ericsson project the number of publications were few and the results were mostly kept within Ericsson for competitive reasons. In parallell with this project, the antenna research group at Chalmers, with Prof. Kildal, Ph.D. student Kent Rosengren and Charlie Orlenius as the main actors, started to work on developing the same method for antenna tests on communication terminals. Their excellent work have been published and successfully implemented in a practical measurement procedure for qualitative measurements on fully assembled and active cell phones in a Reverberation Chamber. This method is called TCP (Telephone Communication Power) and it is used in applied antenna research and for qualitative comparison of the radiation abilities of different cell phones placed close to a human head. Also the Helsinki University of Technology [2] have made work toghether with Nokia that examines the possibility to use the RC as a measurement tool for terminal antenna measurements. Other companies and institutions that have made experiments on cell phones inside an RC are for example ETS Lindgren and National Institute of Standards and Technology (NIST) in USA.

Chapter 1. Introduction

This chapter containes the background of the project together with a problem description. It also gives an introduction to channel modeling and Mean Effective Gain (MEG) measurements as well as a short description of the diversity and Multiple Input Multiple Output (MIMO) concepts.

1.1 Project background

The work behind this thesis can be divided into two parts, one that covers development of the Reverberation Chamber (RC) test method for cell phone antenna testing within production and one that covers the propagation environment modeling in a Scattered Field Chamber (SFC). The different parts are closely related and the main purpose is to show and verify the versatility of the Reverberation Chamber technology for antenna testing situations of many different kinds.

A mobile communication terminal such as, for instance, the cell phone is a portable device that communicates via the air interface with, most commonly, a stationary unit such as the base station. To be able to communicate, the device needs a transmitter and a receiver that is coupled to an antenna. The antenna creates energy that can propagate through the air from the conducted energy that is fed to the antenna via the transmission line, or in the receiver case the opposite, the antenna absorbs energy from the air and transform into conducted energy in a transmission line. The cell phones today include a lot of different systems for communication with other devices, this could be the GSM and/or UMTS (3G) system for ordinary speach transmission or data transmission and it can include the Bluetooth system for communication with headsets and computers. It is also possible to, for instance, receive FM radio, television and GPS signals for positioning by adding hardware to the phone to fit these systems. All these systems use different frequencies and they all need antennas that are suitable for each system and this means a lot of antennas and a lot of different transmitters and receivers. For every system there are guidlines and constraints that are supposed to be followed and to be able to find out if you can meet these constraints you must perform measurements on the device. The easiest way is to make conducted measurements but then you need to equip every system that is integrated in your device with a connection point and since connectors are large and expensive compared to the size and cost of the device this is not always possible. The only possibility that is left is to perform the test via the air interface with an active device. This is not just a problem but also a possibility to test the complete device (including the antenna) in the same mode as the final user would use it. The traditional antenna measurement facilities like the anechoic room or different kinds or near field ranges demands very expensive hardware and the test times, including set-up, is far from usable in high volume testing of devices. The high volume testing could be complete testing of all produced devices or tests on a sample basis from a production line. Also if more sophisticated antennas that include diversity (will be explained in section 1.2.1) and/or active antennas are implemented, the test results will be more dependent on the electromagnetic environment that is used in the test situation. The need to test the device in the same environment as the user environment becomes more and more significant. This is why the second part of this project was performed.

By the time of the early stages of this project the cell phones were tested in different stages during the production. The final tests were performed on fully assembled phones in custom made fixtures that were specialized to fit the different models that were produced. In these fixtures (shielded boxes) things like output power, receiver sensitivity, display characteristics, buttons and acoustics were tested to meet the constraints set by the GSM standard. The output power was measured conducted via an external connector and the antenna was, in this way, by-passed and not active during the measurements. The idea was to develop a new test method that could be implemented in these fixtures and be able to measure some of these characteristics via the air interface and in that way also include the antenna. This new method would also make it possible to get rid of the external connector that was costly and not wanted from a design perspective. This is why the first part of the project was performed.

The Reverberation Chamber technology has been known since at least the 1960’s [3] and a review of the technology is given in [4]. It has been developed as a measurement facility for measurements of the radiated emission and immunity of test objects. It is widely used within the defence as well as the EMC community and it’s theory is well established and confirmed both with theoretical work as well as measurements. The RC theory and the difference between an RC and a Scattered Field Chamber will be explained in Chapter 2 but the fundamental difference is that the RC has some properties like, it creates an statistically isotropic environment and the polarization of the plane waves are distributed according to a statistically uniform distribution over all possible directions. The statistical sense means, for instance, that the environment is isotropic when you consider the ensemble data for a large number of stirrer positions while the environment could be far from isotropic for a single stirrer position These are, as we pointed out, fundamental properties of a well functioning RC and if one (or some) of these properties is violated, the chamber is no more an RC. Therefore, the chamber in which we are to model the propagation environments, must be given a new name. The name that we have chosen was proposed by Paul Hallbjörner at Ericsson AB (former Ericsson Microwave Systems) in Mölndal, Sweden and the name is the Scattered Field Chamber (SFC). In this thesis the name RC will be used to denote the chamber when it comes to explaining theory and describing properties that are derived from RC theory. The name SFC will be used when measurements are presented and when experimental results are presented even though the chamber might work as an RC in some of these experiments.

1.2 Alternative channel models and measurement methods

In this part some other methods to simulate channels are described together with an overview of MEG and the existing methods to evaluate the MEG of mobile terminals. But first comes a short description of the diversity and MIMO concepts.

1.2.1 Explaining diversity and MIMO

The mobile propagation channel is affected by fading and because of this the signal strength of the communication can be very poor from time to time. The attenuation between the transmitter and receiver is however highly dependent on the antenna positions, the polarization of the antennas, the radiation patterns of the antennas and the time. Significant improvement of the received power can thus be obtained if a second antenna is introduced and the antenna with, at the moment, the lowest attenuation is used for communication. The second antenna must in every case be placed in another position or have another polarization etc. than the first one. This ensures that the two possible communication channels are uncorrelated and it is therefore very unlikely that they both have high attenuation at the same time instance. For instance figure 1 shows the correlation coefficient of two, equally polarized, antennas as the function of antenna separation. The function shown in figure 1 corresponds to equation 1 which is given in [5].

$$\rho = J_0^2\left(2\pi\frac{d}{\lambda}\right) \tag{1}$$

The improvement of average signal strength over time can be used to increase the data rate of the communication or to decrease the radiated power from the device. This technique is called antenna diversity and it can be used in either end or both ends of the communication. If antenna diversity is used in both ends and the number of antennas is increased the system is called a Multiple Input Multiple Output (MIMO) system. There are also many different ways to chose or combine the signals from the different antennas and they all give different gains compared to the original Single Input Single Output (SISO) system. Antenna diversity is already used in the base station antennas of European cell based communication systems and diversity in the cell phone is used in Japanese systems. In diversity concepts on mobile terminals the diversity is usually obtained through other methods than the pure antenna separation method since the wavelength of the signal is large in comparison with the size of the mobile terminal and thus it is hard to get uncorrelated signals with only antenna separation.

If we for instance have implemented antenna polarization diversity on the mobile terminal and we want to measure it's performance it is important to measure it in a real environment or in a good model of the real environment. The results would be quite different if it was to be measured in a traditional RC with it's uniformly distributed polarization

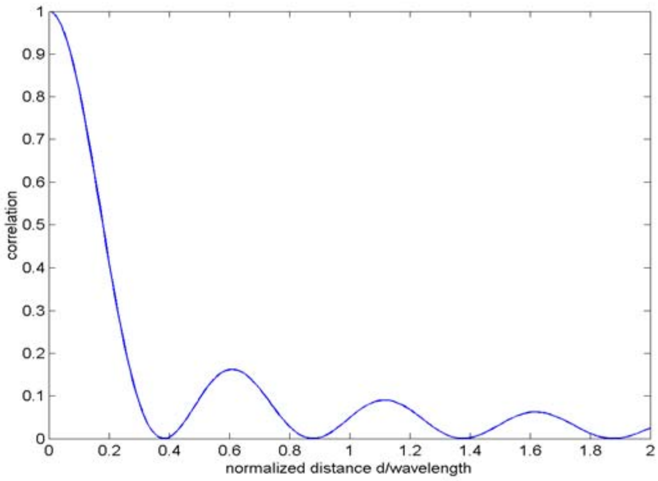

Figure 1. The correlation between two diversity antennas as a function of normalized separation distance d/λ.

than in the real environment that might have one strong, dominant polarization. Since antenna diversity is rising as a possible future technology to be used on cell phones and it is already used on other communication terminals, the need for a measurement tool is obvious. To measure objects in the real environment is tedious and in many cases it is also hard to get good repeatability since conditions like weather and surroundings might change from one measurement to an other.

1.2.2 Mean Effective Gain

The directional gain of an antenna is a measure of the directional properties and efficiency of the antenna [6]. The directional gain of a mobile terminal antenna can not be used to evaluate the effective gain when the terminal is used in a random multipath environment [7]. Another measure of the antenna performance has been proposed and this is the Mean Effective Gain (MEG). The MEG is obtained using equation 2 [7].

$$G_e = \frac{P_{rec}}{P_V + P_H} \tag{2}$$

Where P_{rec} is the mean received power of an antenna over a random route in the environment, P_V is the vertically polarized mean incident available power of an antenna when it is moved in a random route in the environment. Similary P_H is the horizontally polarized mean incident available power of the antenna. This gives that $P_V + P_H$ is the total mean incident available power of an antenna over the route and the MEG is thus the ratio between the mean received power in the antenna divided by the total mean incident available power that arrive at the antenna. It has been shown [8] that the effective gain of mobile terminal antennas strongly depends on the type of antennas and the propagation environments that they are used in. The MEG is directly proportional to the radiation efficiency of the antenna and it is also affected by the directional properties of the environment and the antenna as well as the polarization properties of both the antennas and the environment. This can easily be seen if we look at the expression for the mean received power as shown in equation 3 [9].

$$P_{rec} = \int_0^{2\pi}\int_0^{\pi}\{P_1 G_\theta(\theta,\phi)P_\theta(\theta,\phi) + P_2 G_\phi(\theta,\phi)P_\phi(\theta,\phi)\}\sin\theta d\theta d\phi \tag{3}$$

In this eqation P_1 and P_2 is the mean power received by an isotropic antenna with θ and ϕ polarization respectively. G_θ and G_ϕ are the θ and ϕ components of the antenna power gain pattern and P_θ and P_ϕ are the θ and ϕ components of the angular density functions of incoming plane waves. In [7] a theoretical model for evaluation of the MEG is proposed and it make use of the statistical distributions of the directional properties and the polarization properties of the environment. The model use uniformly distributed plane waves in the azimuth plane and a Gaussian distribution in the elevation plane. Separate distributions are used for the two polarization states and the model is able to predict the MEG of a half-wave dipole that is verified with measurements in an urban area. The MEG can according to equations 2 and 3 be measured or calculated theoretically from simulations. Section 1.2.4 will describe some of the possible measurement methods that are used today.

1.2.3 Channel models

Channel models are used to calculate link budgets and to estimate coverage areas in cellular mobile systems. There are not many examples of hardware channel models available in the litterature. Controlled scattering environments can be built to simulate a real scattering environment [10] [11] but these are usually large in size and/or make use of expensive anechioc chambers as the main building block. The reverberation chamber or the compact box [1] are examples of small and inexpensive channel models but these are restricted to model Rayleigh fading environments with isotropic plane wave incidence and thus have limitations when it comes to measurements of the MEG of terminal antennas. Nakagami-Rice fading play an important role in indoor wireless communication systems [12] and smart antennas (MIMO) make use of the directional properties of the channel and therefore spatial or directional channel models with changable fading properties must be used. There are a few examples of work that examines the possibility to change the propagation environment inside a RC [13]. Also [14] make use of two RC connected via a wave guide in order to simulate MIMO channels with keyholes and local scattering environments around transmitter and receiver.

Software models [15] used for computational evaluation are much more common. The models can be divided into different groups where the first group is the site specific models. To this group belongs models based on measurements and models based on ray tracing. The second group is the geometry based and correlation based stochastic models.

Some channel modeling approaches don't use the directional properties of the channel, in this case the measurements can be performed with just channel impulse response measurements at different positions. The impulse response can be measured with a channel sounder. To get the directional properties of the environment, the impulse response measurement can be combined with a directional antenna that is pointed in different directions to find the 3D directional channel properties. Another method where you don't have the dependency of the directional properties of the directive antenna is to use an antenna array for data collection. The array could be either a real antenna array with many antenna elements or a virtual array where one antenna is placed in many different positions to simulate an array. The virtual array can only be used when the channel is static with respect to the measurement time and the real array have drawbacks when it comes to mutual coupling between antenna elements. For geometry based model approaches the directional properties must be extracted from the impulse respones and this is usually made with methods like MUSIC [16], ESPRIT [17] and SAGE [18]. The ray tracing method uses geographical and material data of the surroundings to find the possible ray paths from the transmitter to the receiver. This will naturally give the directional properties of the channel directly since it is based on the propagating rays. This kind of models will be site specific since the geometry is based on deterministic scatterers.

More general models can be created with stochastic approaches like the geometry based stochastic channel model (GSCM). Here the scatterers are chosen stochastically according to some probability function. The impulse response is then found with a simplified ray tracing method. As an example the EGPROM model [19] uses measurement data to determine the statistical distribution of the scatterer parameters.

The software models can be combined with models of the terminal antennas (and the whole terminal) to find the overall behaviour of the terminal inside the environment. In this case the calculations are built on the antenna model and not the physical antenna itself. As pointed out by [20] the efficiency of printed antennas, often used in terminals, is very hard to predict with theoretical calculations. The feed network loss and the surface wave excitation will reduce the efficiency considerably and factors like surface roughness, tolerance effects and spurious radiation is also hard to account for in theoretical calculations. Measurements on the real antenna is often the only reliable way to find the efficiency of the antenna. Therefore it is often more reliable to measure the physical antenna than to rely on theoretical models and calculations.

1.2.4 MEG measurement methods [21]

As mentioned in section 1.2.2 the MEG of communication terminals can be both calculated theoretically and measured. The measurements can be performed on the terminal in the real environment but these kind of measurements are time consuming and hard to repeat due to the changing nature of the real environment. The MEG can also be evaluated with methods that are partly measured and partly calculated.

The Cost 273 Final report has made a summary of the different methods available to measure the radiated performance of communication terminals. In this summary the Reverberation Chamber (RC) method, the circular and spherical multi-probe systems and the controlled scattered field measurements are mentioned. The traditional Anechoic Chamber (AC) method with rotation of the test object can also be added to the list of available methods although it is not very practical. The RC method is well known and explained later on in this thesis. It’s limitations when it comes to MEG measurements lies in the fact that the environment is always isotropic with uniformly distributed polarization states of the plane waves. These are fundamental properties of a well functioning RC and they restrict the MEG measurement abilities of the RC. The other three methods are all performed in anechoic rooms and the only difference is the movement of the test object or the measurement array. In traditional AC measurements the test object must be rotated to find the 3D radiation pattern, this is very tedious and the measurement time for a full sphere measurement with an acceptable angular resolution can take several hours. In the circular multi-probe system the test object (or measurement array) must be rotated around one axis only. This will give shorter test times of about a few minutes. In the spherical multi-probe system it is not neccessary to roatate the test object nor the probes and a phase retieval network will make it possible to measure the complex radiated performance with a spectrum analyzer and thus it is possible to measure active mobile terminals without cable connections. All these methods measure the radiation pattern of the terminal and if the MEG is to be found, the measurements must be combined with calculations dealing with weighting factors of the desired environment. The controlled scattered field measurements make use of an anechoic chamber with scatterers placed inside to create multiple propagation inside, this method has possibilities when it comes to changing the 3D plane wave distribution (even though it isn’t mentioned) and also to some extent the polarization distribution.

1.3 Problem description

The first part of this thesis, the project regarding production test has the aim to investigate the possibility to use the Reverberation Chamber as a measurement tool in electronic production of cell phones. When the project was introduced the antenna function on the fully assembled cell phone was not tested at all and the antenna could, in practice, be disconnected from the rest of the components and still pass the final test. The final tests were made in a test fixture and conducted via an external connector that disconnected the antenna during the tests. Since the miniaturization and the design as well as the cost of each unit is very important the external antenna connector was about to disappear from future cell phone models and thus a new method to perform the final tests via the air interface must be invented. No specific constraints were set to be matched by the new method but the method should be able to detect if the phone radiates or not. The limitations in measurement time and accuracy was to be evaluated together with an investigation of the possible other limitations that were associated with the new method. In short this project aims at:

- Investigating the possibility to use the RC for final tests of radiation or no radiation of cell phones in electronic production.
- Find the limitations in measurement time and uncertainty of the RC method.
- Perform simple cable bound and active cell phone measurements inside the chamber in order to find other limitations of the test method.

The second part of the thesis, regarding the propagation environment modeling aims at showing how to create a hardware realized directional channel model (simulator) of different propagation environments inside the specialized Reverberation Chamber. The chamber, called Scattered Field Chamber (SFC), could then be used to measure the performance, for example the Mean Effective Gain, diversity gain and MIMO capacity of communication terminals in different environments. The propagation parameters: plane wave incidence, polarization, amplitude statistics and time delay is to be modeled in the chamber to fit measurement results from real environments. Even though the project aims at modeling all of these propagation parameters at the same time we have no illusions about being able to show exactly how to model every possible real environment in the chamber. This kind of work would include standardization of the different propagation environments and this is far beyond the scope of this thesis. As well as in the production test case no constraints were set on the modeling accuracy compared to real environments but the project was to show correlation of measurement results on communication terminals from the real environment and the model. In short this project aims at:

- Showing how to alter the propagation environment parameters plane wave incidence distribution, polarization, amplitude statistics and time delay profiles inside a Scattered Field Chamber.
- Inventing hardware realizations that are implementable all together.

- Showing correlation between measurement results (of for instance the MEG) for communication terminals in the model and in the real environment.

1.4 Method

This thesis is mainly built on experiments and measurement results and the interpretation of the outcome of these. Measurements have been performed in different Reverberation Chambers located at Flextronics in Linköping, FOI (Swedish Defence Research Agency) in Linköping and at Örebro University. In addition to these measurement facilities support and feed back has been given by Sony Ericsson in Lund, Ericsson AB in Kista and Gothenburg and by SAAB Bofors Dynamics in Karlskoga.

In all measurements some kind of Reverberation Chamber is used and also sometimes modified to fit the purpose of the measurements. A simple illustration of communication between two antennas in an RC is shown in figure 2. The used RC:s are of different sizes and they have stirrers of different types and therefore they will be more or less suitable as measurement facilities for different frequency ranges (see Chapter 2). Often the experiments start out on the smallest and also least expensive RC with some preliminary measurements and rough modifications that are supposed to act as indications of the probable measurement results. If more accurracy is needed we have carried out measurements in larger, more complex and expensive chambers to validate the results from the small chamber. These measurements also have the benefit of more sophisticated instrumentation. The measurements on passive, cable bound terminal antennas are usually performed with Network Analyzers for good measurement precision and control of the complex amplitudes, while the active measurements use spectrum analyzers to measure the power and base station simulators to control the terminal. Except the antennas under test we have used, mostly broadband horn antennas designed for the frequency range 800 MHz to 3GHz also in some case a logperiodic dipole antenna for approximately the same frequency range, as complementory antennas during the measurements. In the small chamber, WLAN antennas of patch type and self constructed dipole and monopole antennas have been used since the available space is more limited. These measurements are then restricted to a single frequency since the bandwidth of these antennas are much smaller compared to the bandwidth of the broadband horn or the logperiodic antenna.

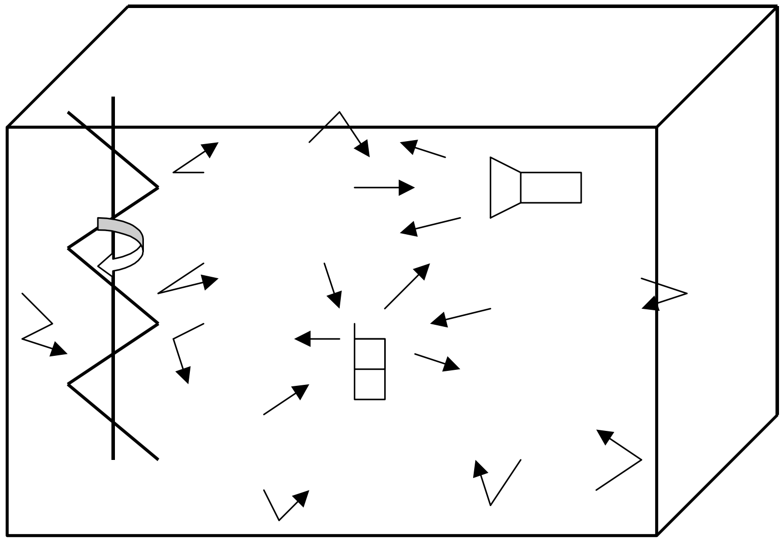

Figure 2. The communication between two antennas in a Reverberation Chamber – a multi-reflection environment.

In any case, the assumption that the unmodified chambers work properly as RC:s has been used (according to the theory given in Chapter 2). This means that we have assumed the chambers to be large enough to create complex over-moded cavities and have stirres that are efficient enough to create ensamble properties (for many independent stirrer positions) like isotropy, field uniformity and uniformly distributed polarization states. This will also make sure that the antenna reflection coefficient will be the same as in free space, again under the constraint that we consider the ensamle complex mean value. We have also assumed that the sometime (for some stirrer position) large absolute value of the antenna reflection coefficient doesn't affect the active terminal performance.

In some experiments some propagation parameter has been changed inside the chamber but we do not want to change the fundamental function of the chamber so we need to check if the chamber still works as an RC. In order to check if the chamber still works as an RC the Rayleigh distributed amplitudes or exponentially distributed power has been used as a ”figure of merit”. Therefore you will often find plots of the power or amplitude distribution compared to a theoretical distribution in the experiments and this is to check if the modifications did affect the fundamental function of the chamber. In almost every case the Rayleigh fading property is wanted in the chamber and if we have violated this property the chamber function is probably affected in an unwanted way and this is easily seen in these distribution plots. This ”figure of merit” should be seen as an engineering tool since the complete theory of the amplitude statistics of RC:s (or SFC:s) with non-isotropic plane wave incidence isn’t established yet. In the propagation environment modeling we have used small anechoic boxes with apertures and these are shielded boxes on the outside and their interior is covered with absorbing material, often planar material due to space limitations but in some case, when applicable, pyramidical absorbers have been used for better performance in sensitive directions. The assumption that these materials completely absorbs the energy that incident on the material is often used in our practical work but the non-ideal properties of these materials will ofcourse affect the measurement results. Many of the mechanical structures used are self constructed from cheap materials such as cardboard, copper tape and aluminium foil and because of this they are not optimized for maximum performance but rather considered as prototypes that are easy to modify.

1.5 Scientific contribution

The scientific contribution of this thesis is mainly from the second part regarding the propagation environment modeling. This work shows how to simulate and alter different propagation environment parameters to fit real propagation cases. By showing that these propagation paramenters can be altered in the chamber we show that there is reason to belive that a hardware directional channel model can be realized with a SFC. This chamber can for instace be used to measure the MEG of different antenna configurations on mobile terminals. It is important that the communication terminal is tested in a model of the real environment to obtain correct and relevant results. Especially when antenna diversity and MIMO are implemented the environment becomes more and more significant. Diversity concepts on cell phones will surely be implemented within a few years in European systems to increase the data rate or to reduce the output power used in the communication.

The first part that covers the development of the measurement method for production tests is very much applied and intended as an investigation of the possibility to use the method and find the limitations for this application.

In this chapter we have given the background of the project and we have given a description of the problem. We have also given an introduction to diversity and MIMO, Mean Effective Gain (MEG), channel modeling in general and to MEG measurements on communication terminals. Finally we gave a description of the method and scientific contribution of this thesis.

Chapter 2. The Reverberation Chamber and the Scattered Field Chamber

In this chapter we present the RC theory and we make a distinction between the RC and the SFC. We also point out some problems that might occur when we are using a small RC for antenna measurements. Finally we present some measurement results of antennas in the chamber and a comparison with results preformed with another measurement method.

2.1 Fundamental RC characteristics

The Reverberation Chamber (RC) is an electrically large (compared to the wavelength), shielded, resonant cavity equipped with some kind of mode stirring device. The cavity is usually rectangular in shape but variations might occour [22], in general, shapes that tend to create focuses of the waves like spherical or cylindrical is not so convenient since the fields inside the cavity should be statistically uniform within a large volume. This means that the mean value of the fields taken over a large number of stirrer positions will be the same independent of the position in the chamber, as long as you are more than half a wavelength [23] away from any mechanical structure in the chamber. The environment is also isotropic which means that the plane wave incidence towards a test object will be the same from any direction around the object. Every chamber has a lowest usable frequency and it is set by the size and complexity of the chamber and by the measurement uncertainty that could be accepted. The uncertainty springs from the statistics and is highly dependent on the mode density and the number of statistically independent resonant modes that could be excited by the stirrers inside the chamber. By optimizing the geometry of the chamber with respect to the mode density for a certain frequency the lowest usable frequency for the chamber could be decrased. Also introduction of diffusors that tends to create an even more complex geometry could decrease the lowest usable frequency [24][25] of the chamber but for the high frequencies these techniques seems useless. Even a wall that seems flat could have a irregularities that create a complex geometry for frequencies with short wavelengths [26]. The optimum stirrer design is also still not decided but investigations [27] show that a large diameter is to be preferred compared to a large hight. Paper E deals with a factor experiment that

Figure 3. The interior of the RC at Flextronics, Linköping Sweden. The picture is taken from a side with a removable side wall and the dual stirrers made out of cupper and the EMC-door (to the left).

examines how the number of uncorrelated samples is affected by changing the size and position of the stirrer and the chamber load. The results of the experiment show that the stirrer size clearly affects the number of possible uncorrelated samples, also the chamber Q-value has the same effect, a high Q-value gives more possible uncorrelated samples. The position of the stirrer did however not show any significant change in the number of uncorrelated samples. The same goes for all four of the possible interaction effects between the parameters, no significant change in the number of uncorrelated samples. Figure 3 shows the interior of a RC equipped with dual mode stirrers (one horizontal and one vertical).

2.2 RC mode theory

For a rectangular cavity with dimensions *a*, *b* and *d* the resonance frequencies are given by equation 4 [4].

$$f_{mnp} = \frac{c_0}{2}\sqrt{\left(\frac{m}{a}\right)^2 + \left(\frac{n}{b}\right)^2 + \left(\frac{p}{d}\right)^2} \tag{4}$$

The variables m, n and p are integers and at least two of them must be non-zero for a physical resonace to occur. The resonance with the lowest frequency is called the fundamental resonance. As the frequency in the cavity is increased the number of possible resonance modes increase and mode stirring is made possible through the mecanical stirrers that change the boundary conditions for the electromagnetic fields inside. The number of modes that can occur up to a frequency f is given by equation 5 [4] and the mode density at a certain frequency is given by equation 6 [4] where V is the chamber volume.

$$N = \frac{8\pi}{3}\cdot a \cdot b \cdot d \cdot \left(\frac{f}{c_0}\right)^3 - (a+b+d)\cdot\left(\frac{f}{c_0}\right) + \frac{1}{2} \tag{5}$$

$$\frac{dN}{df} = \frac{8\pi \cdot V}{{c_0}^3}\cdot f^2 \tag{6}$$

Equation 6 is valid when the frequency is far above the fundamental resonance frequency which means that the chamber is over-moded. To be able to calculate the number of simultaneously exited modes in the chamber we also need to know the chamber Q-value. The Q-value is usually estimated from measurements and both time domain measurements and power transmission measurements can be used. The Q-value is then estimated from equation 7 [4] or 8 [28] respectively.

$$\tau = \frac{Q}{\omega} \tag{7}$$

$$Q = \frac{16\pi^3 V}{\lambda^3}\left\langle \frac{P_r}{P_t} \right\rangle \tag{8}$$

The variable τ is the time constant of the chamber. When using equation 8 we need to compensate for antenna mismatch and antenna losses in the transmit and receive antennas. The number of simultaneously excited modes is then calculated from equation 9 [29].

$$N_s = \frac{8\pi V f^3}{c_0^3 Q} \tag{9}$$

The Q-value will determine the bandwidth of the resonance modes and therefore a small Q-value (loaded chamber) will give a large number of simultaneously excited modes in the chamber.

The motivation for doing the experiment in Paper E was to see if one could take advantage of this large number of simultaneously excited modes and, with an efficient stirrer, create a large number of independent samples. The results of Paper E clearly shows that a chamber with a low Q-value will produce a small number of independent samples and that no interaction effect between the stirrer size and the Q-value of the chamber can be seen. Obviously the large bandwidth of the modes will make it harder for the stirrer to shift the modes in and out of the chamber bandwidth and therefore a large movement of the stirrer is necessary to produce a new, statistically independent sample, leading to fewer possible independent samples over one stirrer revolution.

Since the chamber Q-value is proportional to the time constant, see equation 6, the Q-value will also determine how short pulses that can be used in the chamber.

2.3 RC statistics

Due to the complex nature of the RC all the chamber field theory is based on statistics. To be able to use the field theory for RC:s [28][29] one must be able to produce a large number of independent samples in the chamber. The theory is based on the assumption that we have an infinite number of independent mode structures in the chamber and if we are to use this theory we must be able to at least produce a large number of independent mode structures. How large will determine the uncertainty of the applied theory. It has been shown [23] that the uncertainty of the meanvalue of the received power by an antenna in the chamber is proportional to $\frac{1}{\sqrt{N}}$ where N is the number of independent samples created by the stirrers.

A simple method to determine the approximate number of independent samples that can be produced by the stirrer(s) is to use the autocorrelation function on the measurement data. By shifting the data in the measurement array and then examine the correlation coefficient between the shifted array and the original one can determine the number of shiftings that are necessary to produce uncorrelated arrays. The ”magical” number of the correlation coefficient that is used as a line between correlated and uncorrelated data is often set to $e^{-1} \approx 0.37$. This method is the most widely used but since uncorrelated is not always equivalent to statistically independent the method must be regarded as ”ad hoc” [4]. More complex but also more correct methods that use statistical Goodness of fit tests have been proposed [30].

The basic assumption in the statistical theory is that the electric and magnetic field components have normal distributed real and imaginary parts. The distribution of the amplitude of the fields will therefore be Chi distributed with 2 degrees of freedom (dof). The Chi distribution with 2 dof is also called the Rayleigh distribution and its probability density function is given by equation 10 [31]. The distribution of the phase will be uniform.

$$f(|E_s|) = \frac{|E_s|}{\sigma_N^2} e^{\frac{-|E_s|^2}{2\sigma_N^2}} \quad s = x, y, z \text{ (cartesian coordinates)} \tag{10}$$

In equation 10 σ_N is the standard deviation of the normal distributions of the real and imaginary parts. The mean value and the standard deviation of the Rayleigh distribution are given by equations 11 and 12 [31] respectively.

$$\text{mean value}(|E_s|) = \sigma_N \sqrt{\frac{\pi}{2}} \tag{11}$$

$$\sigma = \sigma_N \sqrt{2 - \frac{\pi}{2}} \tag{12}$$

The total field will be distributed according to the Chi distribution with 6 dof but more important is that the power will be distributed according to the Chi^2 distribution. One component of the power and also the power captured by any linearly polarized antenna in the chamber [28] will be distributed according to the Chi^2 distribution with 2 dof which is the same as the exponential distribution. The pdf of the exponential distribution is given by equation 13 [31].

$$f\left(|E_s|^2\right) = \frac{1}{2\sigma_N^2} e^{-\frac{|E_s|^2}{2\sigma_N^2}} \tag{13}$$

The mean value and the standard deviation are given by equations 14 and 15.

$$\text{mean value}\left(|E_s|^2\right) = 2\sigma_N^2 \tag{14}$$

$$\sigma = 2\sigma_N^2 \tag{15}$$

To examine if the data follows a certain distribution one can use statstical tests like Goodness of fit tests and Kolmogorov-Smirnov tests [32].

2.4 The Scattered Field Chamber (SFC)

The SFC is in principle a RC but to be able to model different propagation environments one might have to change some of the fundamental characteristics of the RC and therefore a new name has been introduced. Even if the measurements on fully assembled cell phones where to be done via the air interface it has been proposed [33][34] that cable bound measurements can be done directly on the antenna to characterize it. During the development of the measurement method this was also a way to limit the measurement uncertainties. Paper A deals with some problems that were discovered while doing these initial cable bound measurements and they are also summarized in the following sections 2.4.1 and 2.4.2.

2.4.1 Position dependence

When measuring the antenna reflection coefficient [35] in the chamber not only the reflection from the antenna port will be measured. Also the reflections from the chamber will, to some extent, be absorbed in the antenna and give a contribution to the reflection coefficient measured by, for instance, a Network analyzer. RC theory however give that the complex mean value of the reflection coefficient contribution from the chamber will be equal to zero for a large number of stirrer positions. This means that if the reflection coefficient is to be measured in the chamber, the mean value of the measured coefficient will give the reflection coefficient obtained in free space. The advantage is obvious since the RC is a controlled environment that is inexpensive to build and it is not affected by weather conditions or other surrounding disturbances. In Paper A an experiment was performed to examine the position dependence of the test object. According to RC theory there should be no dependence on the positioning of the test object as long as it is placed more than half a wavelength [23] from any mechanical structure in the chamber. In the experiment, the test object (antenna) was placed in 81 different locations in the chamber, all fulfilling the above mentioned criterion. The complex mean value of the reflection coefficient over a large number of stirrer positions was then calculated for every position and represented by a plus sign in figure 4. In figure 4 is also shown, as a square, the complex mean value of all these 81 complex mean values and the free space measured S_{11} represented by a circle. Figure 4 clearly shows that the mean value varies a lot between the different positions of the test object, however if the mean value of all the 81mean values is calculated it fits the free space measured S_{11} quite well. The conclusion to this must be that the chamber is a bit too small compared to the used frequency (GSM 900) and thus it doesn't work properly as a RC at these low frequencies. Movement of the object to deal with such a problem has been proposed [36].

2.4.2 Unstirred power

Paper A also deals some with the matter of unstirred power in the chamber. A more thorough investigation of the matter can be found in [37]. When measuring the transmission between two antennas in the chamber, for instance to find the radiated power from a device, and plotting the measured data in complex format it can look something like figure 5. If the chamber is well functioning as an RC the complex mean value of all the scattered waves should be zero and the average amplitude can be found as the average distance from the origin to the

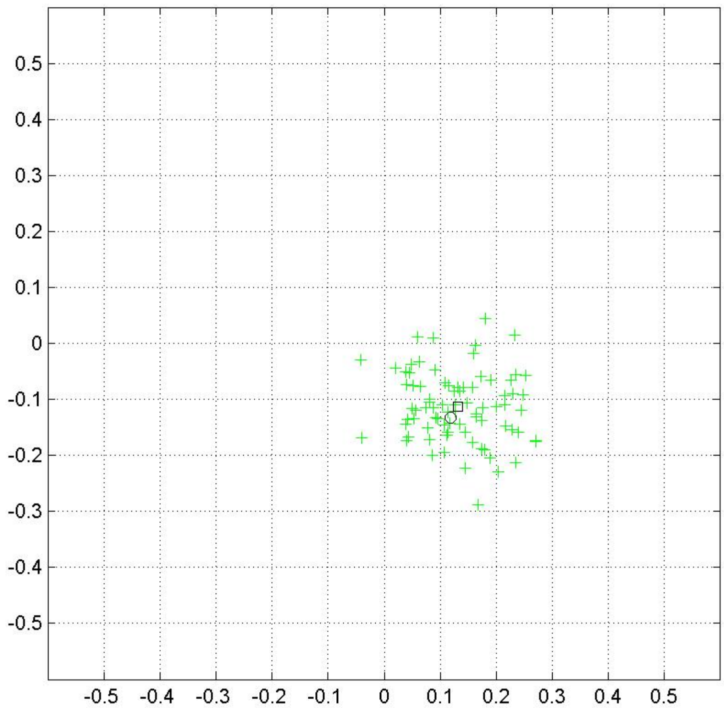

Figure 4. The mean values for the 81 different positions of the test object shown as plus signs. The mean value of these 81 mean values shown as a square and the measured free space S_{11} shown as a circle.

data samples. Figure 5, however, clearly shows an offset of the complex mean value. This offset can be interpreted as unstirred power or expressed in other terms, some direct propagation between the antennas. The larger the offset compared to the scattered amplitudes, the larger the amount of unstirred power. This unstirred power can be caused by inefficient stirrers, small or lossy chambers or even worse a combination of the above mentioned problems. If we for instance were to calculate the mean value of the amplitude of such data shown in figure 5, the calculated mean value would be completely wrong. The problem is however easy to solve since we only have to subtract the offset from every data sample and then recalculate the mean value of the amplitude. Only when we are measuring both amplitude and phase this kind of correction can be made, it is not possible to compensate for this

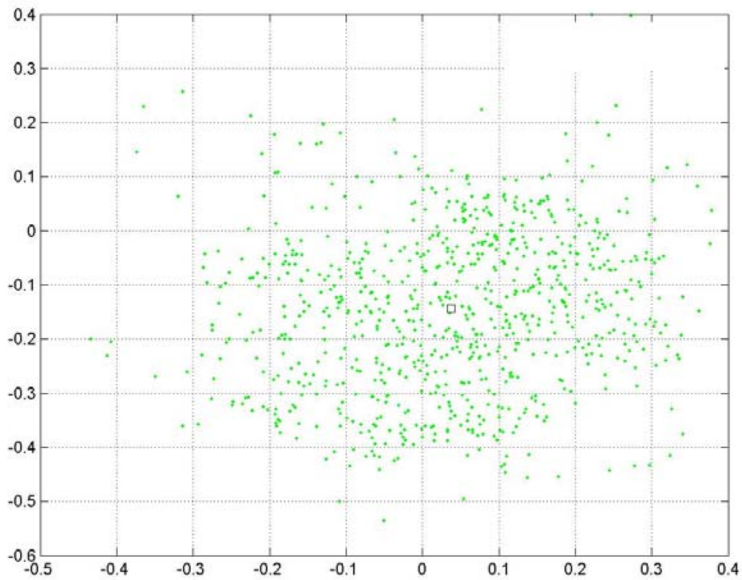

Figure 5. A complex plot of the transmission coefficient S_{12} between two antennas in the chamber. The unstirred power can be seen as an offset of the mean value.

kind of error when measuring only the amplitude. Later on in this thesis and in Paper H we will show how the unstirred power can be used to create environments with amplitude statistics according to other distributions than the Rayleigh distribution.

2.5 Production tests on active cell phones

Paper B shows some results from measurements on active cell phones inside a SFC. Figure 6 shows the measurement set up for an active measurement. The control channel antenna (CCA) is used to maintain the communication between the cell phone and the base station. For some stirrer positions the attenuation between two antennas in the chamber is very high (due to the fading), this can cause a disconnection of the active device due to the low signal strength. To reduce this fading effect the CCA is directed towards the cell phone and uses the recently described unstirred power to maintain a lowest signal level that exceeds

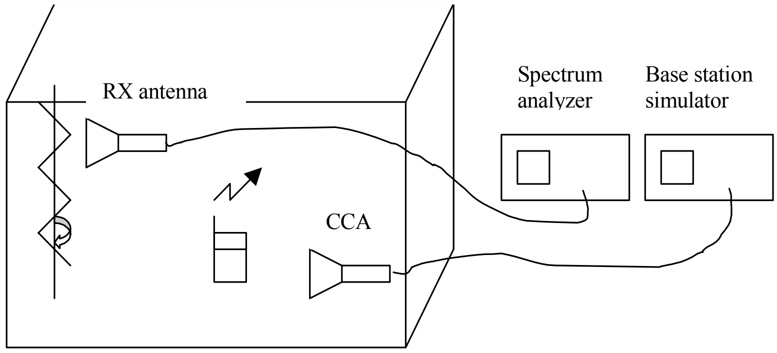

Figure 6. The measurement set up for active cell phone measurements. CCA is the Control Channel Antenna and it is directed towards the cell phone to reduce the fading and maintain the communication for every stirrer position.

the disconnection limit. The distance between the CCA and the cell phone antenna is dependent on the chamber Q-value and the stirrer efficiency, the higher Q-value and the better stirrer efficiency the shorter the distance must be to be able to use the effect of the unstirred power.

The relative radiated power of 4 different cell phones (T1-T4) was measured in the SFC. T1 was measured 30 times trying to keep the same conditions for all measurements except that the phone was taken out of the chamber and then replaced to the same position between every measurement. The phones T2-T4 were measured 10 times each and the results are shown in figure 7. The variation between the measurements can be explained with RC statistics. It has been shown [23] that the variation of the mean values between different measurements can be expressed as an interval of uncertainty according to equation 16.

$$d = 10 \cdot \log\left(\frac{1+\frac{k}{\sqrt{2N}}}{1-\frac{k}{\sqrt{2N}}}\right) \tag{16}$$

In equation 16 N is the number of independent samples obtained from the stirrer(s) and k is 1.96 for 95% confidence [32] given by the standard normal distribution. From measurements and estimation of the number of independent samples with the autocorrelation method we

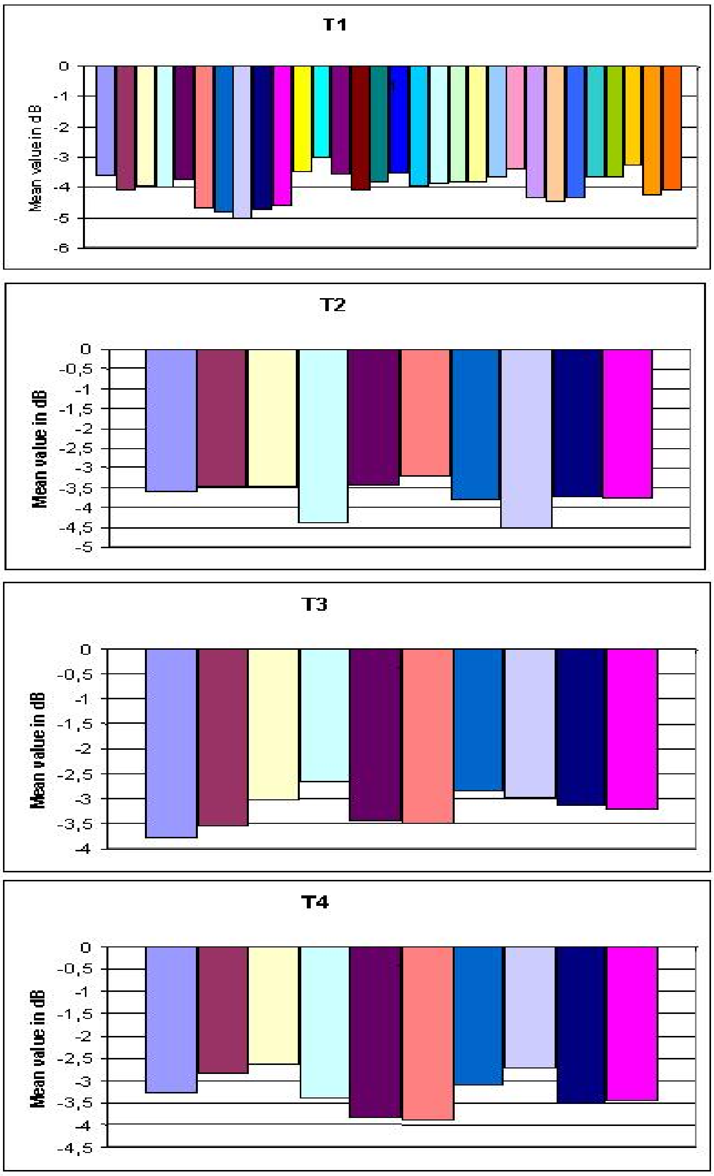

Figure 7. Relative radiated power of the cell phones T1-T4 measured in the SFC. The bars corresponds to the 30 or 10 different measurements carried out on the same phone.

estimated the number of N to be 100 for the given case. Equation 16 will give us an interval of uncertainty of 1.2 dB. This value seems reasonable if we look at the variation of the mean values in figure 7, some value lie outside the given estimated interval but this can both be natural due to the statistical nature of the interval or due to an over estimation of the number of N.

Two of the phones were also measured in an Anechoic Chamber (AC) and table 1 shows the comparison of the results between the two different measurement methods. Note that the values from the SFC is relative and the values from the AC is given as an absolute power level so the resemblance of the levels is only due to coincidence. Table 1 shows that both the AC measurements as well as the SFC measurements shows that the difference in radiated power between phone T1 and T4 is about 1 dB. A more thourough investigation of the correlation between different measurement facilities can be found in [38].

Phone	T1	T2	T3	T4
Mean 1-10	-4.3	-3.7	-3.3	-3.2
Mean 11-20	-3.7			
Mean 21-30	-3.9			
Mean total	-4.0	-3.7	-3.3	-3.2
TRP AC	-4 dBi			-3 dBi

Table 1. Comparison between measurements of the relative radiated power in the SFC and measurements of the Total Radiated Power (TRP) in an Anechoic Chamber (AC). Telephone T1 has been measured 30 times and telephones T2, T3 and T4 are measured 10 times. Only T1 and T4 are measured in the AC.

In this chapter we have described the RC theory. We have also described the problems with position dependence and unstirred power and how to deal with them when doing antenna measurements in a small RC. Finally we showed some measurement results that confirmed the theory of chamber measurement uncertainty and repeatability and a comparison with measurement results from an Anechoic Chamber antenna measurement.

Chapter 3. Propagation environment modeling

In this chapter we will present the propagation parameters that we want to model in the chamber. Then we will present experimental results showing how to model the parameters of interest and short discussions about the limitations of the modeling and ideas for further experiments.

3.1 Propagation parameters of interest

The received signal in an antenna can be expressed as a function of 5 parameters as shown in equation 17.

$$P_r = f(\theta, \phi, p, a, t, \varphi) \tag{17}$$

The parameters θ and ϕ represent the angle of incidence of the plane waves, p represents the polarization of the waves, a the amplitude, t the time and φ the phase angle of the plane waves. All these parameters affects the received power in the antenna and all parameters except time is of interest when measuring the antenna characteristics. Time is not an important parameter since all the antennas are passive devices that don't change characteristics with time. If future systems include something like time diversity it would also become a parameter of interest.

3.2 Measurements on real environments and parameter modeling

To be able to model different real environments we need to examine how the above mentioned parameters behave in the real environments. Measurements performed by Helsinki University of Technology and Ericsson AB has been our main sources of information. As mentioned in section 1.3 the intention is not to show exactly how to model a certain environment but to show how to alter the propagation parameters one by one and with hardware that is implementable all together. This will hopefully provide the readers with ideas and the tools needed to model the environment of their interest.

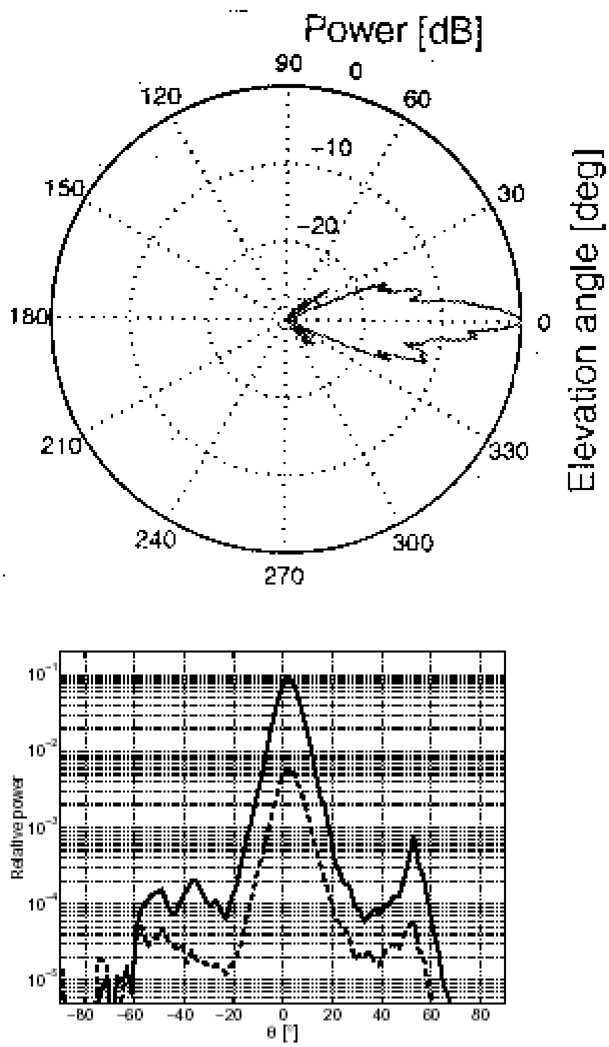

Figure 8. Measured power distribution in the elevation plane of two different environments, the above is an indoor office environment [40] at 5 GHz and the one below is an outdoor urban environment [39] at 2 GHz.

3.2.1 3D Plane wave distribution

The 3D incident plane wave distribution around the antenna is important because the antennas have radiation receiving patterns of different kinds. For instance an antenna that has a directive pattern in the vertical direction is quite worthless if placed in an environment with a plane wave distribution only in the horizontal plane. The test results would show something else if the antenna was tested in an isotropic environment like the RC. Even if small terminal antennas are not very directive they still have radiation patterns that differ from the isotropic (omni directional) antenna model. Measurements on real environments show that the 3D plane wave distribution can vary from almost omnidirectional in one plane to very directive in the other [39][40]. Especially indoor office environments can show very directive patterns when the waves are guided by the corridors and the doorways to enter an office. It seems that a common characteristic of many environments is that the distribution in the elevation plane is far from uniform but rather some kind of exponential decaying function of the elevation angle. Figure 8 [39][40] shows some examples of this.

The first efforts to alter the plane wave distribution in the chamber was made with single absorbing material plates as described in Paper B. This experiment was not so successful and the effect of the absorbing plates was quite poor but still visible. In Paper C new experiments were designed and this time the reduction of the plane waves was significant. Although the examples in figure 8 shows the plane wave distribution in elevation plane we have carried out all of our measurements in the azimuth plane. This is because of the more simple mechanical set-ups that you can achieve when measuring in the azimuth plane rather than the elevation plane. The results are however interchangable and only dependent on how you place the objects relative to each other inside the chamber. The pricipal setup is shown in figure 9 and we use a Schwartzbeck braodband horn antenna as the rotatable receiving antenna. The experiment measures the transmission coefficient between two antennas in a SFC with a Network Analyzer. The transmit and receive antennas are both broadband horn antennas that are directive with an approximate directivity of 7 dB for the used frequency 1000 MHz. The transmit antenna is pointed away from the receive antenna and directed at a stirrer to obtain the best possible mode stiring performance of the chamber. The receive antenna is placed on a rotatable platform and directed in different directions in the azimuth plane. Figure 10 and 11 shows the received power from different directions in the azimuth plane, absorbers are placed in the 0 and 180

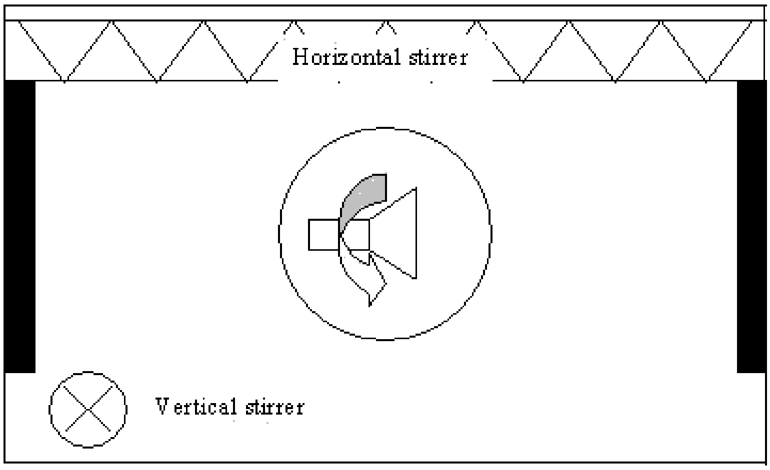

Figure 9. The measurement setup for received power in different directions. The black pieces are absorbing material and the chamber is seen in a cut from above.

degree directions in figure 11 and measurements are carried out for a large number of frequencies between 800 MHz and 3 GHz. The plot containes a lot of different frequencies and it is not important to see exactly how each frequency behaves. The imporatant thing is to see that the received power has a tendency to decrease in the direction of the absorber in figure 11 compared with the more random variations that you will find in figure 10. When you load the chamber with absorbers the Q-value will decrease and the chamber will become less efficient as a reverberation chamber. It is therefore important to examine the field's amplitude statistics to see if it still follows the Rayleigh distribution. Remember that the amplitude statistics (or power statistics) is our ”figure of merit” to see if the chamber still works properly even after the modifications. In this case the received power was compared to the exponential distribution. Figure 12 shows the visual comparison between the theoretical distributions and the measured distributions for the frequencies 1 GHz and 2.4 GHz. Clearly the absorbers are more critical, changing the power statistics, in the low frequency range since the chamber already is close to it's lower frequency limit and it is harder to acheive an over-moded cavity in the lower frequency region. From figure 11 we see that the variation of received power is not that large as in the real environments shown in figure 8. Paper D and F continues this work with the 3D power distributions and

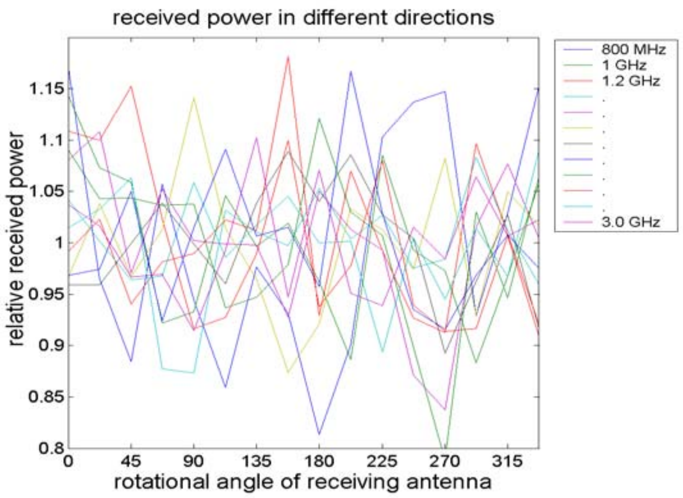

Figure 10. The received power from different angles in the azimuth plane, no absorber is present.

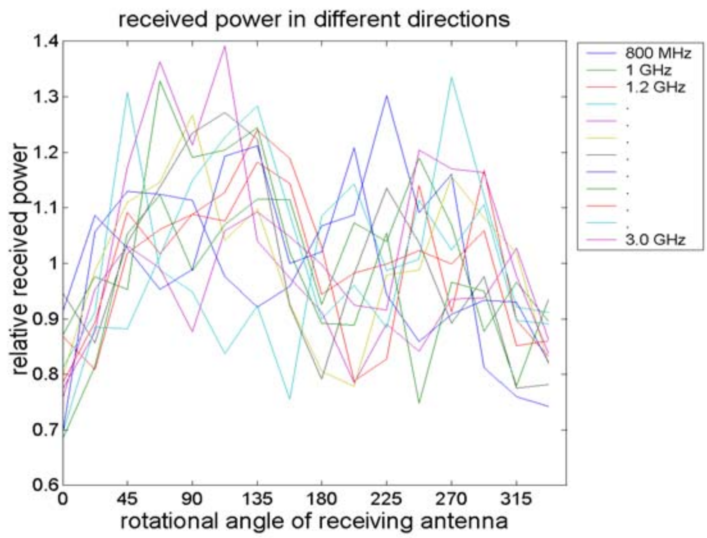

Figure 11. The received power from different angles in the azimuth plane, absorbing plates in the directions 0 and 180 degrees.

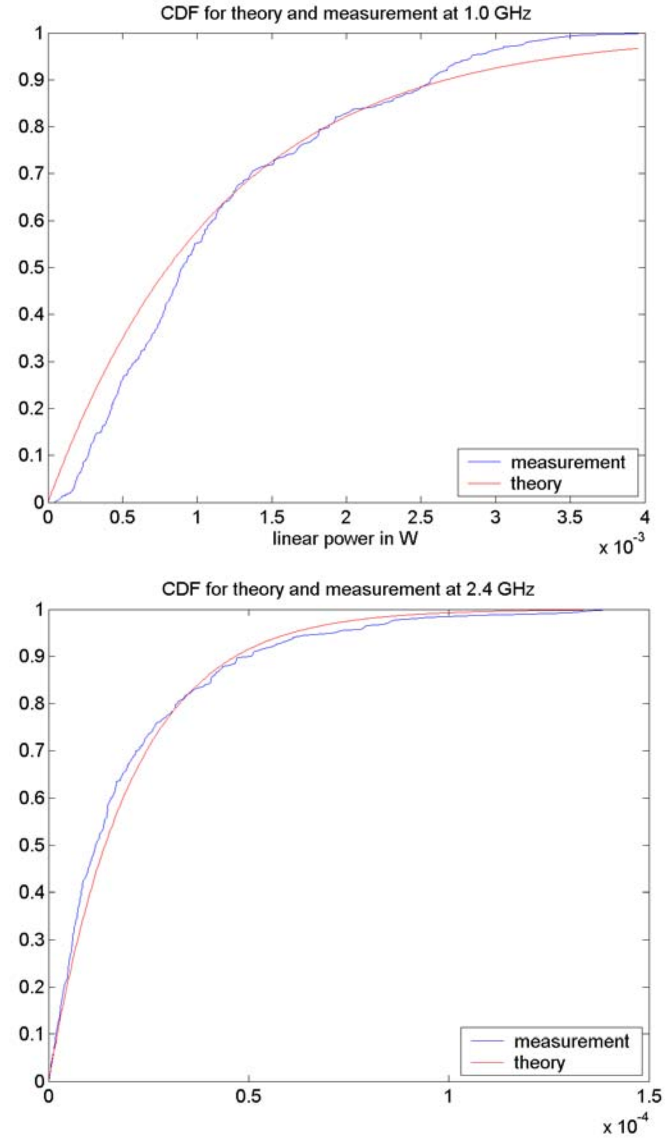

Figure 12. The received power statistics of the measurements compared to the best fit theoretical distributions.

this time an anechoic box with apertures is placed inside the chamber. This creates a larger variation in the received power and also the loading of the chamber is less severe since the anehoic box is shielded on the outside and only the aperture areas give large contributions to the loading of the chamber. Figure 13 shows a measurement set up and figure 14 some results of the received power distribution from a circular aperture. Again a broadband horn antenna was placed on a rotatable platform and the transmission coefficient was measured with a Network Analyzer. The transmit antenna was placed in the reverberation chamber and the receive antenna was placed inside the anechoic box (also placed inside the RC) as shown in figure 13. The aperture is in the 0 degree direction as shown in figure 14. Also this time the distribution of the received power was compared to the theoretical best fit exponential distribution to see if the transmitted waves into the anechoic box still follows Rayleigh distributed amplitudes. Figure 15 shows the results of the visual comparison and this time the logarithm of the power is plotted, this is to magnfy the lower end of the distribution which is the more important one when it comes to antenna diversity aspects.

The conclusion of these experiments must be that the 3D power distribution can be changed with the help of an anechoic chamber with aperture(s) that is placed inside the SFC. Also the field statistics of the received waves inside the box still shows good resemblance with theory, even in the lower tail of the distribution. In this case the RC acts as a generator of the Rayleigh distributed signals and the anehoic box, in which the terminal under test will be placed, with it's apertures will be the environment model. Apertures are placed in the directions of the incoming waves of the real environment and they are designed, according to aperture antenna theory, to create approximately the same beam shapes as in the real environment.

Paper F also shows that the antenna used to measure the received power will affect the measurement results, the lower the gain of the antenna the more under-estimated the directional properties of the aperture becomes. It might be possible to produce an even more directive pattern inside the anechoic box if, for instance, an antenna array is placed on the inside of the box and the array is fed from an aperture in the box. This is however not realized in any experiment so far. It should also be possible to measure the directional properties of the model in the same way as it is done in a real environment, the problem is the space limitations since the antenna arrays used to measure directional properties of real environments occupy large space and the models that we have built is so far small in comparison.

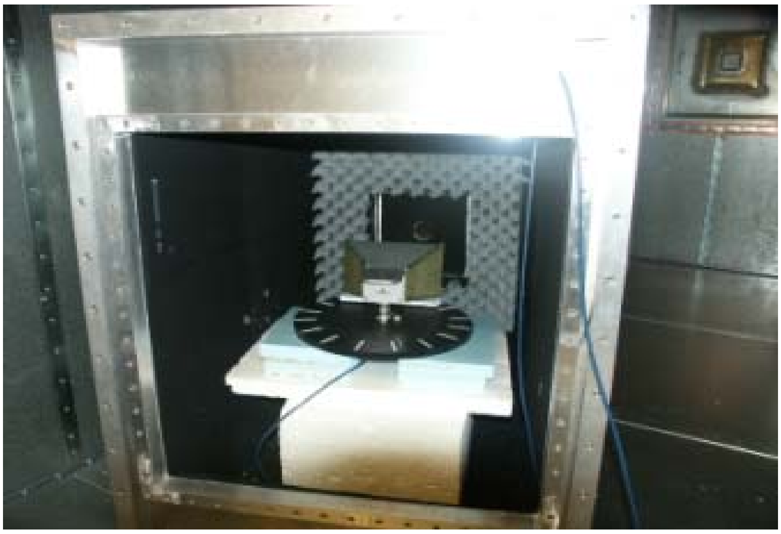

Figure 13. Measurement of the received power distribution from a circular aperture.

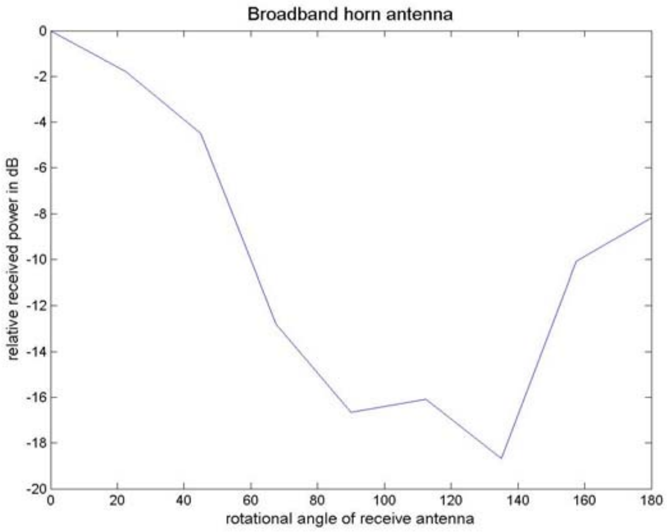

Figure 14. The received power distribution of the measurement shown in figure 10. Aperture in the 0 degree direction.

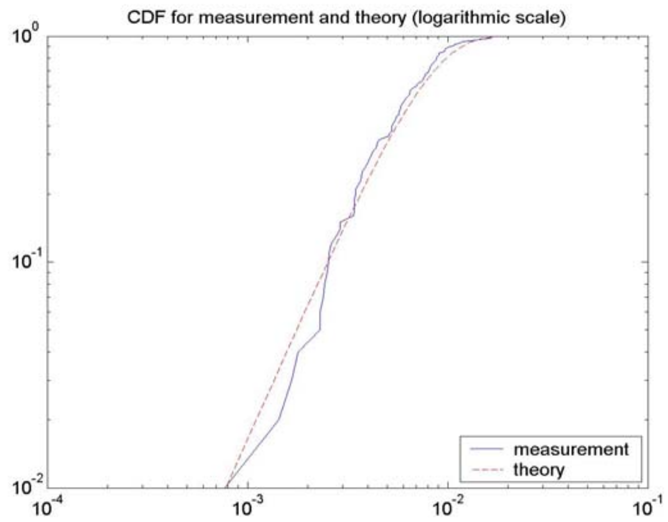

Figure 15. The statistical distribution of the received power inside the anechoic box. The scale is logarithmic to highlight the lower tail of the distribution.

3.2.2 Polarization

The polarization of the environment is also a factor that significantly will affect the MEG of a terminal. Measurement results from real environments often refer to the cross polarization ratio (XPR) and that is a ratio between the power that can be collected from waves having a certain desired polarization state (often the transmit antenna polarization) compared to the power that can be collected from waves with a polarization state orthogonal (cross polarized) to this desired polarization. Since the XPR can vary between different environments we also need to be able to vary the polarization distribution in the SFC. Measurements on real environements have shown [41] that the polarization state of the transmit antenna is preserved in many cases and most dominantly if the waves are guided by a street canyon or something similar. The RC creates a uniformly distributed polarization state of the plane waves inside. In order to linearize or at least create XPR that are unequal to 0 dB we use aperture design.

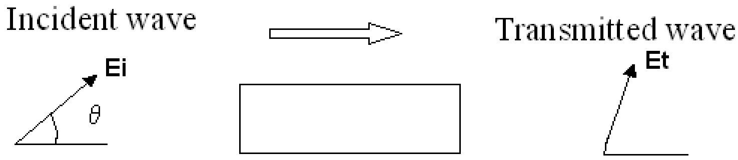

Figure 16. The case study for FDTD simulations of transmitted field through rectangular apertures.

Paper G covers the polarization modeling and also some very simple FDTD simulations to support measurements and the results are summarized below.

When we are using the apertures to control the plane wave incidence (as shown in section 3.2.1) we can also use the geometry of the apertures to control the polarization of the waves from that direction. The RC creates waves that are polarized with uniform distribution over all directions. When these waves are transmitted through an aperture the aperture will, due to it's geometry, act as a polarization filter. Simple FDTD calculations have been performed to see the polarization filtering effect of rectangular apertures of different dimensions. The principal case study is shown in Figure 16 and the idea is to let plane waves with polarization along an angle θ with respect to the horizontal x-axis, be transmitted through an aperture. The plane waves have frequencies between 1.8 and 2.0 GHz. The results from FDTD simulations and also from measurements show that waves that are polarized with an angle θ = 5° according to figure 16 will contain a larger proportion of vertically polarized waves when they have been transmitted through the aperture. For instance the aperture of size 15×125 mm will force the waves to have polarization angles in the interval 30-40° after passing through the aperture. The aperture of size 35×125 mm will produce waves that have polarization states in the angular interval 5-23° and 95% of these waves will be in the interval 5-14° and only 5% in the interval 14-23°. The same results are repeated for incident plane waves with polarization angle 45° and 85°. The thinner aperture will force the polarization to become more polarized than the wider aperture. This means that the waves are ”polarization filtered” by the aperture to have a larger proportion of vertically polarized field than the incident field, and the amount of ”filtration” is decided by the aperture thickness. From this and Paper G we can conclude that the wave polarization can be filtered by a simple rectangular aperture. The random polarization of the incoming plane waves, created by the RC, can possibly be linearized to fit a desired XPR for the transmitted waves. By adjustment of the height of the aperture the amount of linearization can be controlled. It might also be possible that some kind of polarization filter such as thin wires in one direction of the aperture can be used to reduce the amount of waves with polarization parallel to the wires. This is not yet realized in any real experiment. The results of the numerical simulations were also confirmed with some measurements presented in Paper G.

3.2.3 Amplitude statistics

As discussed in chapter 2.4.2 the unstirred power can be used to control the fields amplitude statistics in the chamber. It is well known that the amplitudes can follow Rayleigh statistics or Rice statistics depending on the amount of direct propagation that is present in the environment. The distribution will affect the MIMO channel characteristics and can be an important factor to model for MIMO measurements in the chamber. Paper H shows how to alter the statistics of the received amplitude by introducing more or less unstirred power in the chamber.

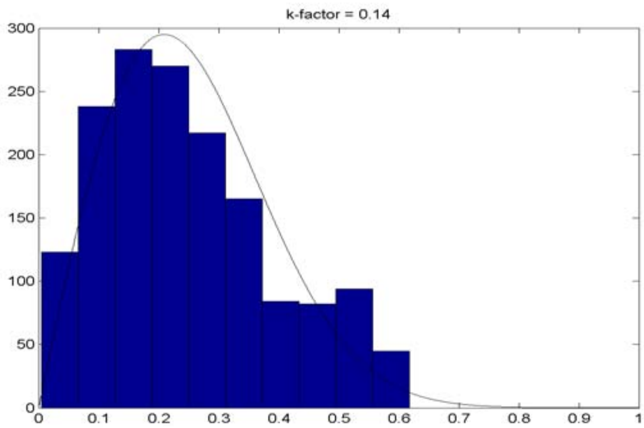

Figure 17. Sample histogram and estimated Rice distribution for antennas directed away from each other in the empty chamber.

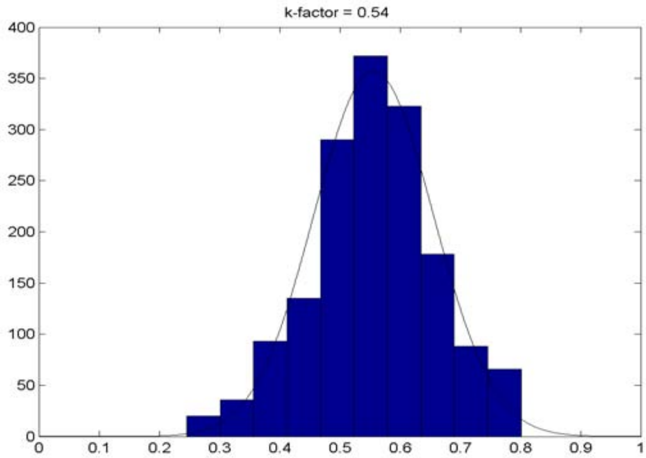

Figure 18. Sample histogram and estimated Rice distribution for antennas placed 7 cm apart directed towards each other and lined up to have the same direction of polarization.

For a well functioning RC the amplitude statistics follow the Rayleigh distribution, this has so far been our ”figure of merit” for a well functioning chamber. Real environments show amplitude statistics that range from Rayleigh distributed to different degrees of Rice distributions. The Rice distribution appears when there is one component that is dominant with respect to the others and one usually refer to a direct propagation path between the transmit and receive antenna. The Rayleigh distribution can be seen as a spezialized case of the Rice distribution with no dominant component present. The Rice and Rayleigh distributions describe the short term variations of the signal envelop around a mean value. The mean value it self is also affected by a long term variation due to the path loss between the transmitter and receiver and this variation can be described with a lognormal distribution [42]. Our modeling only consider the short term variation that can be described with the Rice distribution.

The experiment measures the transmission coefficient between two antennas with a Network Analyzer. The antennas are of patch type used for WLAN communications and their directivity is approximately 9 dBi according to the manufacturer. In the experiment the antennas are directed away from each other or pointed directly at each other and the distance between them is varied. Also the polarization of the two antennas are lined up in different ways to alter the amount of direct propagation between them. The distribution of the received amplitude is then examined for different positions and directions of the antennas and compared with a best fit Rice distribution. Figure 17 shows the distribution of the amplitudes when the antennas are directed away from each other. In this case the statistics should follow the Rayleigh distribution (according to RC theory) but this small chamber that is used in the experiment is not an ideal RC at the frequency used and it doesn't have a very efficient stirrer so the distribution will be Ricean with k-factor 0.14, which is at least close to a Rayleigh distribution. Figure 18 shows the amplitude distribution when the antennas are directed towards each other at a distance of 7 cm. This distribution is a Rice distribution with k-factor 0.54. Paper H shows that the antenna positions, directions as well as the total loading of the chamber affects the obtained distribution, also the antenna directivity will probably affect the results. Due to this the correct way to change the distribution must be decided from time to time, but on the other hand the fact that there are so many variables that affects the distribution will give a lot of freedom to construct a measurement case that suits the given constraints. We have been able to show that distributions that range from almost Rayleigh up to Rice distributions with k-factor 0.5 can be created in the SFC. These results show that there is reason to belive that any Rice distribution in this range can be modeled inside the SFC.

3.2.4 Time delay profiles

The relatively small size of the SFC will give much shorter delay times than many outdoor propagation environments. The chamber Q-value will affect the impulse response of the chamber and this could be a way of altering the time delay in the chamber. Some experiments have been performed where a part of the energy in the chamber is transmitted through a delay path and then inserted into the chamber again with an antenna. The measurement set-up is shown in figure 19. A pulse is created by the signal generator and fed into the chamber, this signal is also taken as a reference signal in the oscilloscope. Some part of the energy in the chamber is absorbed by the antennas below and transmitted through the delay line and then fed again into the chamber. The delay path is made out of long transmission lines and in our case the lines were coaxial lines that gave high loss and thus the need of an amplifier was neccessary. The amplifier gain was tuned to the loss of the cable but careful not to exceed it, otherwise the delay path would

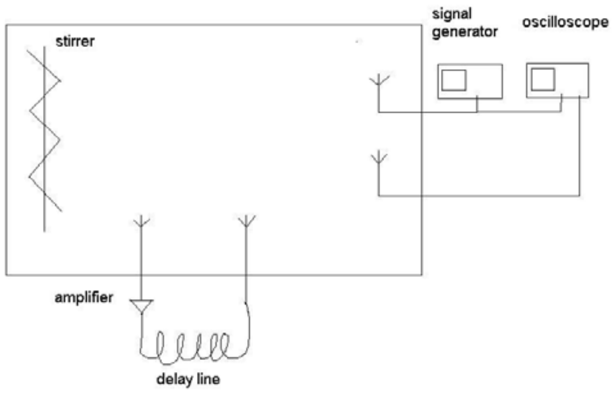

Figure 19. The measurement set-up for time delay measurements.

function as a gain loop and the input signal to the amplifier could increase unlimited until the amplifier burns. A better way is to use fiber optical cables with small losses but the hardware was not available for us. One can also imagine some kind of delay path into the ether and then reflected back from a large object into the chamber but this will also introduce large losses compared to the signals reflected only on the inside of the chamber. Another way is to use channel simulators to control the delay and even the amplitude and phase of the waves that are inserted into the chamber but this kind of equipment is very expensive.

It might also be possible to control the input power that is transmitted into the chamber with software and hardware to produce a certain time delay profile directly on the chamber input but again this will demand complex and expensive hardware. The experiment with the coaxial delay line did extend the time delay profile of the chamber and added some new ”taps” to the profile. These results are not yet published and the work has to be extended before this is done. As mentioned before in the thesis, the power delay profile of the environment doesn’t affect the antenna measurements since the antennas, at least this far, are passive devices that don’t change with time so the need to alter this variable is only for future technologies that might be introduced in mobile communication systems. The coherence time and doppler shift of real propagation environments might also be possible to simulate with variable stirrer speed and movement of the device under test respectively.

In this chapter we have shown ideas and measurement results on how to model the propagation parameters, plane wave angular distribution, polarization, amplitude statistics and time delay profile. Figure 20 shows an example of how the total setup for measurements on an active mobile terminal could look like. This setup measures the radiated power of a terminal in a certain environment and the terminal is placed inside the Anechoic box on a rotating platform to simulate movement in the environment.

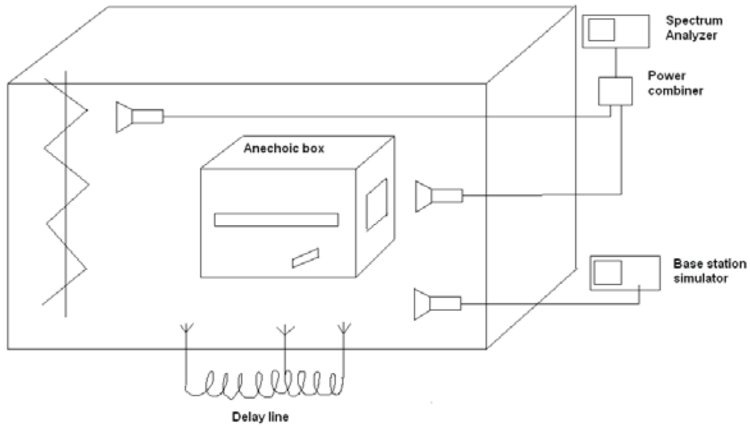

Figure 20. The suggested total setup of a measurement of the radiated power in a modeled environment. The terminal is placed on a rotating platform inside the Anechoic box.

Chapter 4. Conclusions

The conclusions will be divided into two parts, one that covers the production tests of cell phones and one that covers the environment modeling.

Production tests

This work shows that it is possible to use the RC (or SFC) to test cell phones in production, at least to test that the antenna connection is performed properly. The test time could be reduced into a couple of seconds and the tests could be performed on a sample basis or on every individual depending on the production rate. The test time will be dependent on the complexity and accurracy of the tests and if many functions are to be tested via the air interface the test time could significantly increase. For simple tests of radiation or no radiation the above mentioned test times could be accomplished however for this simple test it exists less complex test methods like for instance near field ”sniffing”. The more complex the tests become the more important it is to be able to control the matter of unstirred power and position dependence as described in this thesis. Factors like these will affect the measurement accurracy. All measurements presented in this thesis are relative measurements, for measurements of absolute levels the need for calibration is introduced. Chamber calibration with well specified sources and antennas can be performed. Figure 21 shows a suggested case for production line tests of cell phones, more than one phone can be tested simultaneously and energy leakage can be prevented through the quarter wave transmission lines of wave guide type on each side of the chamber.

Propagation environment modeling

If we are to compare the available methods to calculate or measure the Mean Effective Gain (MEG) of a mobile terminal we end up with completely different approaches. First we have the all software calculation approach where a model of the terminal is used to calculate the radiation pattern and this pattern is then combined with the weighting factors of the desired propagation environment to give the MEG. This method does not include the physical terminal at all and there are offcourse drawbacks with this. Second we have the methods

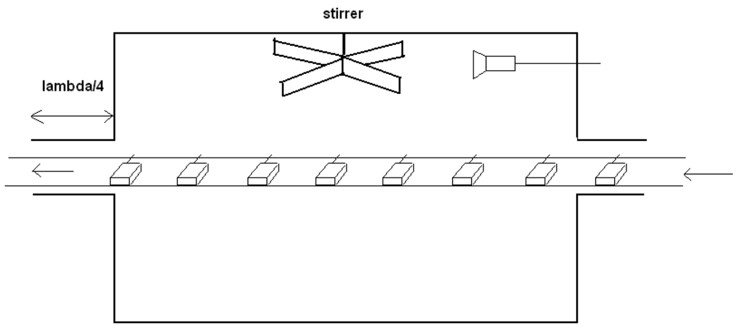

Figure 21. A suggested case for production line testing of cell phones. Several phones can be tested simultaneously and energy leakage is prevented by the quarter wave transmission lines in each end of the chamber.

that measure the radiation pattern of the terminal and then calculate the MEG with software. The measurement of the radiation pattern includes the use of expensive and large measurement facilities like near field probe ranges and/or anechoic rooms. The measurements are in most cases also quite time consuming and the need for nearfield to farfield transformations is also necessary in many cases. The third method is to measure the MEG directly in a hardware model like the SFC or in the real environment. Since the measurements in the real enviroenment is very time consuming and hard to repeat a good model that has good repeatability and short measurement times would be preferable. The SFC is basically an RC and this is an inexpensive and simple measurement facility that occupies a small volume compared with the other hardware methods. The measurement times are in the order of seconds or maybe a few minutes so the method is also fast compared to the others. It also provides the possibility to measure complete active communication terminals such as cell phones, Bluetooth units etc. without cable connection or modification. Measurements via the air interface on active units like these might be the only possibility since they often lack external connection possibilities and modification will affect the measurement results.

The work in the articles gatherd in this thesis show that it is possible to alter the important propagation parameters inside the SFC. It has been shown that the 3D plane wave distribution can be controlled with a shielded anechoic box that is placed inside a RC. The distribution of plane waves is then controlled with apertures in the anechoic box. The same apertures can be designed to control the polarization of the plane waves that is transmitted into the anechoic box. The field amplitude statistics can be altered with antennas that creates direct propagation (unstirred power) and give rise to different levels of Rice statistics. This technique is also implementable together with the others as shown in Paper H. An efficient way to alter the time delay profiles of the environment is however not yet invented. Some initial experiments have been performed but some hardware is missing for further experiments to be performed. The rapid changes in plane wave incidence shown in for instance indoor environements [40] have not been realized in the SFC. The measurements show that the apertures creates less directive environments, however it has been shown [43] that it isn't that important, for the measurement results of the MEG, to model the plane wave incidence very precise. It is more important to model the polarization distribution since it contributes a whole lot more to the measured MEG. This is not so hard to imagine since the terminal antennas tend to have almost omnidirectional (at least in one plane) radiation patterns but usually have a more precisely preferred polarization state.

Finally it would have been nice to make correlation studies between measurements in a real environment and measurements in the SFC model of the same environment. Unfortunately no feasible measurement data was available and no measurement equipment was available to make the neccessary measurements in a specific environment. We would have needed, for example, an outdoor measurement including all the discussed propagation parameters in an urban environment that was made recently and along a specific route. This was not available to us at the moment. Although we haven't been able to prove the resemblance between our model and a real environment we think that, by showing how to alter the important propagtion parameters we have reason to belive that a hardware directional propagation model can be created within the SFC.

References

[1] Arai, Urakawa, ”Radiation Power Measurement Using Compact Shield Box”, Proceedings of ISAP´96, Chiba Japan, (1996).
[2] Krogerus, ”Comparison of methods for measuring total radiated power and radiation efficiency of handset antennas” Master Thesis, Helsinki University of Technology, Espoo, Finland, 1999.
[3] Mendéz, ”A new approach to electromagnetic field-strength measurements in shielded enclosures” Wescon Technical Papers, Western Electronic show and Convention, Los Angeles, USA, 1968.
[4] Bäckström, Lundén, Kildal, ”Reverberation Chambers for EMC Susceptibility and Emission Analyses” URSI The Review of Radio Science 1999-2002, (2002).
[5] Ahlin, Zander, ”Principles of Wireless Communications” Studentlitteratur, 2 ed., ISBN 91-44-00762-0.
[6] Balanis, ”Antenna Theory – Analysis and design”, 2nd ed, John Wiley & Sons Inc., 1997, ISBN 0-471-59268-4.
[7] Taga, ”Analysis of mean effective gain of mobile antennas in land mobile radio environments”, IEEE Transactions on Vehicular Technology, Vol. 39, No. 2, 1990.
[8] Arai, Igi, Hanaoka, ”Antenna-gain measurement of handheld terminals at 900 MHz”, IEEE Transactions on Vehicular Technology, Vol. 46, 1997.
[9] Jakes, ”Microwave Mobile Communications”, New York, Wiley, 1974.
[10] Alayon Glazunov, ”Terminal antenna performance measurements in anechoic chamber with fictitious scatterers”, Cost 273, TD 02-143, 2002.
[11] Olsson, ”Test of smart antenna properties in a simulated scattered field environment”, RVK 02, Kista, Sweden, 2002.
[12] Karasawa, ”Multipath Propagation Theory and Modeling in Wideband Mobile Radio: The ETP Model, Connecting Propagation and Systems”, The Radio Science Bulletin, No. 302, 2002.
[13] Carlberg, Kildal, Wolfgang, Sotoudeh, Orlenius, ”Measurements with lossy objects in reverberation chambers and their effect on polarization and elevation dependence of the field statistics”, Nordic Antenna Symposium Antenn ’03, Kalmar, Sweden, 2003.
[14] Liénard, Degauque, Laly, ”Mode stirred chamber for simulating MIMO channels”, Cost 273 TD 04-024, 2004.
[15] Molisch, ”Modeling of Directional Wireless Propagation Channels” The Radio Science Bulletin, No. 302, 2002.

[16] Schmidt, ”Multiple Emitter Location and Signal Parameter Estimation”, IEEE Transactions on Antennas and Propagation, AP-34, 1986.
[17] Roy, Paulray, Kailath, ”ESPRIT – A Subspace Rotation Approach to Estimation of Parameters of Cissoids in Noice”, IEEE Transactions on Acoustics, Speech and Signal Processing 34, 1986.
[18] Fleury, Tschudin, Heddergott, Dahlhaus, Pedersen, ”Channel Parameter Estimation in Mobile Radio Environments using the SAGE Algorithm”, IEEE Journal of Selected Areas in Communications 17, 1999.
[19] Sánchez, Sánchez, ”EGPROM: An Empirical-Geometrical Propagation Model to Simulate Radio Wave Propagation and Diversity Reception”, Computer Applications in Engineering Education, Vol. 7, No. 2, 1999.
[20] Pozar, Kaufman, ”Comparison of Three Methods for the Measurement of Printed Antenna Efficiency”, IEEE Transactions on Antennas and Propagation, Vol.36, No. 1, 1998.
[21] Cost 273, Final report.
[22] Leferink, Boudenot, van Etten, ”Experimental Results Obtained in the Vibrating Intrinsic Reverberation Chamber”, IEEE EMC Europé Symposium 2000, Brügge Belgien, (2000).
[23] Kostas, Boverie, ”Statistical Model for a Mode-Stirred Chamber”, IEEE transactions on electromagnetic compatibility, vol. 33, (1991).
[24] Petirsch, Schwab, ”Investigation of the field uniformity of a mode stirred chamber using diffusors based on acoustic theory”, IEEE transactions on electromagnetic compatibility, vol. 41, (1999).
[25] Höijer, Andersson, Lundén, Bäckström, ”Numerical simulations as a tool for optimizing the geometrical design of reverberation chambers”, Proceedings of 2000 IEEE International Symposium on Electromagnetic Compatibility, Washington DC USA, (2000).
[26] Corona, Ladbury, ”Reverberation Chamber Research-Then and Now: A Review of Early Work and Comparison With Current Understanding”, IEEE transactions on Electromagnetic compatibility, vol. 44, (2002).
[27] Lundén, Bäckström, ”Predictions of stirrer Performence in Reverberation Chambers”, The 2003 Reverberation Chamber, Anechoic Chamber and OATS Users Meeting, Austin TX USA, April 2003.
[28] Hill, ”Electromagnetic Theory of Reverberation Chambers”, NIST Technical Note 1506, (1998).
[29] Lehman, ”A statistical theory of electromagnetic fields in complex cavities”, Interaction Notes, Note 494, (1993).

[30] Bäckström, Lundén, Wellander, ”Evaluation of Stirrer Efficiency in FOI Mode-Stirred Reverberation Chambers”, FOI Scientific Report FOI-R-0250-SE, ISSN 16501942, (2001).
[31] Kotz, Johnson, Read, ”Encyclopedia of statistical sciences”, Wiley-Interscience, ISBN 0 471 05546-8.
[32] Ross, ”Introduction to Probability and Statistics for Engineers and Scientists”, 2nd edition, Harcourt Academic Press, ISBN 0-12-598472-3.
[33] Rosengren, Kildal, Carlsson, Lundén, ”A new method to measure radiation efficiency of terminal antennas”, 2000 IEEE AP-S Conference on Antennas and Propagation for Wireless Communication, Waltham Massachusetts USA, November 2000.
[34] Kildal, Carlsson, Yang, ”Measurement of free-space impedances of small antennas in reverberation chambers”, Microwave and Optical Technology Letters, Vol. 32, No. 2, January 2002.
[35] Hallbjörner, ”Reflective antenna efficiency measurements in reverberation chambers”, Microwave and Optical Technology Letters, Vol. 30, No. 5, September 2001.
[36] Rosengren, Kildal, Carlsson, Carlsson, ”Characterization of antennas for mobile and wireless terminals by using reverberation chambers: improved accuracy by platform stirring”, Microwave and Optical Technology Letters, Vol. 30, No. 20, September 2001.
[37] Otterskog, ”Produktionstest av mobiltelefonantenner i modväxlande kammare”, Licentiatavhandling, Örebro Studies in Technology 7, 2002.
[38] Serafimov, Kildal, Bohlin, ”Comparison between radiation efficiencies of phone antennas and radiated power of mobile phones measured in anechoic chambers and reverberatin chamber”, Proc. IEEE Antennas and Propagation Society International Symposium, Vol. 2, San Antonio, TX, USA, 2002.
[39] Kalliola, Experimental analysis of multidimensional radio channels, Thesis for the degree of Doctor of science in Technology, Helsinki University of Technology, 2002.
[40] Medbo, Berg, Spatio-Temporal Channel Characteristics at 5 GHz in a Typical Office Environment, IEEE VTC Fall 2001
[41] Toeltsch, Laurila, Kalliola, Molisch, Vainikainen, Bonek, ”Statistical characterization of urban spatial radio channels”, IEEE Journal on selected areas in communications, Vol. 20, No. 3, p. 539-549, April 2002.
[42] Parsons, ”The mobile propagation channel”, 2nd ed., John Wiley & Sons Ltd, 2000, ISBN 0-471-98857-X.

[43] Alayon Glazunov, Pasalic, ”Comparison of MEG and TRPG of practical Antennas” IEEE Symposium on Personal, Indoor and Mobile Radio Communications, Barcelona, Spain, 2004.

Publications

Paper A. M. Otterskog, ”Antenna reflection coefficient measurements in a Scattered Field Chamber”, presented at The 2001 Reverberation Chamber, Anechoic Chamber and OATS Users Meeting, Bellevue Washington USA, (2001).

Paper B. M. Otterskog, K. Madsén”Cell phone performance testing and propagation environment modelling in a Reverberation Chamber”, presented at The 2003 Reverberation Chamber, Anechoic Chamber and OATS Users Meeting, Austin Texas USA, (2003).

Paper C. M. Otterskog, K. Madsén ”On creating a nonisotropic propagation environment inside a Scattered Field Chamber”, Microwave and Optical Technology Letters, vol. 43, no. 3, November 2004.

Paper D. M. Otterskog ”Environment simulations for MEG measurements inside reverberation chamber”, Cost 273, TD 05-017.

Paper E. M. Otterskog ”The influence of stirrer size and chamber load on the number of uncorrelated samples created in a reverberation chamber”, presented and published at IEEE EMC Zürich 2005.

Paper F. M. Otterskog ”Modelling of propagation environments inside a Scattered Field Chamber”, presented and published at the IEEE VTC Spring 2005, Stockholm.

Paper G. M. Otterskog ”Polarization control in a Scattered Field Chamber”, submitted to Microwave and optical technology letters.

Paper H. M. Otterskog ”Altering the amplitude statistics in a Scattered Field Chamber”, submitted to IEEE Transactions on Antennas and Propagation.

Antenna reflection-coefficient measurements in a Scattered Field Chamber

Magnus Otterskog (magnus.otterskog@tech.oru.se)
Institution of technology, Örebro University
S-701 82 Örebro, Sweden

Introduction

The Reverberating Chamber (RC) is since many years used for EMC-measurements. Lately the the interest for other applications of the RC has arised. One possible application is antenna efficiency measurements inside a RC. By doing antenna measurements inside a RC you loose the information of the directional properties of the antenna. This is a minor drawback especially when we are dealing with non-directional antennas as small terminal antennas with almost isotropic radiation patterns. The radiation efficiency of the antenna is a more interesting parameter and the RC could be a tool for measurements of this and other parameters of the antenna. The method of RC compared to traditional methods is, less time consuming than the 3D-pattern integration method and more practical than the Wheeler cap [1] method (lack of space, small bandwidth). Both developers and manufacturers of small terminal antennas could use the RC to test the efficiency of the antennas. Especially the electronic production industry is interested in a fast method for verification of the antenna function. For this purpose Ericsson Mobile Communications in Sweden has built a RC in order to evaluate the method of production testing of terminal antennas. Recently a part of the Ericsson Mobile Communications in Sweden became Flextronics International so the chamber is now at Flextronics in Linköping, Sweden. The chamber is designed to cover the frequencies from 800 MHz and upwards [2]. The dimensions of the chamber are (height × width × depth) 200 × 145 × 85 cm. The chamber is equipped with dual modestirrers, one horizontal and one vertical according to figure 1.

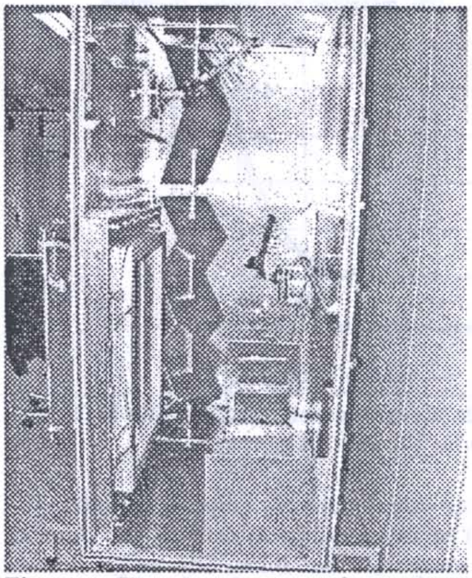

Figure 1: The chamber seen from the removable side wall.

The strirrers are non-symmetrical in order to produce as many different standing wave patterns as possible over one stirrer rotation. The chamber is also equipped with a removable side wall and an EMC-door. The hight of the chamber could also be decreased by a movable wall inside the chamber. We call this rather small RC a Scattered Field Chamber (SFC). We are also interested in creating different field distributions inside the chamber. It has been shown [3] in simulations that a field with more modes in azimuth-plane can be created with different dimensions of the chamber. This special non-isotropic field distribution is more like the multipropagation environment that we see in some environments in real life. One can also change the amount of direct wave between the antennas inside the chamber in order to create a special field distribution [4]. The statistical distribution of the electrical field could in this way be changed from Rayleigh to Rice to Gauss just by increasing the amount of direct propagation between the antennas.

The RC characteristics of the SFC

Measurements have been made to characterize the chamber. The field statistics has been compared with the ideal Chi^2-distribution. Since the lowest frequency used in the chamber is 800 MHz this is the frequency that is the most critical one. Figure 2 shows a compairson between the measured field statistics and the ideal Chi^2-distribution.

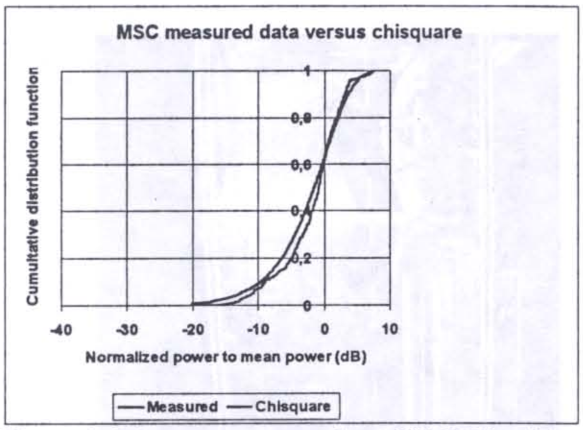

Figure 2: Measurements made at 800 MHz with logperiodic TX and RX antennas.

We placed two logperiodic dipole antennas (TX and RX) in two opposite corners of the chamber pointing away from each other. Still we get a rather poor fit between the measured and the theoretical curve and this could be explained by a direct propagation between the antennas. In order to minimize this direct propagation we placed a conducting sheet of foil between the antennas. The result of this is shown i figure 3. We also replaced the logperiodic TX antenna with a horn antenna. This was to reduce the backlobe of the TX antenna and by doing this also decrease the direct propagation between the antennas. The result of this is shown in figure 4.

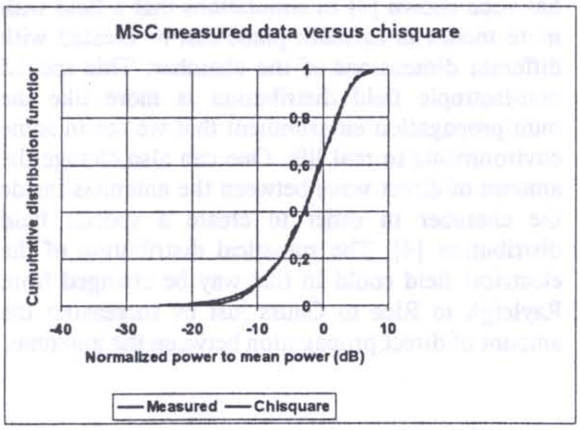

Figure 3: Measurements made at 800 MHz with logperiodic RX and TX antennas and a conducting foil to reduce direct propagation betwen the antennas.

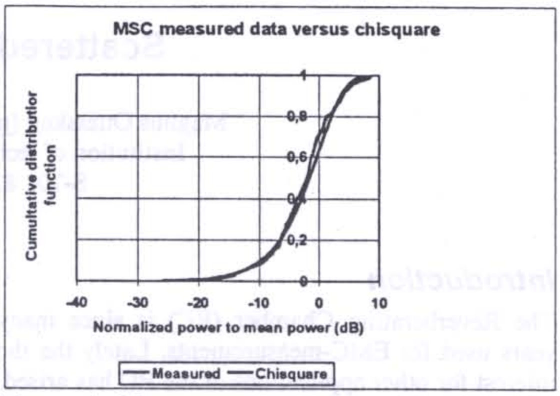

Figure 4: Measurements made at 800 MHz with horn TX antenna and logperiodic RX antenna.

Measurements of the complex S-parameters in the SFC

S11 measurements on a cellular phone antenna

Since our aim with this project is to measure antenna efficiency of a complete cellular phone inside the SFC we first need to investigate how the chamber affects the characteristics of the antenna. To do this we measure the complex reflection coefficient Γ, which is the same as S11, of the phone antenna. In order to measure the S11 we soldered a short semi-rigid cable to the antenna on a phone. Also, the phone is placed far away ($>\lambda$) from any wall or stirrer. Measurements of S11 were then made in free space and inside the chamber. The result of such a measurement is shown in figure 5.

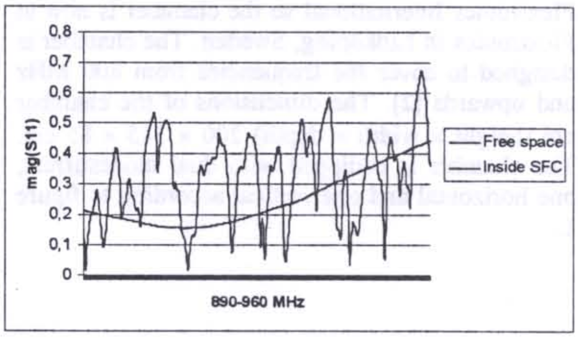

Figure 5: The magnitude of S11 in free space and inside the SFC for one position of the stirrers and over the frequency-band 890-960 MHz.

The random variation around the free space S11 is due to the random reflections from the chamber walls that add up constructively or destructively at the location of the phone antenna. However there is more to it than this. We know that the real and imaginary part of S11 both have a normal distribution. Calculating the mean value of the real and imaginary part of the complex S11 for 40 different stirrer locations and then produce the magnitude of S11 gives a curve shown in figure 6.

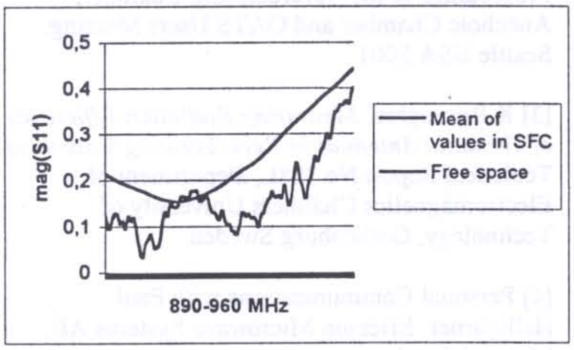

Figure 6: Comparson between the free space S11 and the mean of the S11 inside the SFC.

More information about the S11 can be obtained by looking at a plot in the complex plane. In figure 7 and 8 two plots (different frequencies) of the complex S11 is shown for different stirrer locations. Also the point for the free space S11 is shown for comparson.

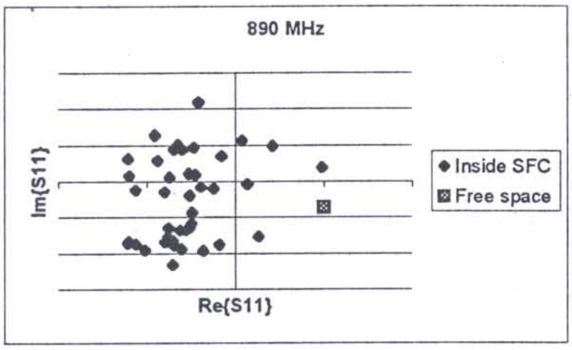

Figure 7: Complex comparison of S11 inside SFC and S11 in free space at 890 MHz.

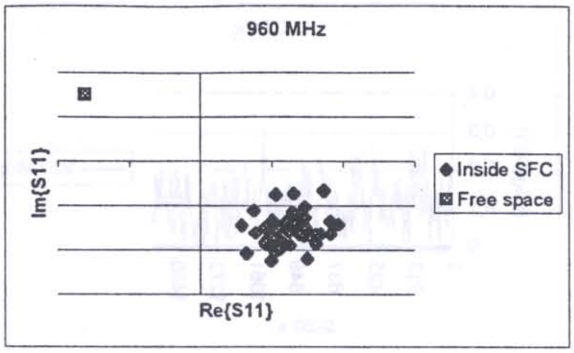

Figure 8: Complex comparison of S11 inside SFC and S11 in free space at 960 MHz.

From this we se that the difference between S11 in free space and inside the chamber is quite large even if the magnitude of S11 sometimes give another impression. The big difference of S11 can be explained by a possible direct propagation[5]. This means that there is some amount of unstirred energy that is reflected back into the antenna. This is not so hard to see since we are using a non-directive antenna it is hard to direct the enegy into a corner or on a stirrer. This means that some part of the energy will make a clear reflection at a side wall and come back unstirred at the location of the phone antenna. We have also examined the variance of S11 for different positions inside the chamber but so far we haven't found any simple dependence. There are still some problems that need to be solved in order to measure the free space reflection coefficient inside the SFC.

S21 measurements between a cellular phone and a receiving horn antenna

A phone is placed inside the chamber and the antenna is connected to a network analyzer via a short semi-rigid cable soldered to the antenna. The other port of the network analyzer is connected to a receiving horn antenna inside the chamber. The horn antenna is pointing towards a corner and a stirrer in order to minimize the direct propagation between the antennas. The horizontal stirrer is set to rotate with a speed of 20s/revolution and the vertical stirrer is set to rotate with a speed of 2.5s/rev. The network analyzer is set to a single sweep of 20 s. A typical measurement series is shown in figure 9.

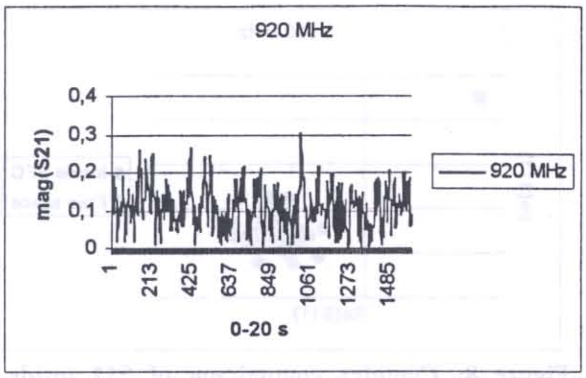

Figure 9: S21 measurements between phone antenna and horn inside SFC.

A complex plot of the S21 parameter gives additional information about the chamber functionality. As before we know that the real and imaginary parts of S21 both have a normal distribution this time with a meanvalue of 0.

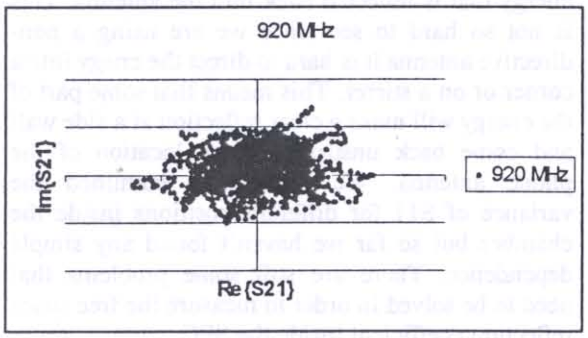

Figure 10:Complex plot of the S21 parameter.

The plot shows that there is no bias to the complex plot and this means that no significant direct propagation between the antennas is present.

Future and on-going work

The position dependence of the magnitude of S11 is to be further examined and also the peaks of the magnitude of S11 must be depressed in order to not disturb the function of the power control chip inside the phone. It has been shown [2] that by inserting absorption material inside the chamber the peaks of S11 can be lowered. More antenna efficiency measurements on phone antennas will be made and compared with measurements made with other methods as the 3D-pattern integration method.

References

[1] H.A.Wheeler, *The radiansphere Around a Small Antenna,* Proceedings of the IRE, Vol 47, August 1959

[2]K.Madsén, P.Hallbjörner, *Reverberating Chamber for Mobile Phone Antenna Tests,* Proceedings of the Reverberating Chamber, Anechoic Chamber and OATS Users Meeting, Seattle USA 2001

[3] K.Rosengren, *Measuring Radiation Efficiency of Terminal Antennas in Reverberating Chambers,* Technical Report No 388L, Department of Electromagnetics Chalmers University of Technology, Gothenburg Sweden

[4] Personal Communications with Paul Hallbjörner, Ericsson Microwave Systems AB, Mölndal Sweden

[5] P.Corona, G.Ferrara, M.Migliaccio, *Reverberating Chamber Electromagnetic Field in Precence of an Unstirred Component,* IEEE Transactions on Electromagnetic Compability, Vol-42, No 2, May 2000

Cell phone performance testing and propagation environment modelling in a Reverberation Chamber.

Magnus Otterskog, Örebro University, Sweden
Magnus.otterskog@tech.oru.se
Tel: +46 19303373 alt. +46 703693874

Kent Madsén, Flextronics International, Sweden
Kent.madsen@se.flextronics.com
Tel: +46 13321899

Abstract

Cellular phones are today more than just telephones without a cable. The cell phone producers are implementing more and more functions into the terminal and the test procedure becomes more and more complex and tedious. The decrease in size of the terminals makes galvanically coupled measurements impossible and the need for a measurement technique that measures via the air interface is obvious. Since the reverberation chamber, which has been used in the EMC society for decades, creates a field with the same statistical properties as the normal, theoretical, communication channel, it is natural to examine whether the chamber is useful as a tool for cell phone antenna measurements.

Cell phone performance testing

Measurements are made on active non-modified cell phones in order to measure the radiated power from the phone for a certain power level. A call is set up between the battery driven phone and a base station simulator. The phone is set to radiate at a certain power level and frequency channel. Avoid putting the power level to the maximum since the phone then becomes most sensible to high VSWR and low battery power. The measurement set up is shown in figure 1. Relative measurements of the radiated power from 4 different phone individuals are shown in figure 2. Phone T1 is measured in 30 measurement series and the other three is measured in 10 series each. The variation of the mean values between different series follows the theory for measurement uncertainty interval shown in [1].

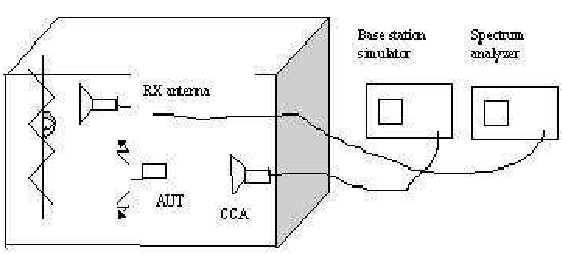

Figure1: Measurement set up for active phones. CCA is the Control Channel Antenna.

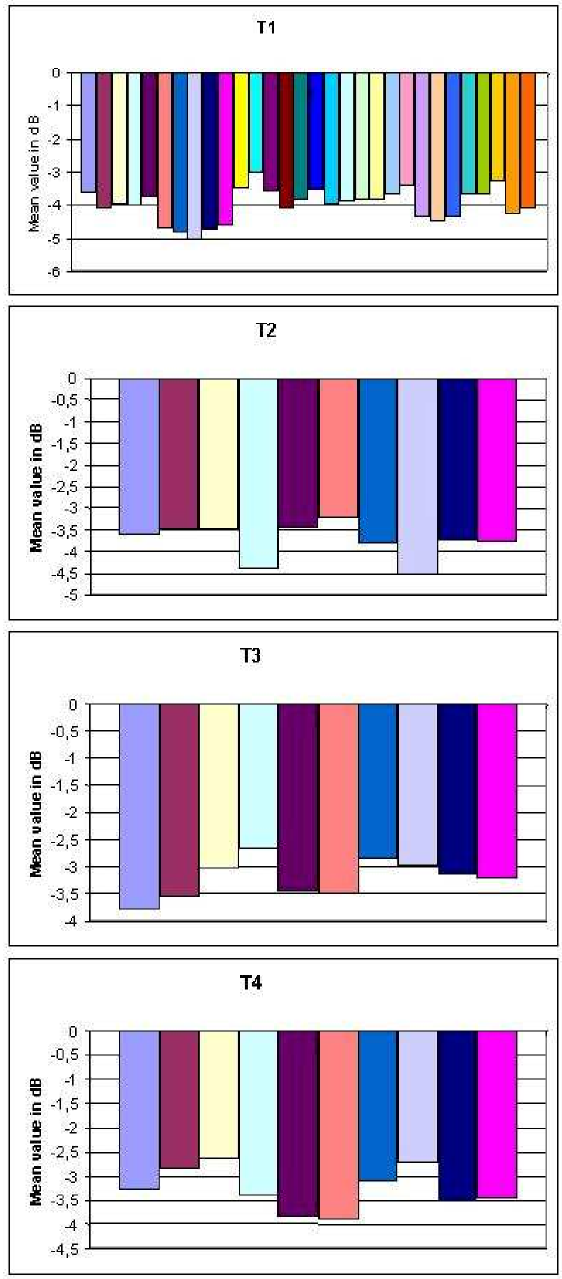

Figure 2: Relative radiated power from 4 different cell phone individuals.

The number of independent samples are estimated to 100 using the e^{-1} method and k is set to 1.96 which is valid for a confidence interval of 95%.

This gives an interval of uncertainty according to (1)[1].

$$d = 10 \cdot \log\left(\frac{1+\frac{k}{\sqrt{N}}}{1-\frac{k}{\sqrt{N}}}\right) = 1.7\,\mathrm{dB} \quad (1)$$

Two of the phone individuals have then been measured in an anechoic chamber and their Mean Effective Gain (MEG) has been computed. Table 1 shows comparison of the results from the two different methods.

Telephone	T1	T2	T3	T4
Mean 1-10	-4,3	-3,7	-3,3	-3,2
Mean 11-20	-3,7			
Mean 21-30	-3,9			
Mean total	-4,0	-3,7	-3,3	-3,2
MEG (Lund)	"-4 dBi			"-3 dBi

Table 1: Comparison of results from two different measurement methods, total radiated power (relative) measured in a Reverberation Chamber and Mean Effective Gain measured in an anechoic room.

Since the measurements made in the Reverberation Chamber is relative it is not useful to compare the absolute levels of the results (even though they, accidentally, show very good agreement). The interesting part is to see how well the ranking of the phones and the relative difference between them agrees between the two different methods.

Propagation environment modelling

In order to test the performance of a cell phone (or another communication terminal) in different propagation environments there is a need to change the environment inside the Reverberation Chamber (RC). The chamber in which the environment is altered from the ideal RC characteristics is called the Scattered Field Chamber (SFC). The SFC is shown in figure 3. So far the focus has been on changing the distribution of plane waves from the isotropic distribution to something else and on how to control the polarisation distribution inside the SFC.

Plane wave distribution

According to [2] each resonance mode can be represented by 8 plane waves. The ideal distribution of these plane waves in a RC is isotropic, however there are several real world propagation environments in which the distribution of plane waves is more concentrated along a certain plane and in order to model this it is desirable to change the distribution of plane waves inside the SFC. In [3] the plane wave isotropy is shown for a certain chamber geometry and it is also shown that the distribution of plane waves can be changed to have

Figure 3: The SFC at Flextronics, Sweden. Dimensions(height×width×depth) 2.0×0.8×1.45 m.

a larger concentration of waves in the azimuth plane by changing the dimensions of the chamber geometry. The problem with this (also shown in [3]) is that this change of geometry is frequency dependent. In order to have a less frequency dependent method we have inserted absorbing material into the chamber and tried to decrease the density of plane waves from certain directions. The chamber cross section (seen from above) with 6 measurement directions are shown in figure 4. Absorbing material is inserted at the right hand wall in order to decrease the density of plane waves from direction 2. The measurements are made with a horn antenna directed in the different directions and the mean (ensemble mean) value of the magnitude of S21 between the horn and a feeding antenna is measured with a network analyser. Figure 5 and 6 shows the ensemble mean of the magnitude of S21 for the 6 different directions for the unloaded case (without absorbing material) and for the loaded case.

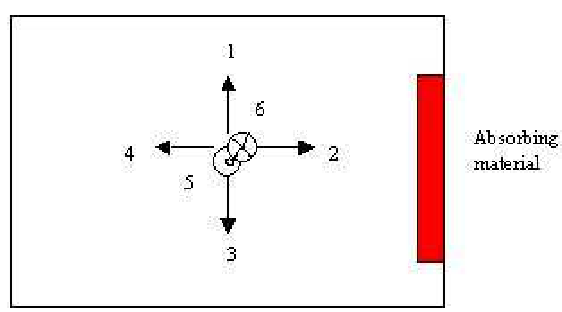

Figure 4: 6 different measurement directions and the location of the absorbing material.

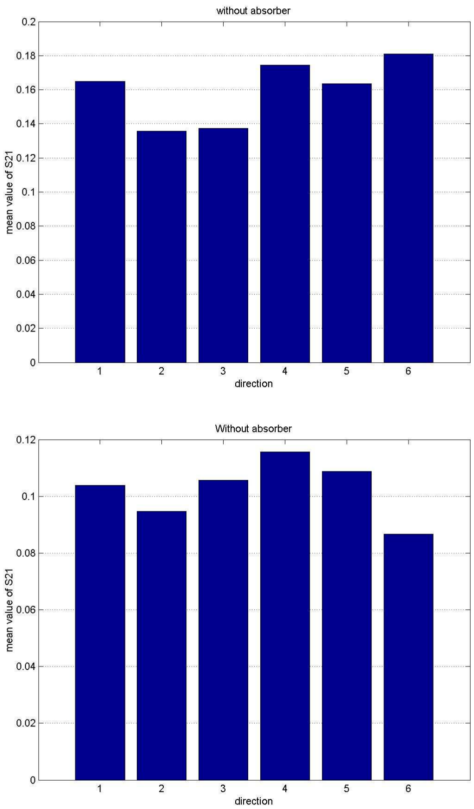

Figure 5: Ensemble mean of magnitude of S21 for the 6 different directions. The above diagram is for 900 MHz and the one below is for 1900 MHz.

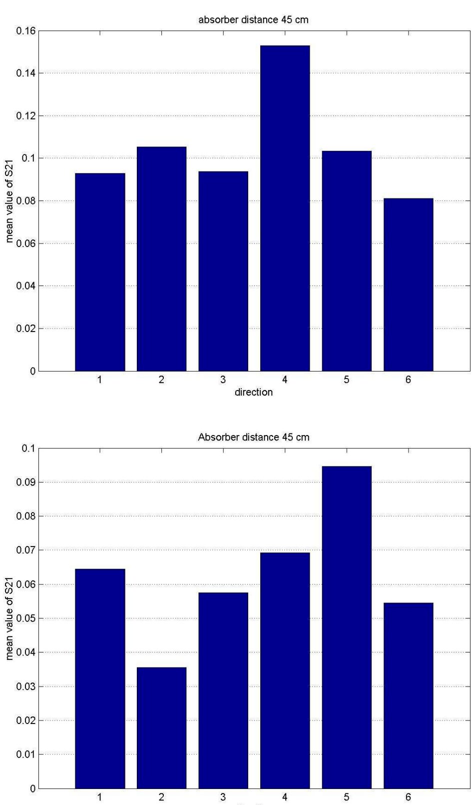

Figure 6: Same as figure 5 with absorbing material placed 45 cm from the measurement antenna.

One can see that the absorbing material clearly decrease the density of plane waves from direction 2 for 1900 MHz but the effect is not obvious for 900 MHz. Moving the antenna closer to the absorbing material will decrease the amount of plane waves from direction 2 as shown in figure 7.

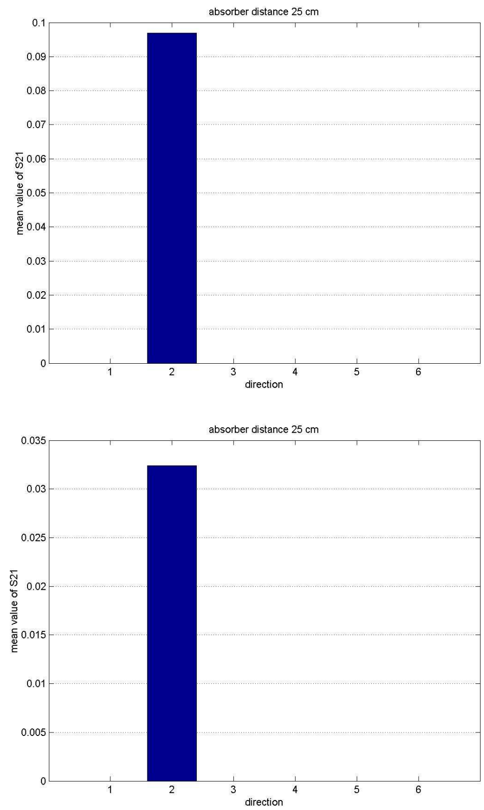

Figure 7: Same as figure 6 but with a distance of 25 cm to the absorbing material. Only direction 2 is measured.

Polarisation distribution

Assuming that we from the beginning had a uniform polarisation distribution i.e. an equal amount of waves polarised in the three polarisation directions *x*, *y* and *z*. The directions are shown in figure 8 as the cross section of the chamber seen from above.

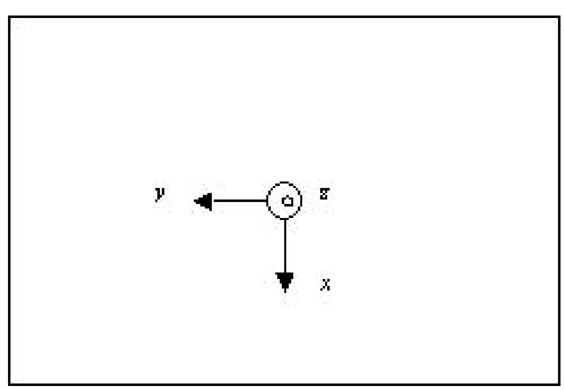

Figure 8: The polarisation directions.

In order to increase the amount of *y*-polarised waves we inserted sheets of aluminium foil hanging from the ceiling and oriented in the *xz*-plane. Measurements were made by rotating a linearly polarised horn antenna (0-180 degrees) in a plane, always pointing in the same direction in order to decrease the effect of a non-isotropic environment. A network analyser registered the ensemble average of the magnitude of S21 between the horn and a feed (log-periodic) antenna. The results from rotating the horn in the *xy*-plane and the *yz*-plane are shown in figures 9-10 respectively.

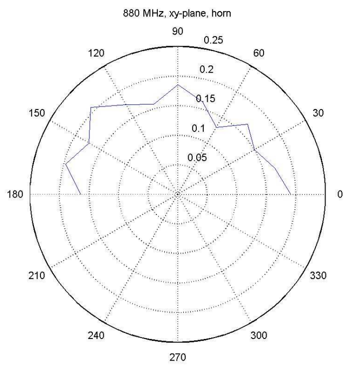

Figure 9: Rotating the horn antenna from 0 to 180 degrees with 15 degrees angle steps in the xy-plane. 0 degrees is in the x-direction and 90 degrees is in the y-direction. The radius shows the ensemble mean of the magnitude of S21. The frequency is set to 880MHz.

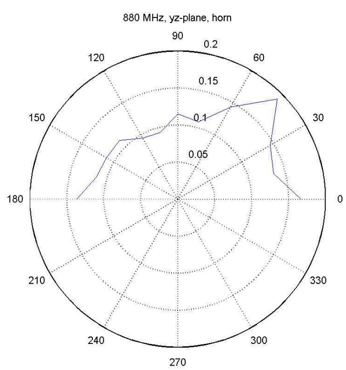

Figure 10: Rotating the horn antenna from 0 to 180 degrees with 15 degrees angle steps in the yz-plane. 0 degrees is in the z-direction and 90 degrees is in the y-direction. The radius shows the ensemble mean of the magnitude of S21. The frequency is set to 880MHz.

No significant effect on the amount of *y*-polarised waves can be seen from this experiment.

We have also examined the polarisation distribution of the empty chamber and the loaded chamber. The loading is made by covering the floor (*xy*-plane) with absorbing material. In this case the ensemble average of the field components *x*, *y* and *z* are measured with an isotropic 3-axis field probe with fibre-optic connection. The results are shown in figures 11-13 for the cases, linearly polarised feed antenna (horn) without and with loading of the chamber and circularly polarised feed antenna without loading of the chamber.

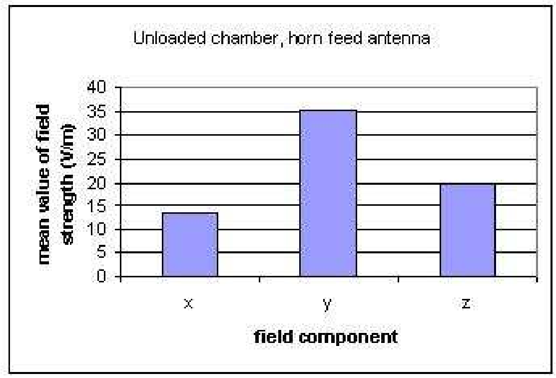

Figure 11: Ensemble average of field components.

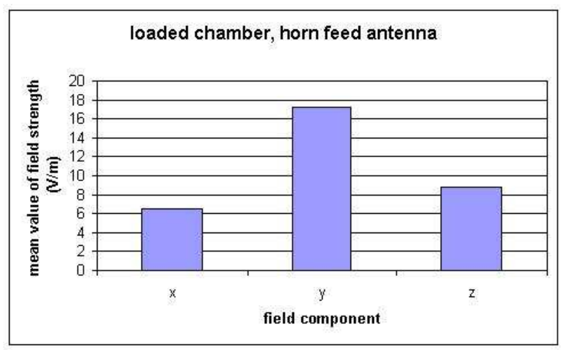

Figure 12: Ensemble average of field components.

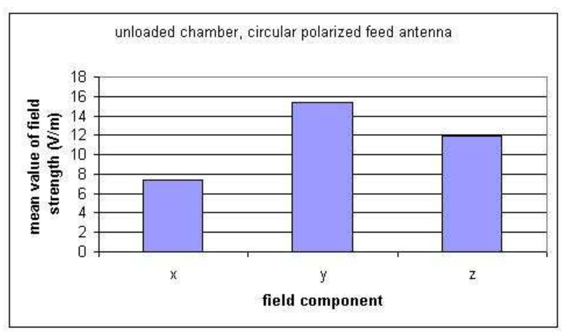

Figure 13: Ensemble average of field components.

This first experiment indicates that the assumption of a uniform polarisation distribution for the empty chamber must be regarded as untrue. Further investigations are needed.

Future work

Further investigations on the plane wave distribution and the polarisation distribution must be made. The aim is to model as many of the important propagation environment parameters as possible in the chamber and then to correlate measurements in the SFC with field trials of different phones in different propagation environments.

References

[1] Kostas, Boverie, ”Statistical Model for a Mode-Stirred Chamber”, IEEE transactions on electromagnetic compatibility, vol. 33, (1991).

[2] Hill, "Plane Wave Integral Representation for Fields in Reverberation Chambers", IEEE transactions on electromagnetic compatibility, vol. 40, (1998).

[3] Rosengren, Kildal, ”Study of distributions of modes and plane waves in reverberation chambers for characterization of antennas in multipath environment”, Microwave and optical technology letters, vol. 30, (2001).

REFERENCES

1. K.L. Wong, Compact and Broadband Microstrip Antennas, Wiley, New York, 2002, Ch. 7.
2. Z.N. Chen and M.Y.W. Chia, Broadband suspended probe-fed plate antenna with low cross-polarization levels, IEEE Trans Antennas Propagat 51 (2003), 345–346.
3. K.L. Wong and T.W. Chiou, Broadband dual-polarized patch antennas fed by capacitively coupled feed and slot-coupled feed, IEEE Trans Antennas Propagat 50 (2002), 346–351.
4. T.W. Chiou and K.L. Wong, Broadband dual-polarized single microstrip patch antenna with high isolation and low cross polarization, IEEE Trans Antennas Propagat 50 (2002), 399–401.
5. W.H. Hsu and K.L. Wong, A dual capacitively fed broadband patch antenna with reduced cross-polarization radiation, Microwave Opt Technol Lett 26 (2000), 169–171.
6. F.S. Chang and K.L. Wong, A broadband probe-fed patch antenna for a DCS base station, Microwave Opt Technol Lett 30 (2001), 341–343.
7. C.W. Su, F.S. Chang, and K.L. Wong, Broadband circularly polarized inverted-L patch antenna, Microwave Opt Technol Lett 38 (2003), 134–136.

ON CREATING A NONISOTROPIC PROPAGATION ENVIRONMENT INSIDE A SCATTERED FIELD CHAMBER

Magnus Otterskog and Kent Madsén
Department of Technology
Örebro University
SE-701 82 Örebro, Sweden
Flextronics Design
Box 1568
SE-581 15 Linköping, Sweden

Received 1 April 2004

ABSTRACT: *A traditional reverberation chamber creates a statistically isotropic test environment. Tests of communication devices may demand different environments to be able to test, for example, the influence of a diversity antenna. Here, a simple way of altering the distribution of plane waves incident on the device under test is presented.* © 2004 Wiley Periodicals, Inc. Microwave Opt Technol Lett 43: 192–195, 2004; Published online in Wiley InterScience (www.interscience.wiley.com). DOI 10.1002/mop.20417

Key words: *reverberation chamber; scattered field chamber; mode stirred chamber; propagation environment; nonisotropic*

INTRODUCTION

Traditional reverberation chambers are used today to create a Rayleigh fading-test environment for wireless-communication devices such as cellular phones. The amplitude of the incoming waves in a Rayleigh fading environment follows the Rayleigh distribution [1]:

$$f(|E_s|) = \frac{|E_s|}{\sigma_N^2} e^{\frac{-|E_s|^2}{2\sigma_N^2}}, \tag{1}$$

where $s = x$, y, or z. The test can, for instance, cover the radiated power [2] or the receiver sensitivity [3] of a device with or without the presence of an artificial human head. The reverberation chamber creates a statistically uniform distribution of plane waves that incident upon the device under test (DUT) [4]. This is an isotropic environment that does not always agree with the typical propagation environment of a communication channel. For example, in [5] measurements on real channels have been reported and it was found that an exponential distribution can describe the distribution of incident plane waves in the elevation plane. Also, in [6, 7], measurements on real channels were reported and the distribution of incident plane waves was found to be far from uniform (isotropic) in some environments.

Figure 1 Interior of the scattered field chamber (SFC). [Color figure can be viewed in the online issue, which is available at www.interscience.wiley.com.]

There is a growing interest in using diversity antennas on mobile communication terminals and also in multiple input, multiple output (MIMO) concepts for mobile communications. In order to examine the effect of diversity antennas placed on a device, one must test the device in the real environment or in a model of the real environment [8]. The first step towards this real test environment has been to create a nonisotropic environment in a specialized reverberation chamber called the scattered field chamber (SFC).

THE SCATTERED FIELD CHAMBER

The SFC used is located at Flextronics in Linköping, Sweden and its interior is shown in Figure 1. The chamber has dimensions $2.0 \times 1.45 \times 0.8$ m and is equipped with dual zigzag stirrers, one is horizontal and the other is vertical. The chamber is also equipped with a table made of Rohacell, which is a low-loss dielectric that can serve as support for the DUT.

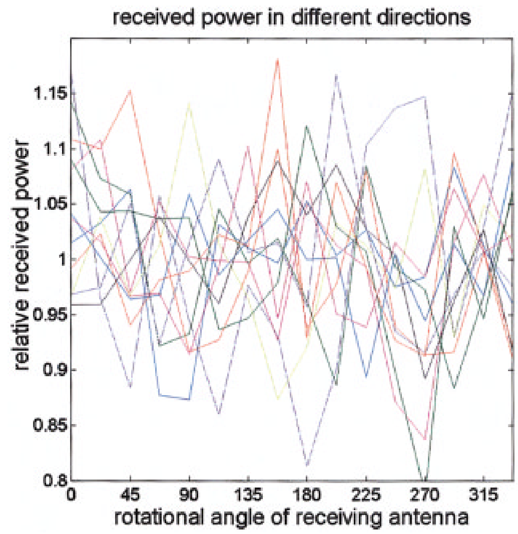

Figure 2 Relative received power as a function of rotational angle of the receiving antenna (the chamber has no absorbers inside). [Color figure can be viewed in the online issue, which is available at www.interscience.wiley.com.]

MEASUREMENTS

It has been shown that the isotropy can be changed with the help of absorbing material placed in the chamber [9]. We used this result to design our experiment, and the experimental set up was as follows. A broadband horn antenna was placed on a rotating platform on the horizontal dielectric table. A stationary log-periodic antenna, pointing away from the horn antenna, was placed in the chamber and the two antennas were connected to a network analyzer. The first measurement was made without any absorber placed in the chamber. The horn antenna was rotated 22.5° steps, resulting in 16 positions for a full turn. For every position, the mean value of P_r/P_t for 401 different stirrer positions was calculated. This was done for frequencies of 800 MHz up to 3 GHz in steps of 200 MHz. The result is shown in Figure 2 as the relative (relative-to-mean) received power as a function of the rotational angle of the horn antenna.

The next experiment was made with flat absorbers of size 61 × 61 cm placed on two opposite walls in the chamber, resulting in a distance between the opening of the horn antenna and the absorbers of 1 m. The reflective data of the absorbers is shown in Figure 3 [9]. The absorbers were placed in the directions 0° and 180°. The same experiment as before was repeated and the result is shown in Figure 4. As can be seen in the figure, the effect of the absorbers is clear: the received power and thus the number of incoming waves is reduced when the receiving horn antenna is pointed in the direction of the absorbers. According to [5, 6], the change of the received power in the different directions of a real environment is typically more than 20 dB. The amount of reduction in our model is not as large, just below 2-dB difference between max and min, so in order to increase the effect of the absorbers another measurement was done, this time with the absorbers closer to the receiving antenna. With the absorbers hanging via wires from the ceiling, at a distance of 0.2 m from the antenna opening, the same experiment was repeated. This time, only three frequencies were measured, but with reference to the previous experiments the effect is assumed to appear for every frequency in between the min and max frequency that is measured. The result is shown in Figure 5. This time, the effect has increased to between 3.8 and 5.5 dB, depending upon the frequency. The received power of the antenna

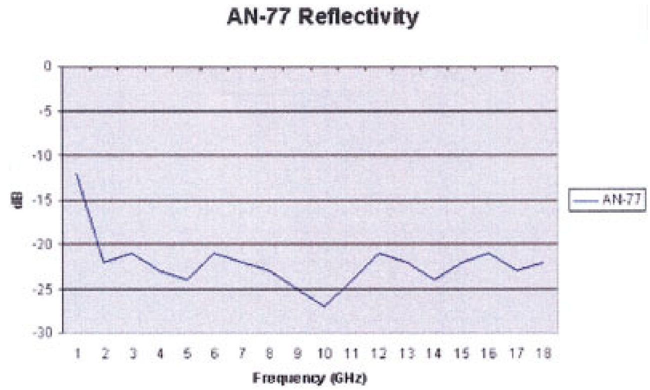

Figure 3 Reflective data of the absorbers used in the experiment. [Color figure can be viewed in the online issue, which is available at www.interscience.wiley.com.]

in a Rayleigh fading environment will follow the exponential distribution [10].

In order to examine the distribution of the received power in our horn antenna, the theoretical distribution is compared with the distribution of the measured data for the frequencies 1, 1.8, and 2.4 GHz when the horn antenna is placed close (0.2 m) to the absorber. The comparisons are shown in Figures 6–8, where the statistics are shown for the cases when the antenna is pointed towards the absorber. As a reference, the distribution for the empty (unloaded) chamber at 1.0 GHz is shown in Figure 9. As can be seen, the agreement with the theoretical distribution is quite poor for the low frequencies and in future work we need to be careful with the loading of the chamber in the low-frequency range in order to still fulfill the criterion of a Rayleigh fading environment. The statistics do not change if we point the antenna away from the absorber; thus, we conclude that it is the total loading of the chamber that will give the poor agreement, rather than the fact that the antenna is placed with its opening close to an absorber.

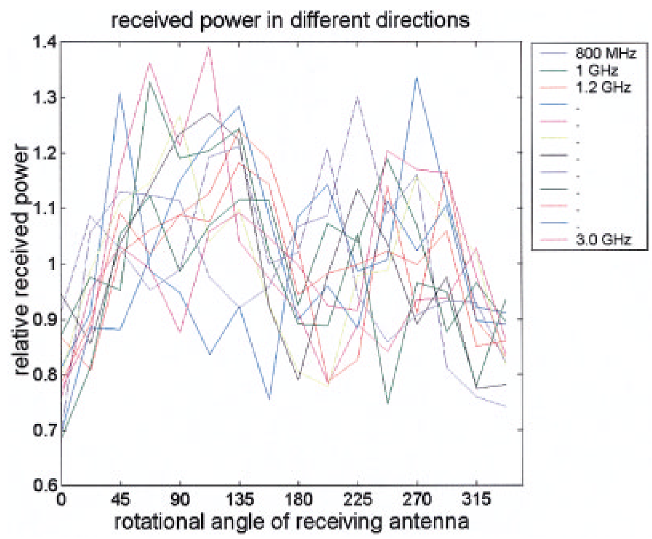

Figure 4 Relative received power as a function of rotational angle of the receiving antenna (the chamber is loaded with two absorbers in the directions 0° and 180°). [Color figure can be viewed in the online issue, which is available at www.interscience.wiley.com.]

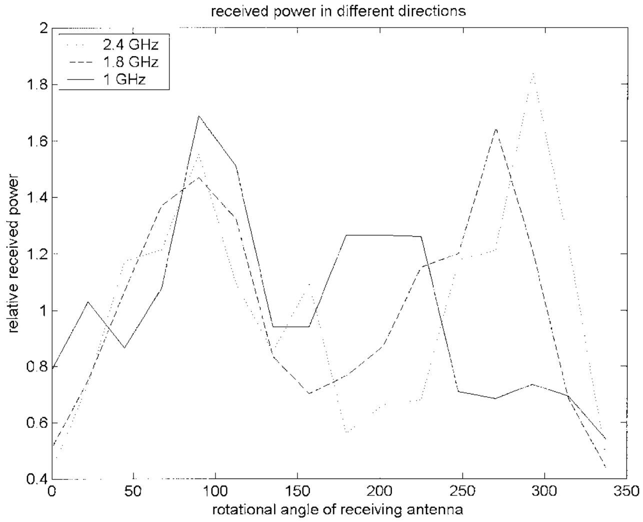

Figure 5 Same as Fig. 3, but this time the absorbers are closer to the receiving antenna (20 cm instead of 1 m)

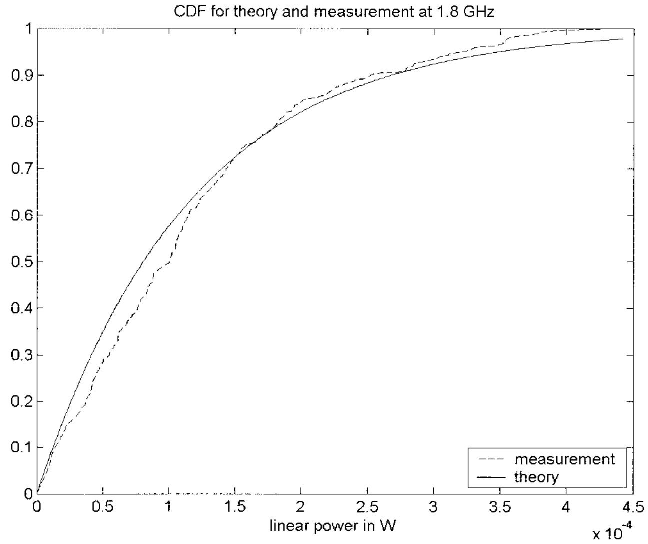

Figure 7 Theoretical cumulative distribution function (CDF) of the exponential distribution compared with the distribution of the measured data for 1.8 GHz

DISCUSSION

The reduction of incoming waves from the directions of the absorbers is probably underestimated with this method, since the receiving horn antenna has a certain beamwidth of its main lobe as well as side lobes in its radiation pattern. Because of this, the reduction of incoming waves will be small at large distances from the absorber, since the antenna will receive waves coming from the outside of the finitely extended absorber. According to [5, 6], the angular distance between directions of max and min values is very much dependent upon the type of environment. For example, in an indoor office environment, the received power can vary more than 20 dB for just a few degrees shift of the direction of incidence. In order to find such fast changes of the received power, measurements with an antenna with a narrow beamwidth are preferable, but as the size of such an antenna would be larger than the horn antenna, it is difficult to accomplish in such a small chamber. Further investigations on how to increase the effect need to be performed in order to fit measurements of real environments [5–7].

CONCLUSION

The distribution of incoming plane waves can be altered with the help of absorbers. The highest reduction obtained thus far is around 5 dB (max to min) and this has been obtained with absorbers placed close to the receiving antenna. The real reduction is probably higher, but due to the nonzero beamwidth of the receiving antenna and the finite size of the absorbers, this is the highest reduction that we can show with this measurement equipment.

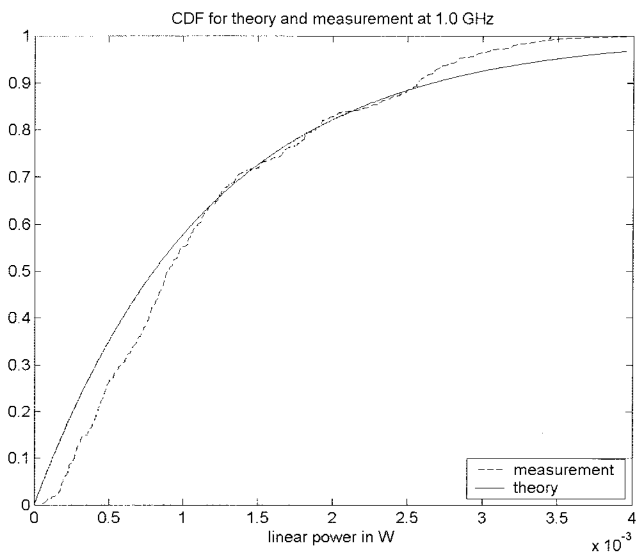

Figure 6 Theoretical cumulative distribution function (CDF) of the exponential distribution compared with the distribution of the measured data for 1 GHz

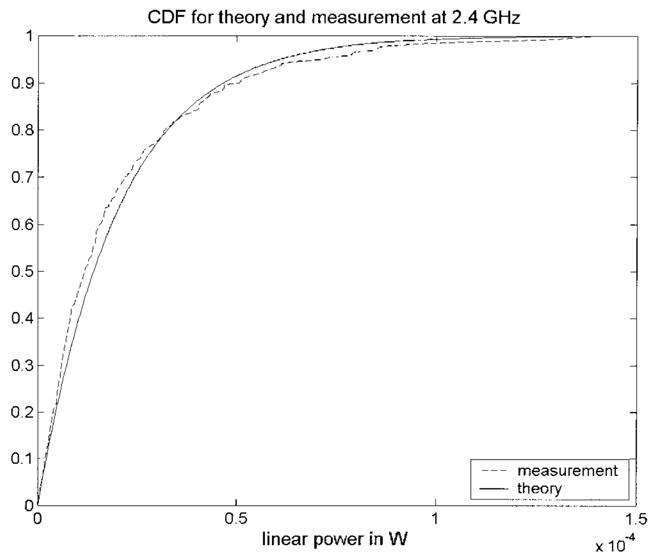

Figure 8 Theoretical cumulative distribution function (CDF) of the exponential distribution compared with the distribution of the measured data for 2.4 GHz

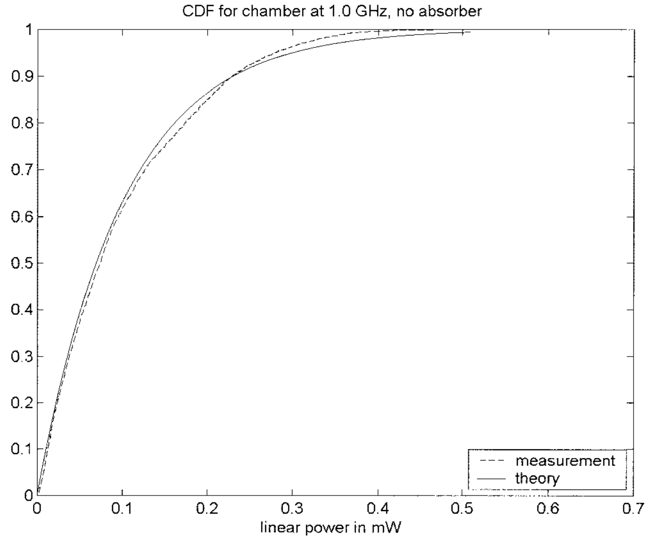

Figure 9 Theoretical cumulative distribution function (CDF) of the exponential distribution compared with the distribution of the measured data for an unloaded chamber at 1.0 GHz

ACKNOWLEDGMENTS

We would like to thank Mats Bäckström and Olof Lundén at the Swedish Defence Research Agency for their valuable comments.

REFERENCES

1. L. Ahlin and J. Zander, Principles of wireless communications, Studentlitteratur, 1998.
2. P.-S. Kildal and C. Carlsson, TCP of 20 mobile phones measured in a reverberation chamber, Bluetest report 2 (available from: Bluetest AB, Chalmers teknikpark, 412 88 Gothenburg, Sweden or via e-mail: simon@kildal.se), 2001.
3. C. Orlenius, N. Serafimov, and P.-S. Kildal, Procedure for measuring radiation efficiency in downlink band for active mobile phones in a reverberation chamber, IEEE Antennas Propagat Soc Int Symp Dig 4 (2003), 731–734.
4. K. Rosengren and P.-S. Kildal, Study of distributions of modes and plane waves in reverberation chambers for the characterization of antennas in a multipath environment, Microwave Opt Technol Lett 30 (2001).
5. K. Kalliola, Experimental analysis of multidimensional radio channels. Doctor of Science in Technology thesis, Helsinki University of Technology, 2002.
6. J. Medbo and J.-E. Berg, Spatio-temporal channel characteristics at 5 GHz in a typical office environment, IEEE VTC, 2001.
7. T. Su, H. Ling, and H. Foltz, Direction-of-arrival statistics of urban propagation channel at 1.9 GHz based on measurement and ray tracing, Microwave Opt Technol Lett 34 (2002).
8. A.F. Molisch, Modeling of directional wireless propagation channels, The Radio Sci Bulletin 302 (2002).
9. K. Madsén and P. Hallbjörner, Reverberation chamber for mobile phone antenna tests, The 2001 Reverberation Chamber, Anechoic Chamber, and OATS Users Mtg, Bellevue, WA, 2001.
10. http://www.eccosorb.com/catalog/eccosorb/AN.asp
11. D.A. Hill, Electromagnetic theory of reverberation chambers, NIST Technical Note 1506, National Institute of Standards and Technology, 1998.

ON THE GENERAL ENERGY-ABSORPTION MECHANISM IN THE HUMAN TISSUE

Outi Kivekäs, Tuukka Lehtiniemi, and Pertti Vainikainen
Helsinki University of Technology
Institute of Digital Communications
SMARAD/Radio Laboratory
P.O. Box 3000
FIN-02015 HUT, Finland

Received 20 April 2004

ABSTRACT: *In this paper, the general energy-absorption mechanism in human tissue is investigated. The purpose is to increase the understanding of this process, which is important, for example, when designing mobile handset antennas with minimized user interaction. The behavior of the electric fields of small antennas located near a lossy dielectric half-space, which consists of several material layers, is studied by numerical simulations. Two different RF sources operating at 900 MHz are used: a half-wave dipole and a patch antenna on a mobile handset chassis. The results show that the peak specific absorption rate (SAR) is not actually related to the antenna current, as has been commonly believed. Instead, the location of the SAR maximums can be explained by inspecting the boundary conditions of the quasi-static electric near-fields of the antenna at the air-tissue interface.* © 2004 Wiley Periodicals, Inc. Microwave Opt Technol Lett 43: 195–201, 2004; Published online in Wiley InterScience (www.interscience.wiley.com). DOI 10.1002/mop.20418

Key words: *antenna; electromagnetic absorption; mobile communications; specific absorption rate (SAR)*

1. INTRODUCTION

Interaction between electromagnetic fields and biological bodies has been extensively investigated, for example, in [1–6]. Research in this area has mainly focused on determining the specific absorption rate (SAR) characteristics and power absorbed in human tissue relating to a certain problem, while the study of the basic interaction mechanism has received less attention. A principal, often-referred-to paper [1] studied the general energy-absorption mechanism in the close near-field of dipole antennas operating above 300 MHz. According to this paper and [2], the surface currents induced by the magnetic fields are the main interaction mechanism, and the coupling of the electric fields is of minor importance. These findings led to a conclusion that the absorption on the surface of a biological body is proportional to the square of the magnitude of the antenna current [1]. However, this conclusion is not supported by the results of [3], in which numerical computation of fat-layer effects on the microwave near-field radiation was presented. A dipole at 915 MHz was located beside a homogeneous muscle phantom with and without a fat layer covering the abdomen. Without the fat layer, the calculated SAR pattern was elliptical around the antenna feed point, which confirms the results of [1]. Instead, with 0.8- and 1.6-cm-thick fat layers on the muscle surface, two SAR hot spots were observed on the fat surface near the ends of the dipole. Nevertheless, no reason for the fat layer effect was provided in this paper.

The purpose of this paper is to increase the knowledge of the interaction mechanism of the electromagnetic fields of small antennas (of size less than a wavelength in free space) with nearby human tissue. Better understanding of the phenomenon is useful, for example, when designing handset antennas with minimized user interaction. We study the behavior of electric fields in the human tissue when a 900-MHz source is located in the close

EUROPEAN COOPERATION
IN THE FIELD OF SCIENTIFIC
AND TECHNICAL RESEARCH

EURO-COST

COST 273 TD(05)017
Bologna, Italy
2005/Jan/19

SOURCE: Department of Technology,
Orebro University,
Sweden

Environment Simulations for MEG measurements inside Reverberation Chamber

Magnus Otterskog
Department of Technology
Orebro University
SE-701 82 Orebro
SWEDEN
Phone: + 46 19303373
Fax: + 46 19303463
Email: magnus.otterskog@tech.oru.se

Environment Simulations for MEG measurements inside Reverberation Chamber

Magnus Otterskog

Dept. of technology, Orebro University, Sweden
magnus.otterskog@tech.oru.se

Abstract: *A specialized Reverberation Chamber is used to create physical models of real propagation environments. The project aims to simulate different real environments by altering the propagation parameters: plane wave incident angles, field amplitude statistics, polarization and time delay inside the chamber. This can be used to measure the MEG and also to evaluate diversity and MIMO concepts on communication terminals. So far it has been shown that the plane wave incident angles and the field amplitude statistics can be altered. Initial experiments has also shown that the polarization and time delay can be changed inside the chamber.*

Introduction

To be able to measure the real performance of mobile terminals used in multipropagation environments we need to measure the terminal in the user environment. It is unpractical and expensive to move around measurement equipment in different real user environments and the measurements are affected by temporary environment characteristics as for instance the weather and the time of year. This is why we have created the Scattered Field Chamber (SFC) which is a specialized Reverberation Chamber in which the propagation environment characteristics can be changed. The Reverberation Chamber, as shown in Figure 1, provides a stabile environment for repeatability and you are also able to control the measurement uncertainty to some extent. Diversity and MIMO concepts can also be relevantly evaluated in the SFC as well as measurements of the Mean Effective Gain (MEG) of antennas (terminals). The propagation environment parameters that are supposed to be controlled are, the 3D angular distribution of plane waves that incident on the terminal, the statistics of the plane wave amplitudes (and phase), the polarization of the incident plane waves and the time spread or power delay characteristics of the environment.

Figure 1. The basic Reverberation Chamber with dual mode stirrers.

The amplitude statistics

It has already been shown by Hallbjörner [1] that the amplitude statistics of the plane waves can be altered between a Rayleigh distribution and a Gaussian distribution. Everything in between these two is the Rice distribution with different parameter values. Figure 2 shows a measurement performed in a real environment [2] and Figure 3 shows how the distribution can be altered in a SFC with Hallbjörners method.

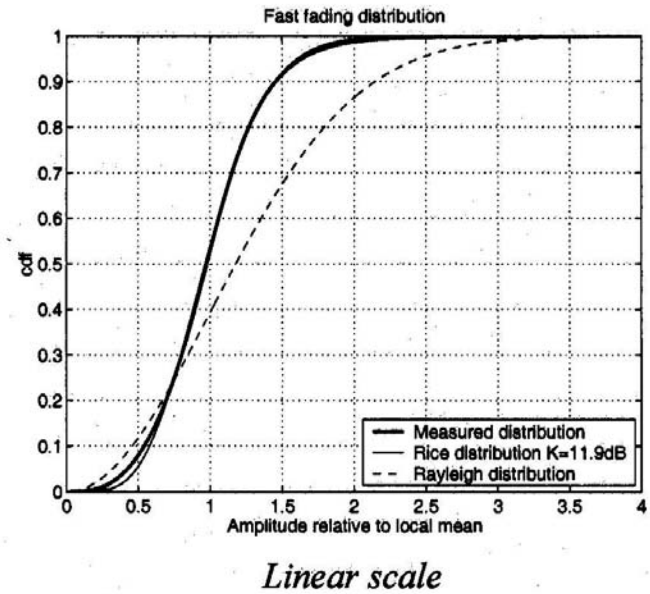

Figure 2. The amplitude statistics of a real environment [2].

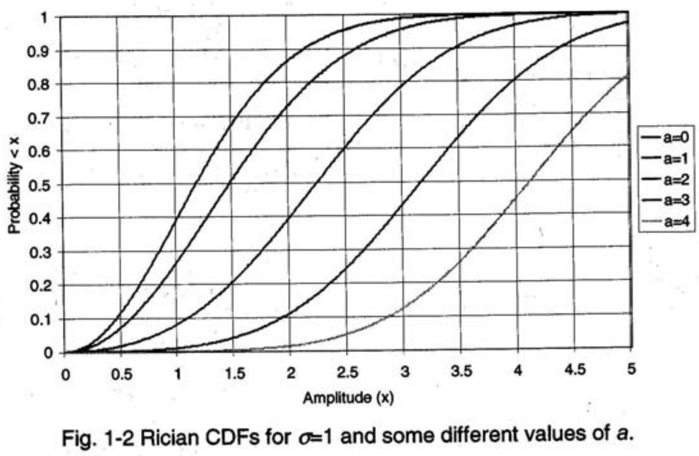

Figure 3. The amplitude statistics inside the SFC with different amount of direct propagation (LOS) [1].

The 3D distribution of plane waves

Experiments have been made with two different methods, the single absorber method and the shielded box method. Starting up with the single absorber method we tried to reduce the amount of plane waves from two directions by placing absorbing plates in these directions. The receiving antenna was rotated 360 degrees in the horizontal plane and the received power was measured for different angles (every 22.5 degrees) of the receiving antenna which in this case was a broadband horn antenna. The results for different frequencies are shown in Figure 4 and Figure 5, Figure 4 is measured without absorbers and Figure 5 is measured with two flat 60×60 cm absorbing plates placed on opposite walls in the directions 0 and 180 degrees inside the chamber.

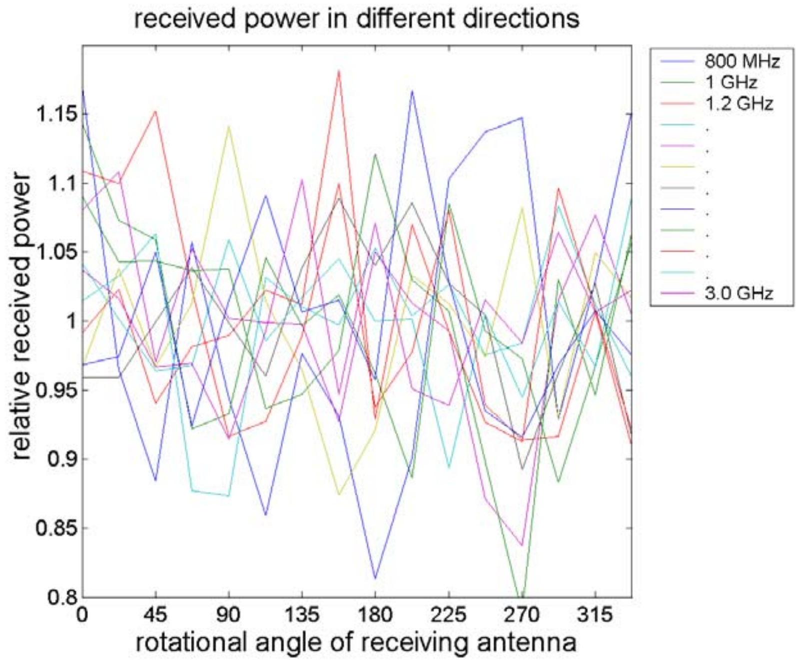

Figure 4. The received power as a function of rotational angle of the receiving antenna, no absorbers.

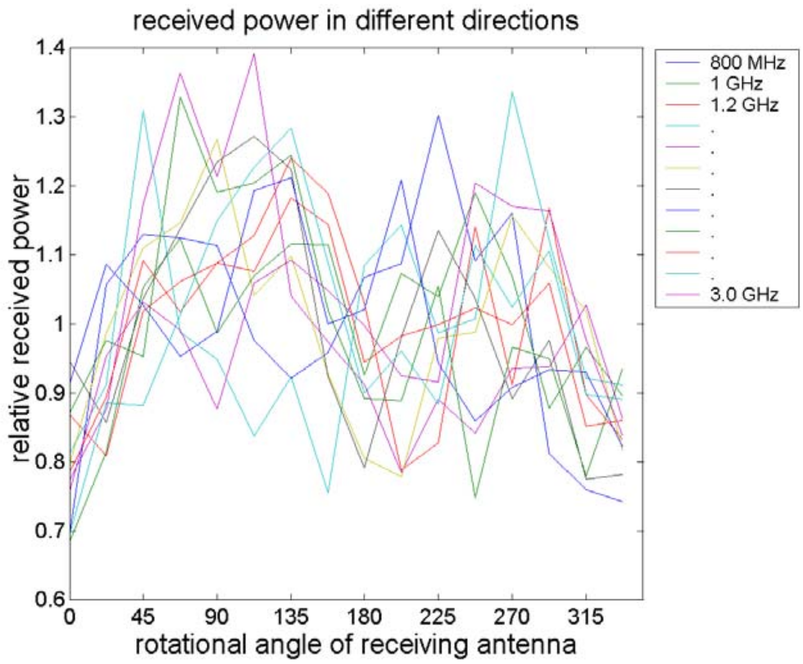

Figure 5. As Figure 4 but this time with absorbers in the directions 0 and 180 degrees.

As we can see the effect of the absorbers is visible but very small. Measurements of real environments [2][3] show that the received power can change as much as 20 dB depending on the direction of reception. A new experiment was carried out, this time with a shielded anechoic box that was placed inside the chamber and the receiving antenna was placed inside the shielded box as shown in Figure 6. Apertures in the anechoic box was used to control the directions of the incident waves upon the receiving antenna which in this case was a WLAN antenna with an approximate directivity of 8 dBi. The result for quadratic apertures of size 8×8 cm in the directions 0 and 180 degrees is shown in Figure 7.

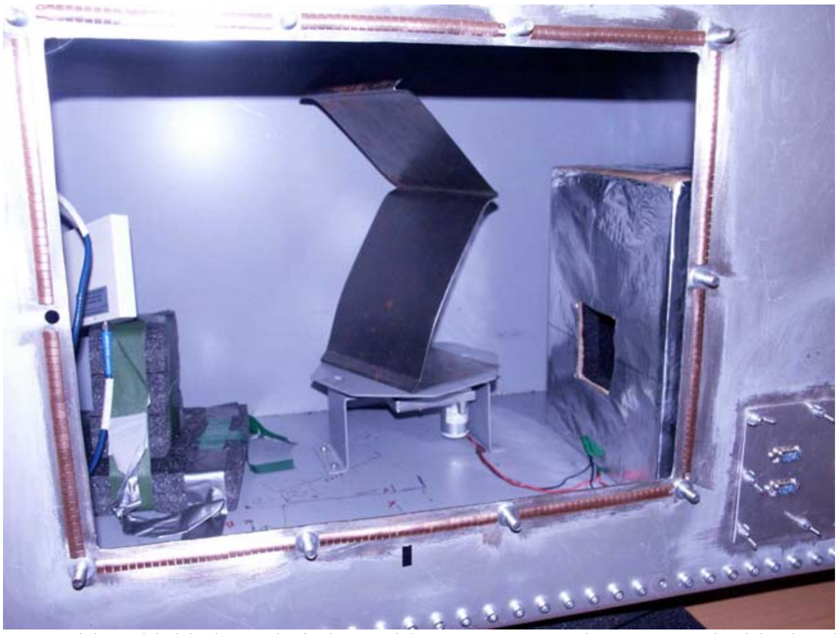

Figure 6. A SFC with a shielded anechoic box with apertures, receive antenna inside the shielded box.

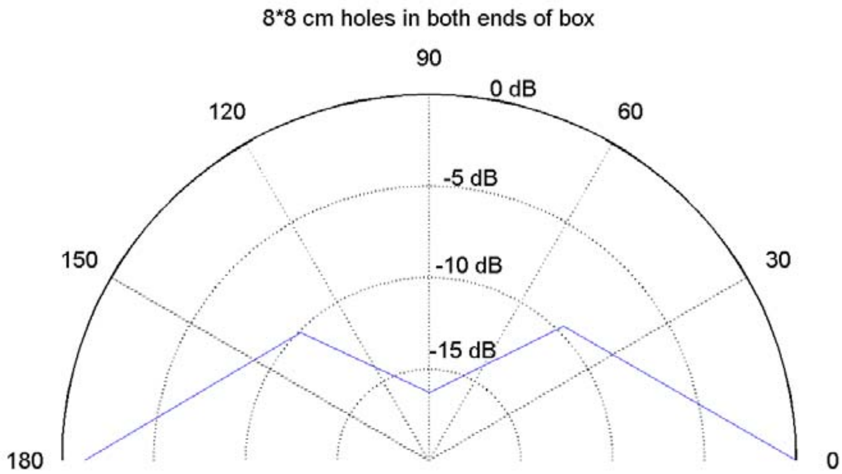

Figure 7. The received power as a function of rotational angle of receive antenna.

As we can see the largest difference in received power is just above 15 dB. Since the receiving antenna directivity is finite and in this case relatively low this will affect the measurement results in a negative way. The antenna will receive quite a lot of energy direct from the aperture even though it is directed away from it. In order to examine how the antenna directivity affected the measurement we performed a similar experiment, this time in a larger Reverberation chamber and with a larger shielded, anechoic box as shown in Figure 8. In this experiment the aperture was circular with a diameter of 6 cm and we used two different kinds of receive antennas, one broadband horn antenna with an approximate 3dB lobe angle of 60 degrees and one standard gain horn antenna with an approximate 3 dB lobe angle of 30 degrees. Figure 9 and 10 show the result for the broadband antenna and the standard gain antenna respectively. As we can see the assumption that the receiving antenna directivity will affect the result in a negative way is true.

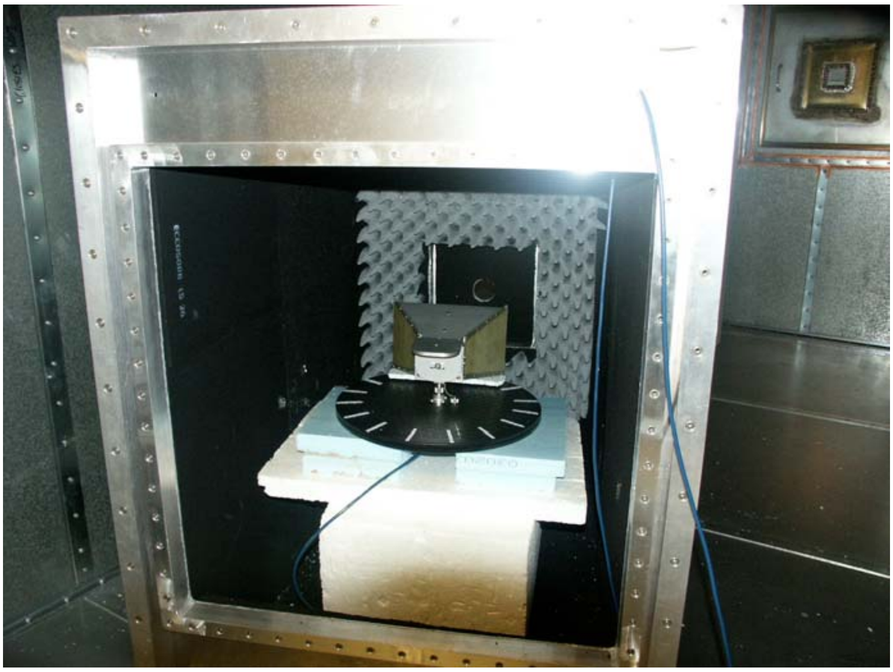

Figure 7. The broadband horn antenna inside the shilded anechoic box with a circular aperture.

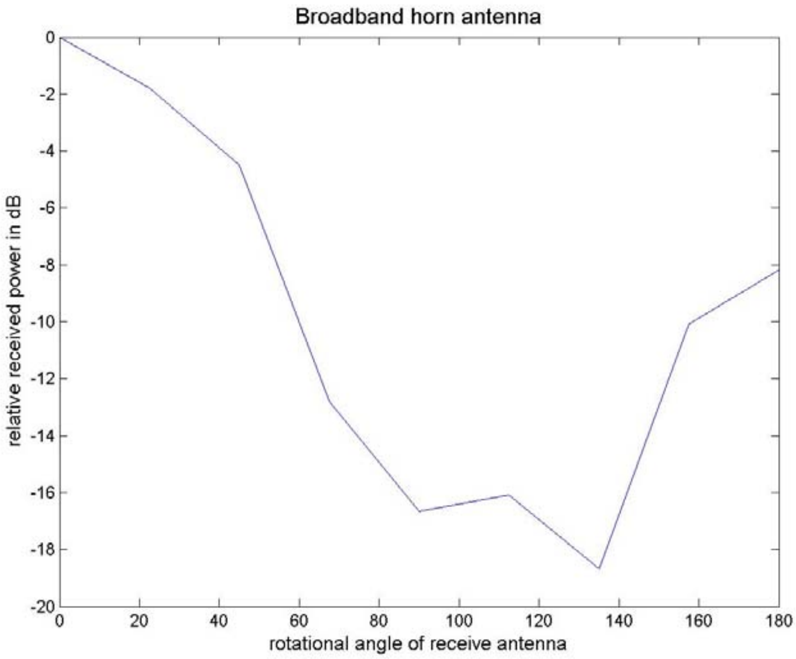

Figure 8. The relative received power for different angles of the broadband antenna.

The amount of change is now around 20 dB and probably limited due to the finite attenuation of the absorbers but this is in the same order as the results from the measurements made in the real environments. The apertures in the shielded box can also be designed to control the polarization of the plane waves from the different directions. This can be made with polarization filters placed in the aperture or by the geometry of the aperture it self.

Conclusions

The method of controlling the 3D plane wave distribution with a shielded anechoic box with apertures seems to be suitable to model real environments. Also the fact that the apertures can be designed to control the ploarization of the plane waves from the different directions is a positive effect.

Limitations in antenna directivity and absorber attenuation are factors that affect the measurement results in a negative way.

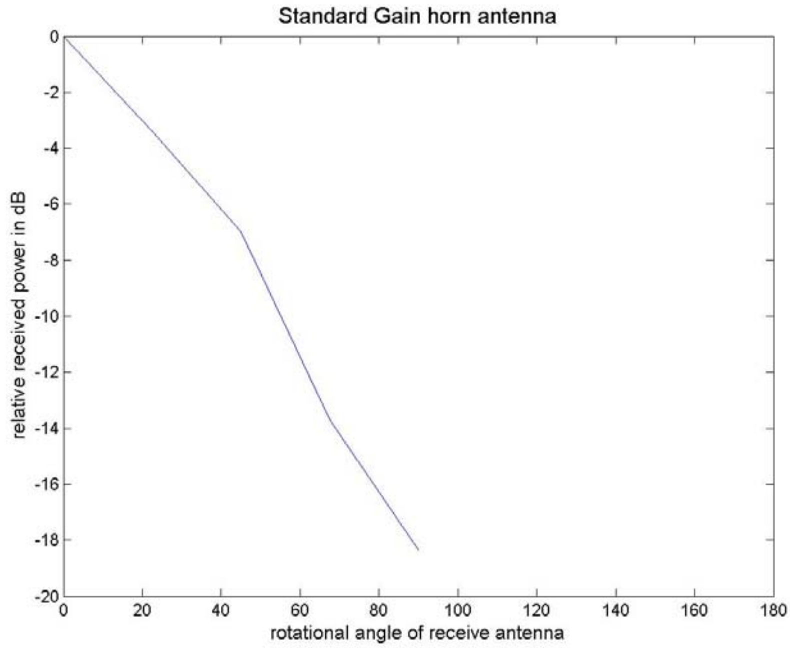

Figure 9. The relative received power for different angles of the standard gain antenna (only 0 to 90 degrees).

Future work

Measurements of the apertures ability to control the polarization is to be performed. Also numerical simulations is made to be able to estimate the directional properties of the apertures without the effect of finite antenna directivity and absorber characteristics. Finally the time spread or power delay is to be changed inside the SFC. Initial measurements have shown that this parameter is possible to alter but it is not examined to which extent this can be done.

References

[1] Madsén, Hallbjörner, "Reverberation Chambers for Mobile Phone Antenna Tests", *The 2001 Reverberation Chamber, Anechoic Chamber and OATS Users Meeting,* Bellevue WA USA, 2001.

[2] Kalliola, "Experimental analysis of multidimensional radio channels", *Thesis for the degree of Doctor of science in Technology*, Helsinki University of Technology, 2002.

[3] Medbo, Berg, "Spatio-Temporal Channel Characteristics at 5 GHz in a Typical Office Environment", *IEEE VTC Fall 2001*, 2001.

The influence of stirrer size and chamber load on the number of uncorrelated samples created in a reverberation chamber

Magnus Otterskog, Ph.D.-student
Department of technology
Örebro University
Sweden
magnus.otterskog@tech.oru.se

***Abstract*-A 2^3 factor experiment is carried out in order to examine the effect on the number of uncorrelated samples (NUS) that is created in a reverberation chamber. The three factors that are examined are stirrer diameter, stirrer position and chamber Q-value. The most interesting factors, chamber Q-value and stirrer diameter, are then examined in a 3^2 factor experiment and presented with simple regression models.**

I. Introduction

When using a reverberation chamber for measurements of many kinds an interesting parameter is the number of uncorrelated samples NUS. The NUS gives the uncertainty that you can obtain in your measurements and it is a result of the statistical properties that you use when working with a reverberation chamber. The NUS is commonly supposed to be related to the number of different mode structures that you can obtain with the mode stirring device of your chamber. In order to obtain this different mode structures one have showed that the stirrer should be electrically large [1] in order to give enough frequency shift for the eigenmodes created by the cavity structure. A large frequency shift of the eigenmodes will enable modes to be shifted in and out of the bandwidth of the cavity and thus excite a new set of modes for each new stirrer position (cavity structure). This will add randomness to the mode stirring of the chamber. Lots of work have been made [2] [3] to find stirrer configurations that will give the best possible statistical field uniformity in the chamber and it has also been showed [2] [4] that use of several stirrers will increase the stirring efficiency. The number of simultaneously excited modes in the chamber is highly related to the chamber Q. An expression for the number of simultaneously excited modes is given in for instance [5] as:

$$N_s = \frac{8\pi \cdot V \cdot f^3}{c^3 \cdot Q} \qquad (1)$$

Here one can see that the number increases with a smaller Q-value of the chamber, which is natural since a smaller Q gives a larger bandwidth of the chamber and therefore a larger number of excited modes. This paper examines if it is possible to build a stirrer efficient enough to take advantage of this larger number of simultaneously excited modes and by stirring, shift more eigenmodes in and out of the chamber bandwidth and increase randomness.

II. The equipment

A small reverberation chamber of size 1×0.5×0.5 m is used and the frequency used is 2.5 GHz. For every test run 801 samples of the relative transmission coefficient, between two small WLAN antennas, are registered with a Network analyzer. The stirrer is driven by a DC-motor and set to rotate (almost) one full turn per test sequence. The stirrers used in the experiments are shown in figure 1 and are, except for the largest one, of zig-zag type. All stirrers are of the same height but they differ in diameter. The chamber Q is controlled with flat absorbers in different sizes that are placed inside the chamber. Finally the stirrer's position can be altered between a central position in the chamber and a position close to a corner.

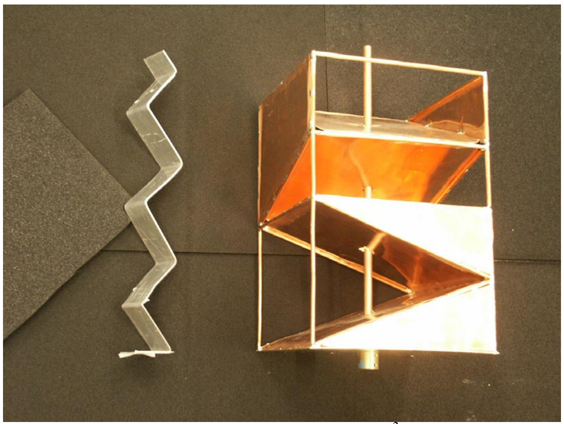

Figure 1a. The stirrers used in the 2^3 experiment.

Figure 1b. The stirrers used in the 3^2 experiment.

III. The 2^3 factor experiment

The full factor experiment [6] examined the response variable, NUS, for two levels of the three different factors, stirrer diameter (SD), stirrer position (SP) and chamber Q (CQ). The response variable matrix is therefore a three dimensional matrix with two levels in each dimension which gives a total of 2^3=8 elements. A minus sign for the factors SD, SP and CQ represent, a small stirrer, stirrer placed in the corner position and a loaded chamber (low Q) respectively. Plus signs represent a large stirrer, stirrer placed in the central position and an unloaded chamber (high Q) respectively. The NUS is obtained by looking at the auto correlation function and searching for the sample shift (offset) that gives a correlation less than e^{-1}. The total number of samples is then divided by the offset and this gives the NUS.

$$NUS = \frac{\text{total number of samples}}{\text{offset (correlation less than } e^{-1})} \qquad (2)$$

Actually, since the interesting parameter is the number of statistically independent samples. And that uncorrelated not always imply statistical independence there are better methods for finding the true number of independent samples see for instance [2] but as long as the total number of samples is the same in all test cases the method is fast and accurate enough. A factor experiment is used for finding factors that significantly affects the response variable. This is called the main effect of the factor and beside this the experiment is also able to detect interaction effects between factors. The response variable matrix looks as shown in figure 2.

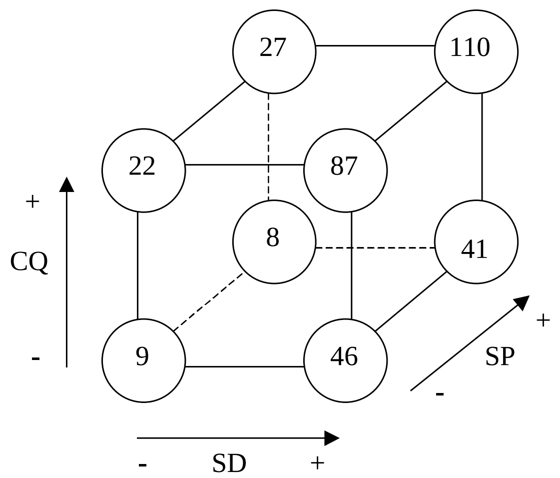

Figure 2. The response variable matrix for the 2^3 experiment. The NUS for every factor combination is given in the circles.

Every value for the different factor combinations is a mean value of three replicated runs with different positions of the transmitting antenna. This means that an estimated variance can be calculated for every factor combination and this will help us draw a useful conclusion later. As we can see a large stirrer diameter and a high chamber Q gives many uncorrelated samples. Calculating the effects from this experiment will give a result shown in Table 1. The effects are presented with the ±1 standard deviation limits.

factor	est. effect	± 1 std
SD (stirrer diameter)	54.5	4.15
SP (stirrer position)	5.5	4.15
CQ (chamber Q)	35.5	4.15
SD*SP	3.5	4.15
SD*CQ	19.5	4.15
SP*CQ	8.5	4.15
SD*SP*CQ	5.5	4.15

Table 1. Main effects and interaction effects on the response variable NUS.

This experiment clearly shows an effect on the NUS for the factors SD (stirrer diameter) and CQ (chamber Q). The experiment also shows an interaction effect between the SD and CQ factors. We also examine the residuals for all the experimental runs and find that the variance seems to increase with an increasing number of independent samples, see figure 3. The residuals are the deviation from the mean value within the three replicated runs for every factor combination. The residuals are supposed to be normal distributed.

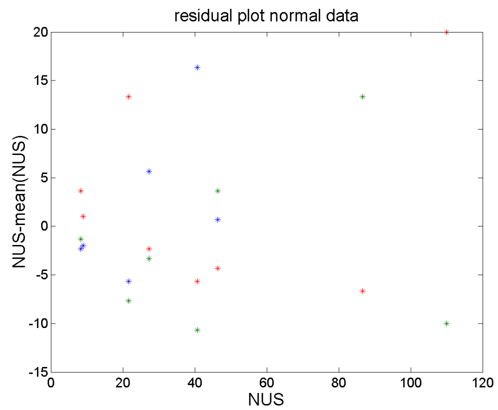

*Figure 3. The residual plot of the 3*8=24 experimental runs.*

The increase of variance as the response variable (NUS) gets larger is a problem. The large interval of the response variable can create non-physical interaction effects [6]. In order to get rid of this [6] and [7] suggests a transformation of the data. In my case the logarithmic function was used to transform the data and this gives a new table of the effects according to table 2.

factor	est. effect	± 1 std
SD (stirrer diameter)	0.66	0.20
SP (stirrer position)	0.029	0.20
CQ (chamber Q)	0.40	0.20
SD*SP	-0.014	0.20
SD*CQ	-0.041	0.20
SP*CQ	0.089	0.20
SD*SP*CQ	-0.0017	0.20

Table 2. Main effects and interaction effects for the logarithm of the response variable.

As we look at the plotted residuals for the logarithmic response variable in figure 4 we see that the variance is more equal and that the normality criterion seems to be better fulfilled. After the transformation the experiment indicates that only the factors SD (stirrer diameter) and CQ (chamber Q) have a significant effect on the number of uncorrelated samples obtained from a chamber. No interaction effects are significant. To further investigate the effect of factors SD and CQ we expand the experiment with a third level of the factors but this time we only examine the two significant factors SD and CQ giving a 3^2 factor experiment.

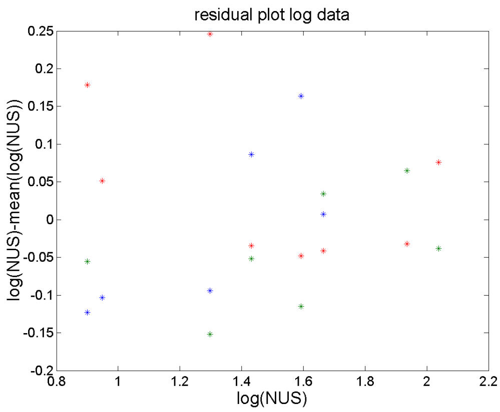

Figure 4. The residual plot of the logarithmic response variable.

IV. The 3^2 experiment

A third level of the factors SD and CQ are introduced and this will give an experiment with a total of 9 factor combinations. The response variable matrix looks like in figure 5. As before the range of the response variable is too high so it needs to be transformed with the logarithmic function in order to create a uniform variance within the experiment. Since we already know that the factors SD and CQ significantly affect the NUS, this experiment is made to find out **how** they affect the NUS. Figures 6 and 7 show the NUS as a function of the stirrer's diameter and stirred volume respectively. The figures also include regression lines found by the least square error method. Both figures show that no interaction effect

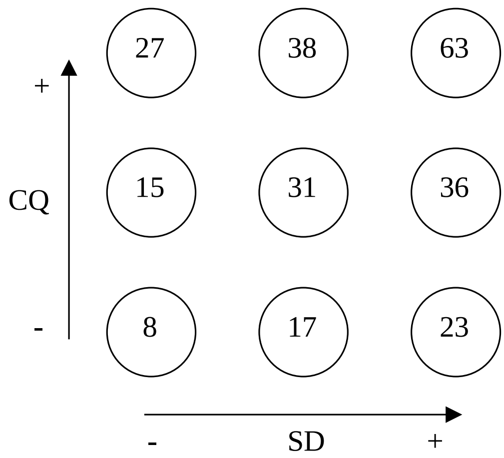

Figure 5. The response variable matrix for the 3^2 experiment. The NUS for every factor combination is given in the circles.

between the factors is present and this makes sense according to the results from the 2^3 experiment. According to the regression lines, the NUS seems to increase proportional to an increase of the diameter of the stirrer rather than to an increase of the volume of the stirrer. For every load case, a fourth point is added to the data before the regression lines are calculated. This extra point corresponds to a stirrer size of 0 that is supposed to give only 1 uncorrelated sample.

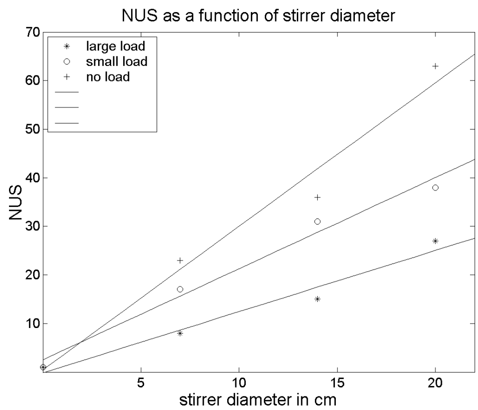

Figure 6. The NUS as a function of stirrer diameter.

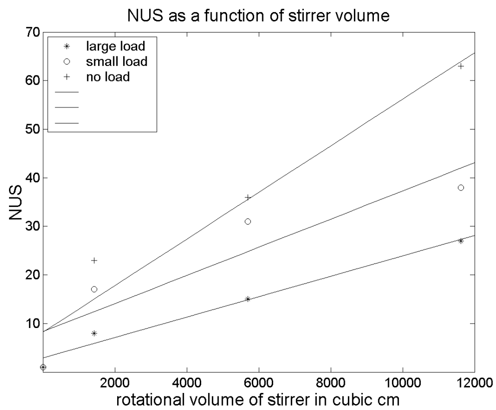

Figure 7. The NUS as a function of stirrer volume.

V. Conclusions

We have found that the NUS is significantly affected by the stirrer's diameter and the chamber's Q-value. A high Q-value and a large stirrer diameter give many uncorrelated samples. We have also found that the stirrer's position does not, significantly, affect the NUS obtained in a chamber. Also, by looking at simple, linear regression lines we conclude that the NUS increase proportional to an increase of the stirrer diameter rather than to an increase of stirrer volume.

VI. Discussion

The initial idea was that an efficient stirrer could take advantage of the low cavity Q and the large number of existing eigenmodes within the band-width of the cavity for a loaded chamber and maybe create a larger NUS than for an unloaded chamber. The efficient stirrer was to create a large amount of eigenfrequency shift and thereby enable a larger number of eigenmodes to be shifted in and out of the bandwidth of the cavity and add more random-ness to the stirring. This idea must be rejected since nothing in the experiment shows any sign of this idea being true. A large number of simultaneously excited modes is thus not something to strive for since it tends to decrease the NUS that can be obtained from the stirrer.

Acknowledgement

I would like to thank Mats Bäckström and Olof Lundén at the Swedish Defence Research Agency, Kent Madsén at Flextronics Design and Paul Hallbjörner at Ericsson AB for their useful ideas and comments.

References

[1] D. I. Wu and D. C. Chang, "The effect of an Electrically Large Stirrer in a Mode-Stirred Chamber" in *IEEE Transactions on electromagnetic compatibility, vol. 31, No. 2*, May 1989.

[2] O. Lundén and M. Bäckström, "Stirrer Efficiency in FOA Reverberation Chambers. Evaluation of Correlation Coefficients and Chi-Squared Tests" in *Proceedings of 2000 IEEE International Symposium on Electromagnetic Compatibility, Washington DC, USA,* 2000.

[3] L. Bai, L. Wang and J. Song, "Effects of Paddle Configurations on the Uniformity of the Reverberation Chamber" in *Proceedings of 1999 IEEE International Symposium on Electromagnetic Compatibility,* 1999.

[4] ¨J. Page " Stirred mode reverberation chambers for EMC emission measurements and radio type approvals or organised chaos" in *Ninth International Conference on Electromagnetic Compatibility, 1994. (Conf. Publ. No. 396),* September 1994.

[5] J. G. Kostas and B. Boverie, "Statistical Model for a Mode-Stirred Chamber" in *IEEE Transactions on electromagnetic compatibility, vol.33, No. 4,* November 1991.

[6] G. E. P. Box, W. G. Hunter and J. S. Hunter, "Statistics for experimenters" John Wiley & Sons, 1978.

[7] D. C. Montgomery, "Design and analysis of experiments", John Wiley & Sons, 1991.

Modelling of propagation environments inside a Scattered Field Chamber

Magnus Otterskog (Ph. D. Student)
Dept. of technology, Örebro University
Örebro, Sweden
magnus.otterskog@tech.oru.se

Abstract—Measurements on communication devices for evaluation of diversity and/or MIMO concepts must be made in the real environment or in a model of the real propagation environment. As a first step towards a complex, physical environment model the plane wave angular distribution, incident on the device under test (DUT), is altered in order to model plane wave angular distributions of real environments. Here a specialized Reverberation Chamber called the Scattered Field Chamber (SFC) is used to create a source of Rayleigh faded plane waves and a shielded, anechoic box with apertures is used to alter the angular distribution of the plane waves incident on the DUT. According to the measurements made, the model seems to be able to produce data that show agreement with measurements made on real propagation environments.

Keywords-propagation environment; modelling; simulation; reverberation chamber; diversity;

I. Introduction

The Reverberation Chamber has been used in the EMC (Electromagnetic Compatibility) community for several years and it has been used as a military test equipment for decades. The Reverberation Chamber [1] is a complex cavity made by a shielded box, usually rectangular, containing some movable conducting structure called stirrer, see Fig. 1. The cavity should have a size that is in the order of 5-10 wavelengths in any dimension to support the assumption that the cavity is overmoded for the frequency that is used. Thus, every chamber has a certain lowest usable frequency that is highly connected to the chamber's size and the uncertainty that can be accepted. Another important factor is the stirrer and how it is constructed [2][3]. The stirrer should, as it moves, change the boundary conditions for the fields inside the cavity and thus create different mode structures inside the chamber. An efficient stirrer will create a larger number of different mode structures than an inefficient stirrer and this will give a larger number of independent measurement samples and a smaller statistical uncertainty. The amplitude of one component of the electric field inside the chamber measured for a large number of different stirrer positions follows a Rayleigh distribution. The received power in an antenna will therefore follow the exponential distribution [4] and this is similar to a real propagation environment without presence of a direct propagation between the antennas. The environment inside the ideal reverberation chamber is also statistically isotropic and statistically uniform. Different versions of the traditional reverberation chamber have been used for measurements of the radiated power [5] and the receiver sensibility [6] of cellular phones for the last few years. These measurements can be made both with and without the presence of an artificial human head. However, in order to evaluate diversity and MIMO concepts on communication devices one must test the device in the real environment or in a model of the real environment. Since measurements of real propagation environments [7][8] show that the environments sometimes are far from isotropic we need to create a specialized reverberation chamber that can have different features than the traditional reverberation chamber, for example a non-isotropic distribution of plane waves that incident on the DUT. For this purpose we have created the Scattered Field Chamber (SFC).

II. Measurements on real environments

Measurements on real propagation environments [7][8] show that the distribution of plane waves that incident on the DUT can vary very quickly. For example in an indoor office environment the received power can vary more than 20 dB for incident angles that is changed only a few degrees. Outdoor measurements in urban environments show variation of the same size but not as rapid angle dependence. Measurements like these give us the guidelines for the environment that we would like to physically model.

III. Shielded anechoic box measurements

A. Small chamber

A combination of the Reverberation Chamber and the Anechoic Chamber is used for the model. A small shielded anechoic box is placed inside a larger Reverberation Chamber, see Fig. 1. The inner walls of the box are covered with absorbing material and the angular distribution of plane waves that incident upon the DUT, placed inside the box, is controlled with apertures in the walls of the box. Here the reverberation chamber is used as a source of Rayleigh distributed plane waves [9] and the shielded box with its apertures is the model of the plane wave environment. We show the relative received power as a function of rotational angle of the receiving antenna in Fig. 2. The measurements shown in Fig. 2 were conducted at 2.45 GHz in a small reverberation chamber of dimensions 1.0×0.5×0.5 meters. The shielded box, that covered the receiving antenna, was a

Figure 1. A small SFC with a shielded anechoic box with apertures.

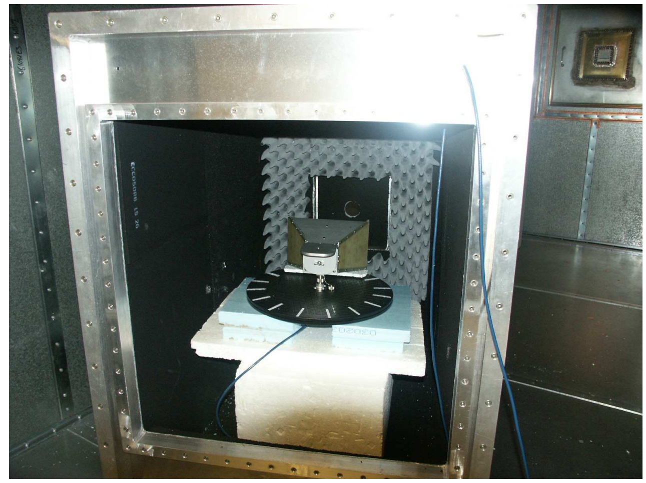

Figure 3. The large shielded anechoic box with broadband horn antenna.

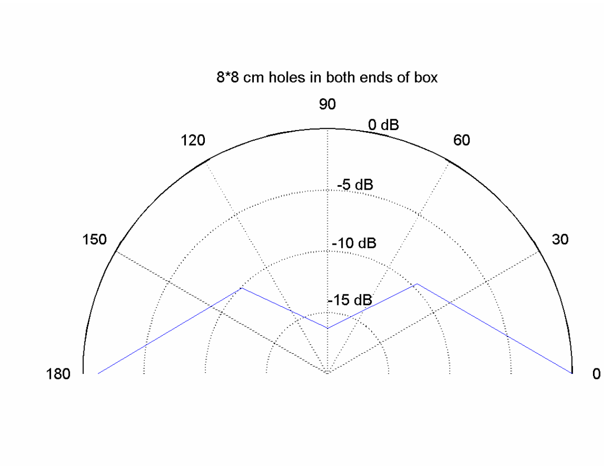

Figure 2. The relative received power as a function of rotational angle of the receiving antenna placed inside the shielded box.

cardboard box covered with aluminium foil and quadratic apertures of size 8 cm in the directions 0° and 180°. The interior of the box was covered with absorbers of type ECCOSORB LS16-22. The receiving antenna was rotated in 45 degrees steps between 0°and 180°. The receiveing antenna was a WLAN antenna with an approximate directivity of 8 dBi. This directivity will give a large 3 dB beamwidth and the antenna will receive a lot of energy directly from the aperture even though it is pointed away from the aperture. This will affect the measurements and the directional properties of the aperture will be underestimated.

B. Large chamber

In order to examine the effect of the finite directivity of the used receiving antenna we have also performed measurements as the ones above but this time in a large reverberation chamber (37 m^3) with a large shielded anechoic box (1 m^3) inside. This time two types of horn antennas with different directivity were placed inside the anechoic box with a constant distance to the aperture. The aperture was a circular aperture of 60 mm diameter and this is shown in Fig. 3. The broadband horn antenna was rotated with 22.5 degrees steps between 0 and 180 degrees giving 9 different directions. The standard gain horn with 22.5 degrees steps between 0 and 90 degrees. The aperture is placed in the 0 degree direction and at a distance of 53 cm from the aperture of the antennas. The relative received power was measured for 51 frequencies between 1.7 and 2.6 GHz. The result of a measurement at a single frequency for the first horn antenna, the broadband horn antenna with an approximate 3 dB beamwidth of 60 degrees for the used frequency, is presented in Fig. 4. The same thing for the other antenna, the standard gain horn antenna with an approximate 3 dB beamwidth of 30 degrees, is presented in Fig. 5. As we can see the reduction rate of plane waves seems to be faster for the standard gain antenna and thus the effect of the directivity of the receiving antenna is significant. Since antennas of finite directivity are used in the measurements the true reduction rates of plane waves from different directions are underestimated.

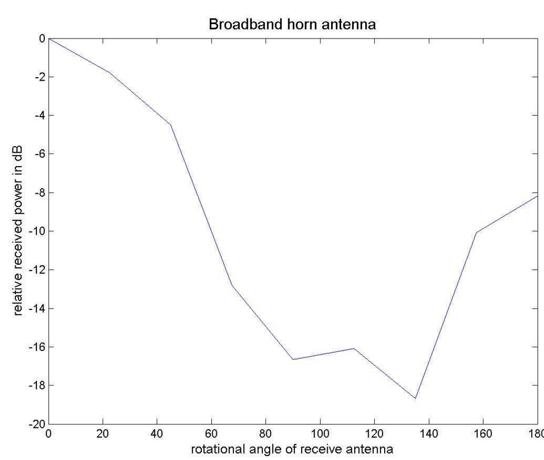

Figure 4. The relative received power as a function of rotational angle of the receiving broadband horn antenna.

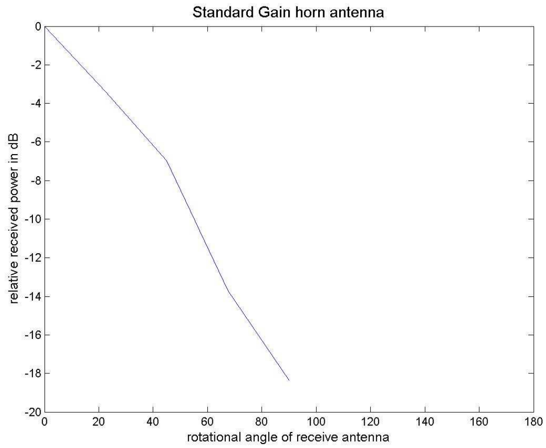

Figure 5. The relative received power as a function of rotational angle of the receiving standard gain horn antenna (only 0 to 90 degrees).

IV. Field Statistics

The statistical distribution of the plane wave amplitudes that is received by the antenna is shown in Fig. 6. The cumulative distribution function (CDF) of the measured data are plotted together with a best fit CDF of a Rayleigh distributed variable. The measurement data are taken for the broadband horn antenna when it is pointed 22.5 degrees away from the circular aperture and the frequency is 2.6 GHz. Fig. 7 shows the same distributions but this time with logarithmic scales in order to enlargen the area for small signal levels.

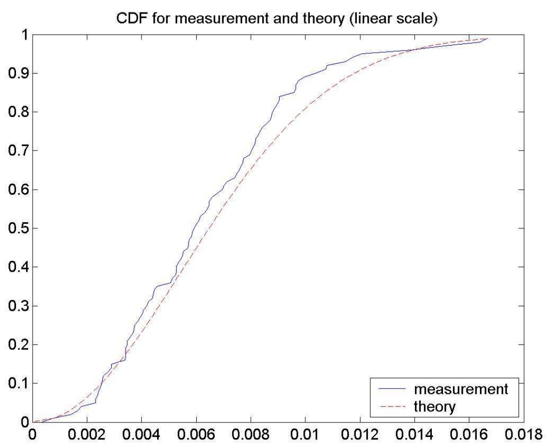

Figure 6. The CDF of measurements compared with best fit theoretical Rayleigh distributed variable, linear scale.

V. Conclusions

The distribution of plane waves that incident upon the DUT can be controlled inside a SFC. The amount of reduction is high when a shielded, anechoic box with apertures is used to control the distribution. Reduction rates of about 20 dB can be obtained. The absorber quality and antenna directivity is

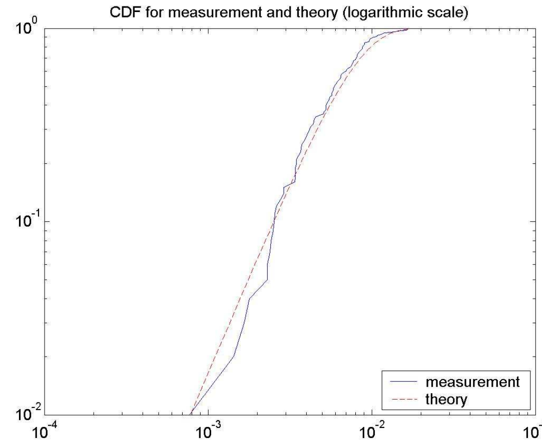

Figure 7. The CDF of measurements compared with best fit theoretical Rayleigh distributed variable, logarithmic scale.

important factors of how large variation and how fast variation with angular shift that you can obtain in the measurements. The use of absorbers with finite attenuation and receiving antennas with finite directivity will underestimate both the possible maximum reduction of plane waves and also the maximum rate of reduction with angular shift of the receiving antenna.

VI. Future Work

Future work includes numerical simulation of the plane wave distribution inside a shielded, anechoic box with apertures as described above. Modelling of the statistics of the incoming plane waves, Rayleigh, Rice or Gauss distributed, has already been shown [10] but will need some further investigations. Methods to control the polarization of the incoming waves and the time spread must also be invented in order to model different real environments. In the end, real field tests on communication devices in different environments will be compared with tests in the SFC and the correlation will be examined.

Acknowledgment

I would like to thank Olof Lundén at the Swedish Defence Research Agency for valuable support when performing the measurements.

References

[1] Bäckström, Lundén, Kildal, “Reverberation Chambers for EMC Susceptibility and Emission Analyses”, URSI the Review of Radio Science 1999-2002, 2002.

[2] Wu, Chang, “The effect of an Electrically Large Stirrer in a Mode-Stirred Chamber” IEEE Transactions on electromagnetic compatibility, vol. 31, No. 2, May 1989.

[3] Lundén, Bäckström, “Stirrer Efficiency in FOA Reverberation Chambers. Evaluation of Correlation Coefficients and Chi-Squared Tests” Proceedings of the 2000 IEEE International Symposium on Electromagnetic Compatibility, Washington DC USA, 2000.

[4] Hill, "Electromagnetic Theory of Reverberation Chambers", NIST Technical Note 1506, National Institute of Standards and Technology, December 1998.

[5] Kildal, Carlsson, "TCP of 20 mobile phones measured in a reverberation chamber", Bluetest report 2 (available from address: Bluetest AB, Chalmers teknikpark, 412 88 Gothenburg, Sweden or from e-mail: simon@kildal.se), Nov 2001.

[6] Orlenius, Serafimov, Kildal, "Procedure for measuring radiation efficiency in downlink band for active mobile phones in a reverberation chamber", IEEE Antennas and Propagation Society International Symposium 2003, Volume: 4, June 22-27, 2003, Pages 731-734.

[7] Kalliola, "Experimental analysis of multidimensional radio channels", Thesis for the degree of Doctor of science in Technology, Helsinki University of Technology, 2002.

[8] Medbo, Berg, "Spatio-Temporal Channel Characteristics at 5 GHz in a Typical Office Environment", IEEE VTC Fall 2001, 2001.

[9]] Svensén, "Reverberation Chamber as a radiation source", The 2003 Reverberation Chamber, Anechoic Chamber and OATS Users Meeting, Austin TX USA, 2003.

[10] Madsén, Hallbjörner, "Reverberation Chambers for Mobile Phone Antenna Tests", The 2001 Reverberation Chamber, Anechoic Chamber and OATS Users Meeting, Bellevue WA USA, 2001.

Polarization control in a Scattered Field Chamber

Magnus Otterskog Ph. D. Student
Dept. of technology
Örebro University
701 82 Örebro, Sweden
magnus.otterskog@tech.oru.se
Tel: +46 703693874
Fax: +46 19303463

Abstract

A way to control the direction of arrival of the plane waves inside a Scattered Field Chamber (SFC) is to use apertures in an anechoic box placed inside the chamber. This work shows how the polarization of these transmitted waves can be linearized from the random polarization produced by the chamber to different levels of linear polarization. The results can be used for propagation environment modelling inside a Scattered Field Chamber.

Key terms: scattered field chamber, propagation environment, polarization, reverberation chamber

Introduction

The reverberation chamber is and has been used used for measurements of electromagnetic compatibility (EMC) for several years, both for emission and immunity measurements. The fact that the ideal reverberation chamber creates a propagation environment that shows Rayleigh distributed field statistics [1] and uniformly distributed phase statistics and that these field statistics are uniform within a working volume also makes the chamber suitable for measurements on mobile communication terminals. The uniformity within the working volume makes the chamber insensitive to positioning of the device under test (DUT). Furthermore the environment is statistically isotropic and the polarization of the plane waves that incident on a test object is uniformly distributed over all directions. These characteristics of the ideal reverberation chamber might be an accurate physical model of a certain propagation environment, for example a pico cell with dense scatterers could have statistics that resembles with the ideal reverberation chamber. This similarity, with a real propagation environment [2], is the main reason why the chamber was used to develop a measurement facility [3][4] that could evaluate the radiation characteristics of active mobile communication terminals. It has also been shown that it is possible to measure the antenna efficiency [5] and diversity gain [6][7] inside a reverberation chamber. The main advantages with measurements inside a reverberation chamber is that the environment is stable, also it is a fast measurement method, in the order of seconds or minutes depending on the number of frequencies and the desired measurement accuracy. Finally the equipment is fairly inexpensive and foolproof .

Since the reverberation chamber has the above mentioned characteristics the possibility to correctly evaluate any diversity or MIMO concept in different propagation environments is quite poor. For this purpose the Scattered Field Chamber (SFC) was created. The SFC is intended to be a specialized reverberation chamber where the propagation characteristics can be altered to fit a certain propagation environment. Recent work has showed that it is possible to alter the direction of arrival (DOA) for the plane waves that incident on the DUT [6][8][9]. The aims of these works have been to create the same DOA profiles that are presented in results from measurements in real propagation environments [10][11][12]. One of the methods used to control the DOA profile inside a SFC uses an anechoic box with apertures to control the direction of the incident plane waves created by the reverberation chamber surrounding the box. The purpose of the work that is presented here is to, experimentally, examine the possibility to control the polarization of the plane waves that propagates through the apertures.

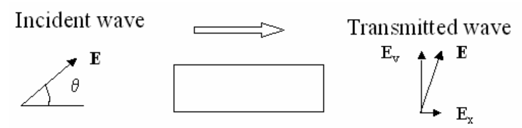

Figure 1. Case study: A plane wave with polarization angle θ with respect to the horizontal axis (x) is transmitted through an aperture. The polarization of the transmitted field is examined and presented as the amount of y-polarized field with respect to the total field transmitted.

Simulations with FDTD

Figure 1 shows a schematic view of the simulated case. The amount of y-polarized field with respect to the total transmitted field is calculated in percent according to equation 1.

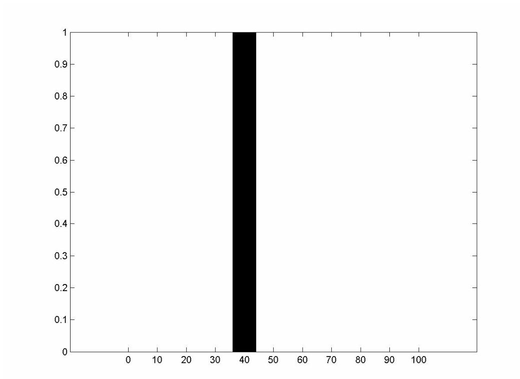

Figure 2a. A hisogram plot of the number of plane waves polarized to a certain extent for an incident field with polarisation angle θ = 5° (according to figure 1) and an aperture of size 125*15 mm.

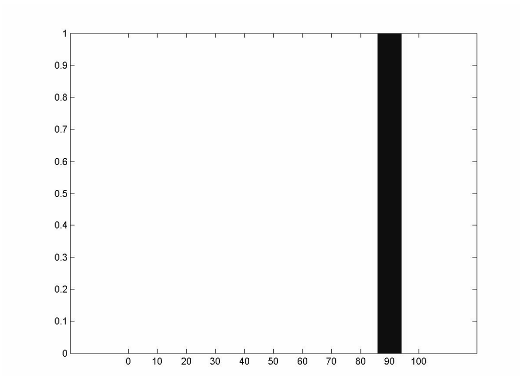

Figure 2b. A hisogram plot of the number of plane waves polarized to a certain extent for an incident field with polarisation angle θ = 45° (according to figure 1) and an aperture size of 125*15 mm.

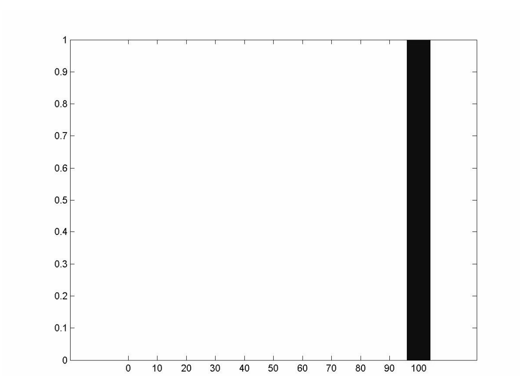

Figure 2c. A hisogram plot of the number of plane waves polarized to a certain extent for an incident field with polarisation angle θ = 85° (according to figure 1) and an aperture size of 125*15mm.

$$\text{y - polarized field in }\% = \frac{E_y}{\mathbf{E}} \cdot 100 \qquad (1)$$

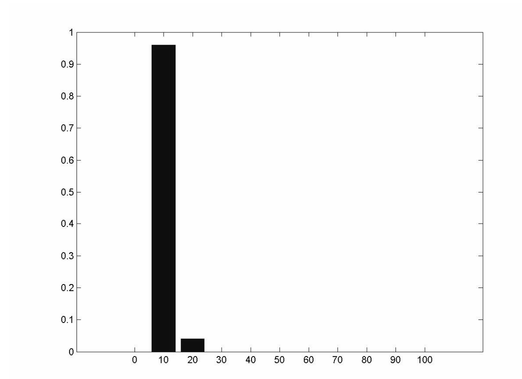

Figure 3a. A hisogram plot of the number of plane waves polarized to a certain extent for an incident field with polarisation angle θ = 5° (according to figure 1) and an aperture size of 125*35 mm.

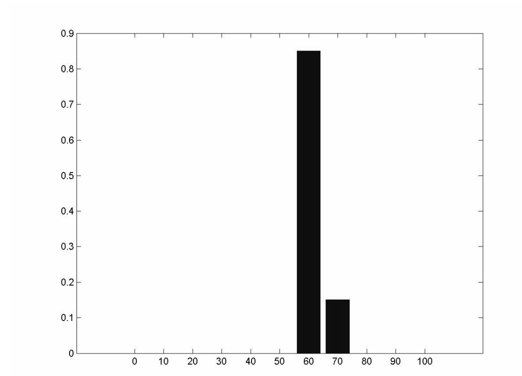

Figure 3b. A hisogram plot of the number of plane waves polarized to a certain extent for an incident field with polarisation angle θ = 45° (according to figure 1) and an aperture size of 125*35 mm.

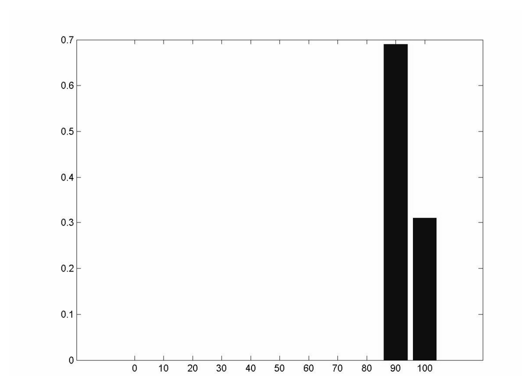

Figure 3c. A hisogram plot of the number of plane waves polarized to a certain extent for an incident field with polarisation angle θ = 85° (according to figure 1) and an aperture size of 125*35 mm.

The simulations are made with FDTD for frequencies between 1.8 and 2.0 GHz and the aperture is rectangular, 125 mm wide and the height is 15 mm in the first case and 35 mm in the second.

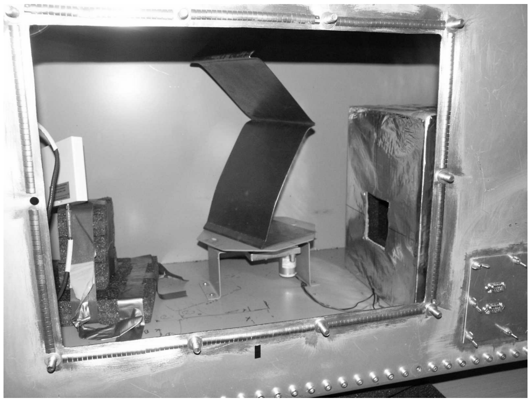

Figure 4. The interior of the small reverberation chamber used for the measurements. In this picture one can see the shielded anechoic box with apertures used to control the DOA of the plane waves [9] although it was not present in the chamber during the measurements presented here.

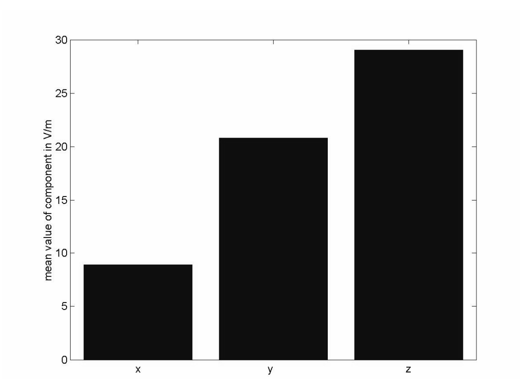

Figure 5. The mean value of the three orthogonal E-field components measured inside the chamber.

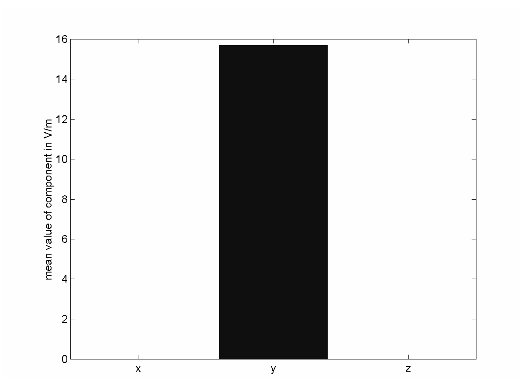

Figure 6. The mean value of the E-field components for the waves transmitted through the 15*100 mm aperture.

In every case the polarization of the incident wave is altered between θ = 5°, 45° and 85°. The results shown in figure 2 and 3 are presented as histogram plots where the number of plane waves, polarized

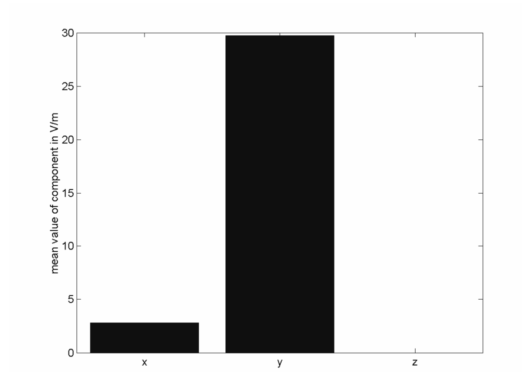

Figure 7. The mean value of the E-field components for the waves transmitted through the 35*100 mm aperture.

to a certain extent according to equation 1, are grouped together to form the histogram.

Clearly the polarization can be controlled and linearized when transmitted through an aperture of this kind. The amount of linearization can in this case be controlled with the aperture height. In

previous work [10] is has been shown that the transmitted field through an aperture, fed by a reverberation chamber, still shows Rayleigh distributed field statistics. This means that it should be possible to create plane wave incidence from a certain direction with a certain polarization distribution and this is to simulate, for instance, a cluster of reflected waves from a building or another large object as can be found in measurements made in real environments [13]. Measurements have also shown that clusters of waves following street canyons in urban environments often are linearly polarized [13]according to the polarization of the transmitter antenna. These clusters also have a certain angular distribution that could be simulated with an aperture.

Measurements

To further validate the results, measurements were made on the transmitted field through an aperture in one of the walls of a small (1*0.5*0.5 m) reverberation chamber shown in figure 4.

Just as in the FDTD-simulated case two apertures were examined, both rectangular, the first of size 100*15 mm and the second of size 100*35 mm. The slightly smaller size of the aperture width is to compensate for the fact that the measurements were made at 2.5 GHz which is a higher frequency than the FDTD-simulated ones. This is due to the available transmit antenna which is a linearly polarized WLAN patch antenna for the 2.5 GHz-band. The polarization was measured with a 3-axis field probe with a sensitivity threshold of about 5 V/m, values lower than this will be registered as a zero.

First the polarization distribution of the complete chamber without aperture was measured, this is to see if there is a polarization imbalance in the chamber itself. The results are shown in figure 5. The figure shows a large imbalance between the three components and the reason is not crystal clear. Since the transmit antenna is y-polarized one might expect the largest mean value for this component if the chamber is equipped with a poor ”mode stirrer” that isn’t able to stir the modes properly. The x-component is aligned with the large dimension of the chamber and this might be a reason for the lower value but for the moment there exist no explanation to why the z-component is larger than the y-component. The polarization imbalance is however a sign of a non efficient reverberation chamber [14] and this is probably because of it’s small physical dimensions (with respect to the used signal wavelength) and it’s rather small, and therefore, inefficient stirrer. The results from transmission through the 100*15 mm aperture is shown in figure 6 and the results from the 100*35 mm aperture is shown in figure 7. The axles are located just as in the FDTD-simulation case, see figure 1. Clearly the field transmitted through the apertures is polarized just as the numerical FDTD-simulations suggested. The components that are shown to be zero in the figures 6 and 7 could exist but the values are to small for the field probe to register. If we would like to compensate for the polarization imbalance of the chamber itself we would have to multiply the size of the x-component with approximately a factor 2. This will still show results that evidently shows the polarization linearization effect of the apertures.

Conclusions

Both numerical simulations and measurements show that the random polarization, produced by a well functioning reverberation chamber, could be linearized to different extent depending on the design of the aperture that the waves are transmitted through. This result could be used for modelling of real propagation environments inside a Scattered Field Chamber. It is also most probable that one can use some kind of polarization filter in the aperture to control the polarization of the transmitted wave, for instance thin parallel wires could be placed in the aperture to enhance the polarization orthogonal to the wires. It is also possible to use arrays of apertures to further control the angular spread of the direction of arrival of the plane waves to the test object and at the same time control the polarization of these waves.

Acknowledgement

The author wants to thank Torleif Martin at the Swedish Defence Research Agency for valuable help with the FDTD-simulations.

References

[1] Bäckström, Lundén, Kildal, “Reverberation Chambers for EMC Susceptibility and Emission Analyses”, URSI the Review of Radio Science 1999-2002, 2002.

[2] Arai, Urakawa, ”Radiation Power Measurement Using Compact Shield Box”, Proceedings of ISAP’96, Chiba, Japan, 1996.

[3] www.bluetest.se

[4] www.fdk.co.jp/whatsnew-e/anbako-e.html

[5] P. Hallbjörner, ”Reflective antenna efficiency measurements in reverberation chambers”, Microwave and Optical Technology Letters, Vol. 30, 2001.

[6] K. Madsén, P. Hallbjörner, ”Reverberation Chambers for Mobile Phone Antenna Tests”, The 2001 Reverberation Chamber, Anechoic Chamber and OATS Users Meeting, Bellevue WA, USA, 2001.

[7] P-S. Kildal, K. Rosengren, J. Byun, J. Lee, ”Definition of effective diversity gain and how to measure it in a reverberation chamber”, Microwave and Optical Technology Letters, Vol. 34, No. 1, p. 56-59, July 2002.

[8] M. Otterskog, K. Madsén, ”On creating a nonisotropic propagation environment inside a Scattered Field Chamber”, Microwave and Optical Technology Letters, Vol. 43, No. 3, p. 192-195, November 2004.

[9] M. Otterskog, ”Modelling of propagation environments inside a scattered field chamber”, 61st IEEE Vehicular Technology Conference (VTC2005-Spring), Stockholm, Sweden, June 2005.

[10] Medbo, Berg, “Spatio-Temporal Channel Characteristics at 5 GHz in a Typical Office Environment”, IEEE VTC Fall 2001, 2001.

[11] Kalliola, “Experimental analysis of multidimensional radio channels”, Thesis for the degree of Doctor of science in Technology, Helsinki University of Technology, 2002.

[12] M. Steinbauer, D. Hampicke, G. Sommerkorn, A. Schneider, A. Molisch, R. Thomä, E. Bonek, ”Array measurement of the double-directional mobile radio channel”, Proc. VTC2000 Spring, 1656-1662, 2000.

[13] M. Toeltsch, J. Laurila, K. Kalliola, A. Molisch, P. Vainikainen, E. Bonek, ”Statistical characterization of urban spatial radio channels”, IEEE Journal on selected areas in communications, Vol. 20, No. 3, p. 539-549, April 2002.

[14] P. Corona, G. Ferrara, M. Migliaccio, ”On polarimetric characterization of the scattering process in reverberating chambers”, The 2003 Reverberation Chamber, Anechoic Chamber and OATS Users Meeting, Austin TX USA, April 2003.

Altering the amplitude statistics inside a Scattered Field Chamber

Magnus Otterskog Ph. D. Student
Dept of technology, Örebro University
Tel. +46 703693874
Fax. +46 19303463
magnus.otterskog@tech.oru.se

Abstract

This work presents different ways of changing the amplitude statistics inside a Scattered Field Chamber. The statistics can be changed by an introduction of a direct propagation path or in this case by introducing some amount of unstirred energy. This is done by pointing the antennas at each other and the amount of unstirred energy can be controlled by the distance between the antennas, the polarization alignment of the antennas and by loading of the chamber. Statistics that range from Rayleigh to Rice with different k-factors can be obtained. The results are also valid if one of the antennas is placed inside a shielded anechoic box with apertures, this is to be able to simultaneously model the direction of arrival profile of a certain real propagation environment.

I. Introduction

The scattered field chamber (SFC) is a specialized reverberation chamber used to physically model real propagation environments [1][2]. Since different environments have different characteristics of propagation variables such as the field amplitude statistics, time delay profile, direction of arrival (DOA) of the plane waves etc., the model must also be able to follow this changing demands of the different environments. The ideal reverberation chamber only has one set of propagation variable characteristics, for instance the field amplitude statistics is Rayleigh distributed [3] and the DOA is isotropic [4]. If a chamber violates one of these characteristics it will no longer be an ideal reverberation chamber and that is the reason for the need of a new name, SFC.

This work deals with the possibility to change the amplitude field statistics inside a SFC. Real propagation environments can show different kinds of statistics, for instance small cells (pico) with large number of scatterers and without prescence of a direct path between the transmitter and the receiver has Rayleigh distributed amplitude statistics. On the other hand, if the environment is a large flat, open area with a substantial amount of direct propagation the amplitude statistics will follow something like a normal (Gauss) distribution. Everything in between these two extreme cases will follow the Rice distribution with different amount of offset or Ricean k-factor. Earlier work [5] has showed that it is possible to change this statistic by introducing a direct propagation or some amount of unstirred energy inside the SFC. This work is based on that idea and expands it for the case where a shielded anechoic box with apertures is used to control the direction of arrival to the test object [2].

II. The measurements

The measurements were performed inside a SFC of size 1*0.5*0.5 m initially constructionally based on an article written by Arai and Urakawa [6]. The chamber is rebuilt several times and can be considered as an experimental chamber not at all optimized for the best functionality. The frequency used is 2.5 GHz and the transmission between two linearly polarized WLAN antennas of patch type is measured by a vector network analyzer. Ideally the amplitude statistics of the chamber will be Rayleigh distributed when the antennas are directed away from each other and the chamber is unloaded. Figure 1 shows a histogram plot of the experimental data together with an estimated Rice distribution (equation 1) with a certain k-factor (offset).

$$f_X(x) = \frac{x}{s^2} e^{\left(-\frac{x^2+k^2}{2s^2}\right)} \cdot I_0\left(\frac{xk}{s^2}\right) \tag{1}$$

The k-factor is found from the complex data plot shown in figure 2 where the real and the imaginary parts of the complex transmission coefficient S_{21} is plotted. The k-factor is estimated to be the amplitude of the offset (from the origin) of the complex mean value of all experimental data points (marked with a

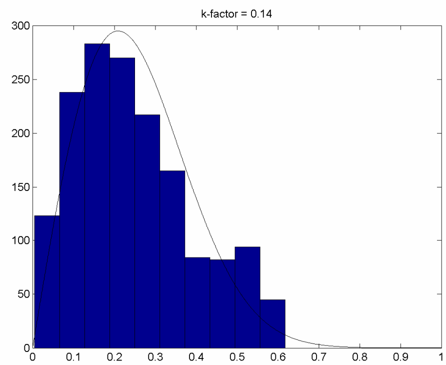

Figure 1. Sample histogram and estimated Rice distribution for antennas directed away from each other in the empty chamber.

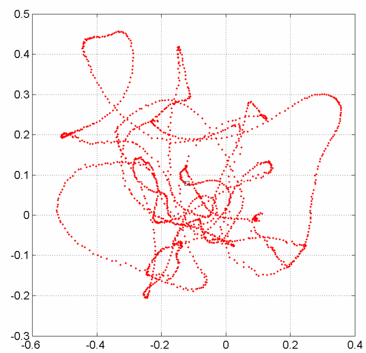

Figure 2. Complex data plot of transmission coefficient S_{21}. The square marks the complex mean value.

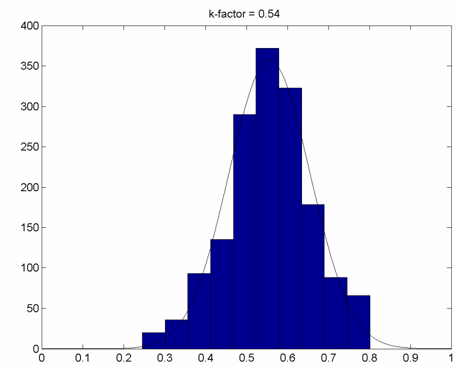

Figure 3. Sample histogram and estimated Rice distribution for antennas placed 7 cm apart directed towards each other and lined up to have the same direction of polarization.

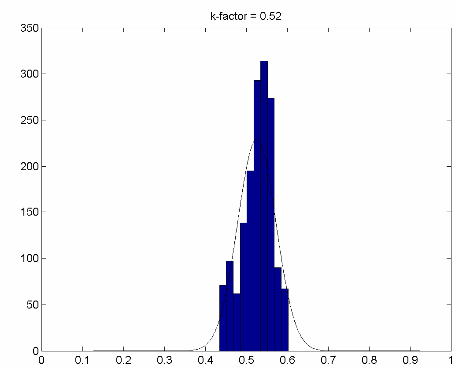

Figure 4. The same as figure 3 but this time with a loaded chamber.

square in figure 2). The other parameter s of the assumed Rice distribution is estimated to be the standard deviation of the two orthogonal normal distributions (real and imaginary part) of the experimental data, for the case when they differ, the mean value of them is taken as s. Figure 2 shows that the amplitude distribution for the case when the antennas are directed away from each other is not, as expected, Rayleigh distributed (Rice with k-factor = 0) but Rice distributed with a k-factor equal to 0.14. This is due to the fact that the mode stirrer in the chamber is a bit inefficient and not able to stir all the energy inside the chamber, some part is left unstirred and this will show as an offset on the complex plot of the data. The used stirrer has a small diameter (due to space limitations) and it has been shown [7] that a large diameter is to be preferred instead of a large height for a rotational stirrer. This small offset will however, as we will see, not affect the ability to show the effect of a larger offset created later on. Next the antennas were placed pointing towards each other only 7 cm (≈ 0.6 λ) apart with the polarization lined up for maximum transmission. The result is shown in figure 3 and the distribution is now clearly not Rayleigh any more but rather a Rice distribution with a high k-factor. Figure 4 shows the same case measured again but this time we inserted a lossy object (absorbing material) into the chamber. The effect of the lossy object will be a decrease in the number of resonant modes that are shifted by the stirerr [8] and therefore the stirrer will be even less efficient and the degree of unstirred energy (direct propagation) will increase leading to an even higher k-factor of the Rice distribution. By increasing the distance between the antennas the amplitude distribution will become Rice distributions with lower and lower k-factor. The figures 5 and 6 shows the results for distances 15 cm and 40 cm respectively. Another factor that can be used to

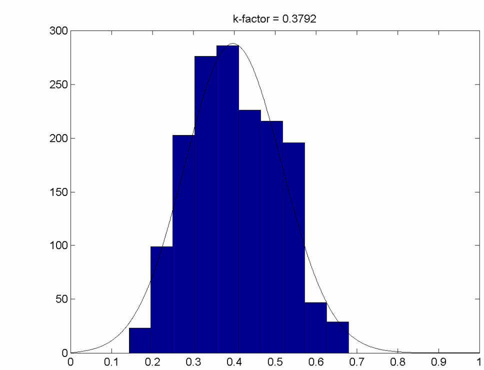

Figure 5. Sample histogram and estimated Rice distribution for antennas placed 15 cm apart directed towards each other and lined up to have the same direction of polarization.

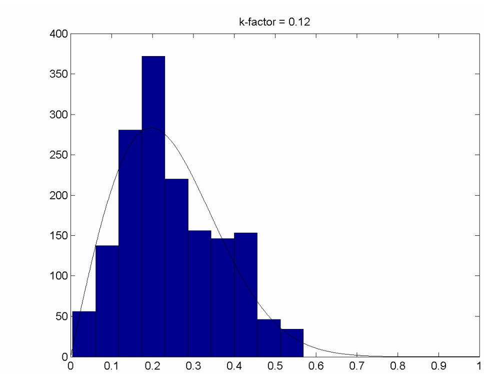

Figure 6. Sample histogram and estimated Rice distribution for antennas placed 40 cm apart directed towards each other and lined up to have the same direction of polarization.

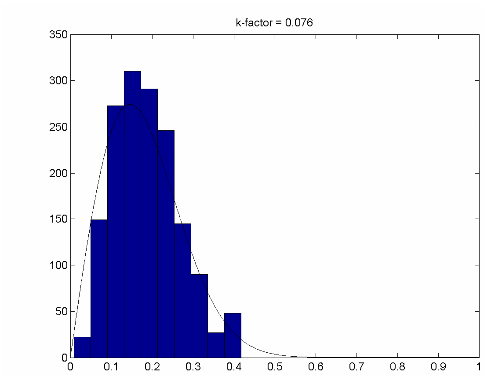

Figure 7. Sample histogram and estimated Rice distribution for antennas placed 7 cm apart directed towards each other and lined up to have a 90 degree difference in direction of polarization.

alter the distribution beside the distance between the antennas is the polarization of the antennas. If the antennas are linearly polarized with large XPR, the distribution can change by

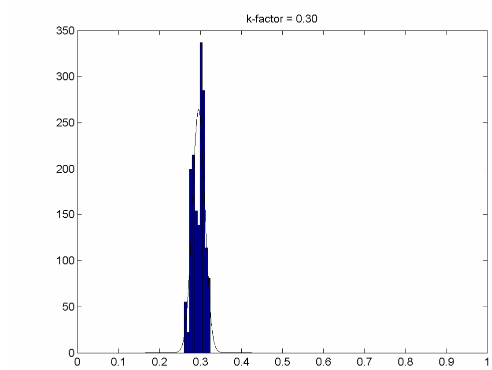

Figure 8. Sample histogram and estimated Rice distribution for antennas placed 20 cm apart directed towards each other and lined up to have the same direction of polarization. The receive antenna is placed inside a shielded anechoic box with an aperture.

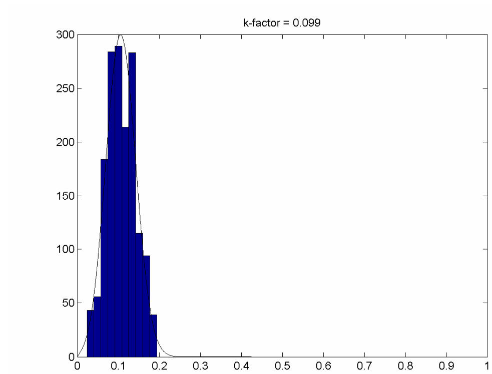

Figure 9. Sample histogram and estimated Rice distribution for antennas placed 40 cm apart directed towards each other and lined up to have the same direction of polarization. The receive antenna is placed inside a shielded anechoic box with an aperture.

just rotating one of the antennas. Figure 7 shows the distribution for antennas placed 7 cm apart but this time with different polarization directions, compare with figure 3 and the difference is obvious.

In former work we have suggested to place a shielded anechoic box with apertures inside the chamber [2]. The apertures are to control the directions of arrival of the plane waves that incident towards the test object. The next experiment is carried out with this shielded box placed inside the chamber and the receive antenna is placed inside this box pointing towards an aperture. The transmit antenna is, as before directed towards the receive antenna and the distance is varied. Figure 8 shows results from a case where the antennas are

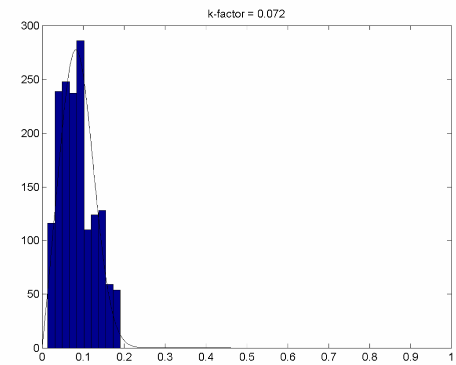

Figure 10. Sample histogram and estimated Rice distribution for antennas directed away from each other. The receive antenna is placed inside a shielded anechoic box with an aperture.

separated 20 cm and it clearly shows a Rice distribution with a large k-factor. When the antennas are moved away from each other the k-factor decreases which is shown in figure 9, the distance in this case is 40 cm. Finally when the transmit antenna is directed away from the receive antenna we obtain the (almost) Rayleigh distributed amplitude again as shown in figure 10.

III. Conclusions and discussion

From the measurements one can easily conclude that it is possible to change the amplitude statistics inside the SFC. This holds for both the case when the transmit and receive antenna is placed inside an empty SFC but also for the case when one antenna is placed inside a shielded anechoic box with apertures. The amount of direct propagation or the value of the Ricean k-factor can be altered by either changing the distance between the antennas, change the load of the chamber, and by this make the stirrer less efficient, and finally by changing the polarization alignment of the antennas. One can always argue that we should have performed some kind of statistical goodness of fit tests on the data, either the Kolmogorov-Smirnov-test or a Chi^2-test, to decide to which extent the data fits the estimated distribution. But for this simple, experimental chamber with a lot of un-optimized parameters, the statistics are not so perfect as you would want them to be, so these results would not enlighten things any more than the graphical plots already do. And since the distance that give a cetrain k-factor will vary a lot between different chambers with different kinds of stirrers and for different antennas and frequencies we found that there is no idea of making such tests but the important thing is to see the principal of the change of distribution.

IV. Acknowledgement

The author would like to thank Paul Hallbjörner for the original idea and for valuable discussions on the subject and also Olof Lundén who always has a lot of valuable information on measurements in reverberation chambers.

V. References

[1] M. Otterskog, K. Madsén, ”On creating a nonisotropic propagation environment inside a Scattered Field Chamber”, Microwave and Optical Technology Letters, Vol. 43, No. 3, p. 192-195, November 2004.
[2] M. Otterskog, ”Modelling of propagation environments inside a scattered field chamber”, 61st IEEE Vehicular Technology Conference (VTC2005-Spring), Stockholm, Sweden, June 2005.
[3] M. Bäckström, O. Lundén, P-S.Kildal, “Reverberation Chambers for EMC Susceptibility and Emission Analyses”, URSI the Review of Radio Science 1999-2002, 2002.
[4] K. Rosengren, P-S. Kildal, ”Study of distributions of modes and plane waves in reverberation chamber for characterization of antennas in multipath environments”, Microwave and Optical Technology Letters, Vol. 30, No 20, p 386-391, Sept. 2001.
[5] K. Madsén, P. Hallbjörner, ”Reverberation Chambers for Mobile Phone Antenna Tests”, The 2001 Reverberation Chamber, Anechoic Chamber and OATS Users Meeting, Bellevue WA, USA, 2001.
[6] Arai, Urakawa, ”Radiation Power Measurement Using Compact Shield Box”, Proceedings of ISAP’96, Chiba, Japan, 1996.
[7] O. Lundén, M. Bäckström, ”Predictions of stirrer performance in reverberation chambers”, presented at The 2003 Reverberation Chamber, Anechoic Chamber and OATS Users Meeting, Austin TX USA, April 2003.
[8] M. Otterskog, ”The influence of stirrer size and chamber load on the number of uncorrelated samples created in a reverberation chamber”, presented at The IEEE EMC Zürich 2005, February 2005.